Unraveling redox metabolism in Escherichia coli

Velasco Alvarez, M.I.

DOI
10.4233/uuid:59b7dcd5-bef9-41e9-80b3-e90412f1d5f8

Publication date
2021

Document Version
Final published version

Citation (APA)
Velasco Alvarez, M. I. (2021). *Unraveling redox metabolism in Escherichia coli*. [Dissertation (TU Delft), Delft University of Technology]. https://doi.org/10.4233/uuid:59b7dcd5-bef9-41e9-80b3-e90412f1d5f8

Unraveling redox metabolism in *Escherichia coli*

Dissertation

for the purpose of obtaining the degree of doctor
at Delft University of Technology by the authority of
the Rector Magnificus, Prof. dr. ir. T.H.J.J. van der Hagen,
chair of the Board for Doctorates to be defended publicly
on Thursday 25th of February at 10:00 o'clock.

by

Mariana Itzel VELASCO ALVAREZ

International Master of Science in Environmental
Technology and Engineering,
IHE Delft Institute for Water Education (The Netherlands),
the University of Chemistry and Technology (Czech Republic),
and Ghent University (Belgium)

Born in Mexico City, Mexico

This dissertation has been approved by the promotor.
Composition of the doctoral committee:

Rector Magnificus	Chairperson
Prof.dr.ir. M.C.M. van Loosdrecht	Delft University of Technology, promotor
Dr. S.A. Wahl	Delft University of Technology, copromotor
Independent members:	
Prof. M.A. Prieto Jimenez	Center for Biological Research, Spain
Prof. G.Q. Chen	Tsinghua University, China
Prof.dr.ir. M. De Mey	Ghent University, Belgium
Prof.Dr. R.A. Weusthuis	Wageningen University
Prof.dr. J.G. Kuenen	Delft University of Technology
Prof.dr.ir. H.J. Noorman	Delft University of Technology, reserve member

The research presented in this thesis was performed at the Cell Systems Engineering section, Department of Biotechnology, Faculty of Applied Sciences, Delft University of Technology, The Netherlands.

This work was carried out within the bilateral research program between the Netherlands (Division for Chemical Science of NWO) and the State of Sao Paolo in Brazil on "Biobased Economy" (FAPESP).

Cover illustration: "*Evolutie*", Piet Mondriaan, 1911
Printed and bound in the Netherlands by Ridderprint BV
ISBN/EAN 978-94-6384-203-7

"Reír nos hizo invencibles. No como los que siempre ganan sino como aquellos que no se rinden." [Laughing made us invincible. Not like those who always win but like those who do not give up.]

Frida Kahlo y Chavela Vargas

To
my family and friends

Summary

A wide variety of microorganisms are increasingly being employed for the production of a broad diversity of compounds, instead of using fossil fuel. The production of such compounds faces different challenges for an optimized production. Identifying the bottlenecks in the synthesis of such products offers the possibility to reduce these bottlenecks and increase the production efficiency. This could lead to economically feasible production of these compounds without utilizing fossil fuels. This thesis focuses specifically on the production of PHB using *E. coli*, by studying the redox modified metabolism.

Different metabolic pathways that might favour the flux towards PHB production were evaluated. More specifically, the bottlenecks in the synthesis and the conditions that might favor or limit its production were carefully analyzed in this thesis. The main bottlenecks in PHB production that have been identified and discussed in literature are the precursor acetyl-CoA and the co-factor NADPH. However, their role has not been entirely clarified in the field of metabolic engineering. Most studies use flux balance analysis to investigate the roles of acetyl-CoA and NADPH.

However, these analyses only provide information about the stoichiometry of a pathway with the flux distribution, while analyzing them through thermodynamics gives the specific reaction that is furthest from equilibrium and therefore a bottleneck for the synthesis of a product. In this thesis we combine both flux balance analysis and thermodynamics for understanding the pathways EMP (Embden-Meyerhof-Parnas pathway), Entner–Doudoroff pathway (EDP), and modified Embden-Meyerhof-Parnas pathway (mEMP).

In **Chapter 2**, the thermodynamic feasibility of each pathway was theoretically analysed for the synthesis of PHB in an ideal condition, that is, the whole substrate (glucose) is used for PHB production. Biomass formation was not included in the analysis to simplify the NADPH sinks. The analysis suggested that the formation of PHB is more sensitive to the ratio AcCoA/CoA than a NADPH/$NADP^+$ ratio. Moreover, the pathway that resulted in a higher flux force efficacy towards PHB was mEMP. Simulations were performed that supported this conclusion.

Following this study, the strain mEMP was investigated in the laboratory and was compared in **Chapter 3**. The strain mEMP was engineered in *E. coli* with the replacement of the genes *gap::ganp* and the knock-out of the gene *zwf* . The modifications increased the PHB flux for mEMP, and production of two molecules of NADPH. The analysis assessed the continuous production of the desired product PHB under carbon limited conditions and oxygen limited conditions. Our results show an observed shift in glycolysis, suggesting that the flux for PHB was increased by oxygen limited conditions. Additionally, a higher AcCoa/CoA was observed during these cultivations. This result was in accordance with the thermodynamic study in Chapter 2.

In order to obtain accurate measurements in Chapter 3, it was desired to implement a small scale method that could detect PHB in the *E. coli* cells from a small amount of samples (1 mL), due to the low working volume of the bioreactors used in the experiments. In **Chapter 4** we describe a method that utilizes labelled ^{13}C-HB as an internal standard for quantifying low concentrations of PHB and providing a higher precision on PHB measurements. The method showed a high level of accuracy.

Samenvatting

Steeds vaker wordt een grote variatie aan micro-organismen gebruikt voor de productie van een divers aantal chemische verbindingen, in plaats van fossiele brandstoffen. De productie van dergelijke chemische verbindingen ondervindt verschillende uitdagingen voor het optimaliseren van productie. Het identificeren van de knelpunten in de synthese van dergelijke producten kan ertoe leiden dat deze knelpunten kunnen worden gereduceerd zodat de productie-efficiëntie kan worden verhoogd. Dit kan leiden tot economisch haalbare productie van chemische verbindingen zonder gebruik te maken van fossiele brandstoffen. Deze dissertatie gaat voornamelijk over de productie van PHB door E. coli, middels het bestuderen van gemodificeerd redox-metabolisme.

Verschillende reactiepaden die de flux richting PHB productie zouden kunnen bevorderen waren geëvalueerd. De knelpunten in synthese, en de condities die de productie kunnen bevorderen or limiteren waren gronding geanalyseerd in deze dissertatie. De voornaamste knelpunten voor PHB-productie die zijn geïdentificeerd en besproken in de literatuur zijn de precursors acetyl-CoA en NADPH. Hun rol is echter niet volledig verhelderd in het werkveld van *metabolic engineering*. De meeste studies gebruiken fluxbalansanalyse om de rol van acetyl-CoA en NADPH te onderzoeken.

Deze analyses verstrekken echter alleen informatie over de stoïchiometrie van een reactiepad met de fluxdistributie, terwijl hun analyse met thermodynamica de specifieke reactie oplevert die zich het verst weg van equilibrium begeeft, en daarom een knelpunt vorm voor de synthese van een product. In deze dissertatie combineren we zowel fluxbalansanalyse als thermodynamica om de reactiepaden EMP (Embden-Meyerhof-Parnas pathway), Entner–Doudoroff pathway (EDP), en modified Embden-Meyerhof-Parnas pathway (mEMP) beter te begrijpen.

In **Hoofdstuk 2** wordt de thermodynamische haalbaarheid van elk reactiepad theoretisch geanalyseerd ten behoeve van de synthese van PHB onder ideale omstandigheden, namelijk dat het gehele substraat (glucose) wordt gebruikt voor PHB-productie. Biomassa-formatie was in deze analyse niet ingegrepen om de NADPH *sinks* te versimpelen. De analyse suggereert dat de vorming van PHB meer gevoelig is voor de ratio AcCoA/CoA dan die van

NADPH/$NADP^+$. Bovendien was mEMP het reactiepad dat resulteerde in een hogere fluxkracht-werkzaamheid. Uitgevoerde simulaties ondersteunen deze conclusie.

In navolg van deze studie werd het reactiepad mEMP onderzocht in een laboratoriumomgeving en vergeleken in **Hoofdstuk 3**.Het reactiepad mEMP was ontworpen in E. coli met de vervanging van de genen *gap:ganp* en de *knock-out* van het gen *zwf* . Deze aanpassingen verhoogden de PHB-flux voor mEMP, en produceerde twee NADPH-moleculen. De analyse toetste de continue productie van het gewenste PHB-product onder koolstof- en zuurstof-gelimiteerde omstandigheden. Onze resultaten tonen een geobserveerde verschuiving in glycolyse, wat suggereert dat de flux voor PHB toenam onder zuurstof-gelimiteerde omstandigheden. Verder werd een hogere AcCoa/CoA waargenomen tijdens de aankweek. Dit resultaat was in overeenstemming met de thermodynamische studie in Hoofdstuk 2.

Om meer accurate metingen te krijgen in Hoofstuk 3, was het nodig om een kleinschalige methode te implementeren die in staat is om lage hoeveelheden PH in *E. coli*-cellen te detecteren vanuit een kleine hoeveelheid monsters (1 mL), vanwege het lage werkvolume van de bioreactoren die werden gebruikt in de experimenten. In **Hoofdstuk 4** beschrijven we een methode die gebruik maakt van gelabelde ^{13}C-HB als een interne standaard voor het kwantificeren van lage concentraties PHB en het verstrekken van hogere precisie voor PHB-metingen. De methode toonde een hoge mate van nauwkeurigheid.

Table of Contents

Chapter 1.

General Introduction

1.1 Bioeconomy and industrial biotechnology

During the last decades, growing concern on climate change has driven the development of new technologies that contribute to a reduction of greenhouse gas emissions. There is an urgency to change the present industrial manufacturing to more sustainable processes [1]. The United Nations sustainable development goals (SDG) for 2030 include new technological sustainability goals, specifically in Goal 9: Industry, Innovation, and Infrastructure (www.un.org) that looks towards enhancing scientific research and developing new alternatives for the transition to renewable feedstocks.

Fermentation processes use renewable feedstocks [2] and are expected to play an important role in the transition to a more sustaianbale society and are becoming an integral part of the chemical industry. However, to compete with current petroleum based production, novel products and more efficient bioprocesses are required [3]. These goals can only be achieved by developing and engineering highly efficient microorganisms [4] by establishing systematic approaches and technologies [5]. One of the complex challenges in metabolic engineering of microorgansms is the unknown regulation of many metabolic pathways [6,7]. A crucial basis for the cellular metabolism are redox processes which generate the catabolic energy and dictate the conversions in the anabolism [8–11]. Redox balances are at the basis of description of cellular metabolism and understanding the redox metabolism is crucial for attaining an efficient and profitable process.

1.2 Polyhydroxybutyrate (PHB) production in engineered *E. coli*

Metabolic engineering towards product formation in most cases will modify the cellular redox balance and state. To study the redox metabolism of different polyhydroxybutyrate (PHB) [12,13] producing strains is analyzed (**Figure 1** shows the product pathway). PHB was the first polyhydroxyalkanoate that was discovered and also the most extensively characterized. Maurice Lemoigne discovered PHB in the 1920s, during a time that had low interest in lipids and little knowledge about polymers. However, the application of polymers became more relevant 30 years after their discovery [14,15]. PHB can be accumulated up to 80% of the dry cell weight as a membrane-enclosed inclusion in several bacteria [16]. The main advantages of using PHB next to the production from renewable resources are 1) the fast, natural degradation, 2) the medical applications, like as capsul material for the controlled drug release or as filaments for surgical sutures [17,18].

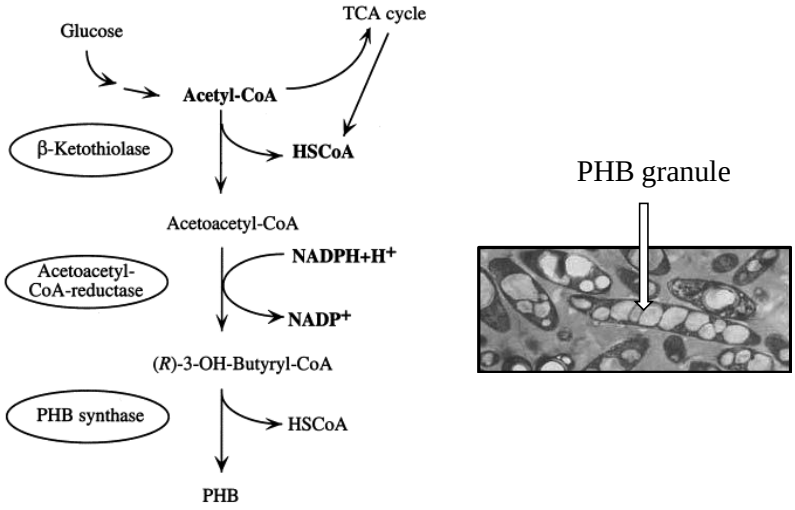

Figure 1. *Left:* Three-step pathway to polyhydroxybutyrate [19]. *Right:* visualization of PHB granules by transmission electron micrograph of recombinant *Escherichia coli* XL1-Blue (pSYLlO5). The image also shows that there is elongation for some cells. Figure modified from Lee at al. [18].

Escherichia coli was chosen as the model organisms because it is well studied and often used in industrial fermentations. Moreover, modified *E. coli* cells have been extensively studied for PHB production [20,21], [22,23]. Furthermore, a large variety of mutants are available from repositories. In **Table 1** the advantages and disadvantages of the use of *E. coli* for PHB accumulation are summarised.

Table 1. Advantages and disadvantages of using *E. coli* for the production of PHB

Advantages	Disadvantages
Accessible genetic tools [24,25]	Filamentation and limited accumulation [23]
Accumulation up to 80% PHB has been achieved (wt/wt) [25]	Sterile conditions needed [26]
No innate depolymerases [27]	Loss or instability of the plasmid based product pathway expression [27]
Easy purification of the polymer compared to natural strains [27]	Limited accumulation capacity [12,23]
Nutrient limitation is not mandatory for accumulation [28,29]	

Some of the challenges mentioned in **Table 1** have been tackled, for instance, the cell elongation. A study demonstrated that a change from rod shape to elongated cell shape improved the PHB accumulation capacity in *E. coli* cells [21].

The current fermentation process developments for PHB production aim at the enhancement of both the yield and process productivity to offer a more competitive process. Batch, fed-batch, or continuous cultures using improved bacterial strains, growing on inexpensive carbon sources combined with multi-stage fermentation systems, have been widely described [18,30]. Continuous production of PHB has been mentioned as an important advantage of using modified strains of *E. coli* [26]. This is different from the traditional PHB production strain *Cupriavidus necator,* where a multistage batch reactor is needed for the effective production of PHB [12,17,23] in a first stage biomass is produced on a balanced medium. When enough biomass is present a nutrient limitation is created which diverts the metabolic fluxes from growth towards PHB accumulation (18). For the two-stage production of PHB a common strategy to increment the productivity of PHB has been applying nitrogen limitation. The advantage of nitrogen limitation is that growth is controlled by nitrogen source [31]. *Alcaligenes lactus*, a natural producer of PHB, was studied under nitrogen limitation in batch and fed-batch conditions. PHB formation was enhanced by nitrogen limitation, and a maximum yield of 0.32 g of PHB/g of residual cells was obtained [32]. The effect of nitrogen limitation has also been studied in engineered strains of *E. coli* expressing a set of heterologous genes from *Streptomyces aureofaciens*, using glycerol as carbon source and a combination of yeast extract

and peptone as the nitrogen source. A maximum PHB accumulation of 60% (w/w) PHB of cell dry weight was obtained [33].

For analysis of metabolism but also production, bioreactor chemostat cultivations are advantageous, since there is 1) optimal control of cell growth rate, and 2) allows to fully characterize the strains employed under controled process parameters such as pH-value, temperature, oxygen supply, and, substrate concentration [26,34]. In addition, on a large scale, chemostat cultivations have several advantages such as greater utilization of installed equipment, smaller equipment size, and shorter down time (i.e. longer cultivations, less frequent cleaning) [31], all leading to lower capital costs. In PHB production, one of the major limitations is that the product is stored intracellularly, hindering the maximal amount of PHB that can be accumulated [18]. Moreover, PHB accumulation occurs when growth is inhibited (e.g. by a limiting nutrient), for continuous production a coupling of growth and PHB production would be needed.

1.3 Suitable substrates for PHB formation

Besides the capital costs also operational costs are limiting industrial PHB production, among others related to the substrate costs. The use of not only a carbon source but also nutrients and minerals that are necessary for bacterial growth create a more substantial obstacle for product formation [35]. Therefore, finding a suitable carbon source that is not only cheap but that can generate a profitable yield is still a current challenge [35–37]. In this line of research, *E. coli* has been used as a promising organism to form PHB since it can be easily manipulated to consume cheap substrates. The most studied carbon source for producing PHB in *E. coli* has been glucose, where a maximum theoretical yield of 1.33 (mol_P/mol_S) can be obtained (see **Table 2**) [35].

The production of PHB through glycolysis produces a redox problem, as it requires NADPH for the synthesis of 3-hydroxybutyryl-CoA. The pathway from glucose to PHB produces 4 NADH, while only one molecule of NADPH (obtained through transhydrogenases or Pentose Phosphate Pathway) is used for PHB synthesis. Therefore, the use of more oxidized substrates than PHB has been one strategy to counterpart redox states substrate/product(s) [33,35,36]. For instance, the synthesis of PHB from gluconate only produces 4 excess electrons, rather than 6 excess electrons produced from glucose. When studied experimentally was attained a PHB flux

yield of 1.6 fold more as also the pathway can be enhanced compared to glucose fermentation [38].

An alternative cheap substrate is the use of xylose or sugarcane bagasse hydrolysate for the formation of PHB [37]. On the other hand, the use of fatty acids (FA) has been a strategy for the forming better of co-polymers (Polyhydroxybutyrate/Polyhydroxyvalerate) [39].

Table 2. Comparison of substrates with respect to degree of reduction (Y) and electron per carbon (Y /C) for PHB production.

Compound	Y	Y /C	C_P/C_S	Theoretical highest product yield (mol_P/mol_S)
Glucose $C_6H_{12}O_6$	24	4.0	0.67	1.33
Gluconate $C_6H_{11}O_7$	22	3.6	0.67	1.22
Glycerol $C_3H_8O_3$	14	4.6	1.33	0.77
Succinic acid $C_4H_6O_4$	14	3.5	1.0	0.77
Xylose $C_5H_{10}O_5$	20	4.0	0.8	1.11
PHB monomer, 3-Hydroxybutyrate $C_4H_8O_3$	18	4.5		

1.4 Metabolic Network Analysis

Metabolic network analysis has developed into a central tool to analyze, design and improve production strains [1]. Especially, a mathematical description of the intracellular reaction network allows to identify and quantify relevant interconnections and links in metabolism thereby enabling a systemic optimization towards defined product pathways [40–44].

Many metabolic network interactions are generated by redox co-factors, precursors as well as energy metabolites. In this thesis, redox co-factors are of special interest and how the redox stoichiometry can influence different metabolic pathways [45,46].

1.5 NADPH regeneration in *E. coli*

The most important co-factors in biosynthetic pathways are NADH, NADPH, and ATP. Most focus has been on NADH and ATP as co-factor. Recently, NADPH and acetyl-CoA have

gained some attention [47–49] which are also essential in the central carbon metabolism. Acetyl-CoA is a precursor for lipids, proteins, and polymers, and NADPH is the reducing power for anabolic reactions. Most of the biosynthetic pathways rely on NADPH, such as lipids, proteins, and DNA synthesis [47]. It is commonly observed that the ratio of NADPH/NADP is higher compared to its non-phosphorylated counterpart NADH/NAD (**Table 3**). It is assumed that the higher driving force from a high NADPH/$NADP^+$ ratio is important for the anabolic reactions like synthesis of lipids. NADH/NAD^+ ratio is more on the oxidized side to accelerate catabolic reactions like the oxidation of glucose to CO_2.

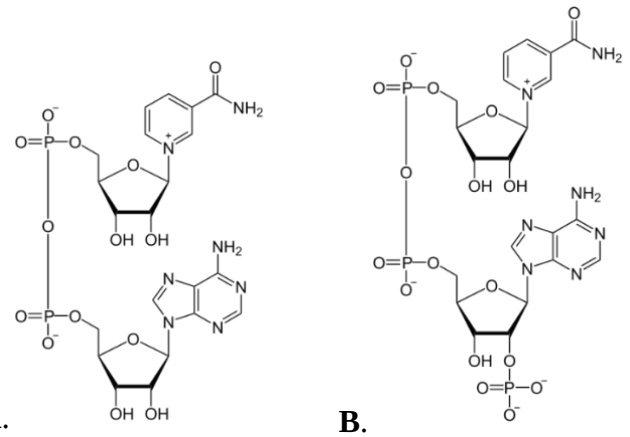

A. **B**.

Figure 2. A: Nicotinamide adenine dinucleotide (NADH) molecule, B: Nicotinamide adenine dinucleotide phosphate (NADPH) [50,51].

The importance of these molecules in the different metabolic processes has increased the interest in studying the regulatory mechanisms in the NAD(P)H and NAD(P) generating systems.

Product pathways commonly involve redox cofactors, especially for relevant reduced compounds like catechin [41], PHAs [14], ε-caprolactone, lycopene [44], NAD(P)H will be required. The consumption of NAD(P)H is in direct competition with biomass production, which could hamper NADPH dependent products.

Table 3. NAD(P) and NAD(P)H oxidized and reduced form [52].

Oxidized form	Reduced form	$E^{0'}$ (volts)	In vivo [Ox.]/[Rd.]	$\Delta_r G'$
NAD^+	NADH	-0.32	3.7-31.3	64.1
$NADP^+$	NADPH	-0.324	0.02-0.95	65.1

Five main sources of NADPH are described for *E. coli*:

1) Pentose Phosphate Pathway (PPP)
2) Entner-Doudoroff Pathway (EDP): glucose-6-phosphate dehydrogenase, and 6-phosphogluconate dehydrogenase,
3) Tricarboxylic acid cycle (TCA): Isocitrate dehydrogenase,
4) Membrane transhydrogenase: Membrane bound transhydrogenase PntAB and,
5) Anaplerotic reactions: $NADP^+$ dependent malic enzyme [53].

Pentose Phosphate Pathway (PPP):

The primarily purpose of the pentose phosphate pathway is the generation of NADPH and the formation of precursors for mRNA and amino acids. In the Oxidative Pentose Phosphate Pathway (OxPPP), there are two main reactions involved in the production of NADPH. The first reaction is catalyzed by glucose-6-phosphate dehydrogenase (gene *zwf*) for the formation of 6-P-Glucono-1,5-lactone, and the second reaction is catalyzed by 6-phosphogluconate dehydrogenase (gene *gnd*) to form Ribulose-5-P. In *E. coli* wild type, approximately 25% of catabolized glucose goes through the PPP, while 2% goes through EDP [54]. Moreover, the flux of NADPH through PPP was observed to have a contribution of 66% *in silico* [55].

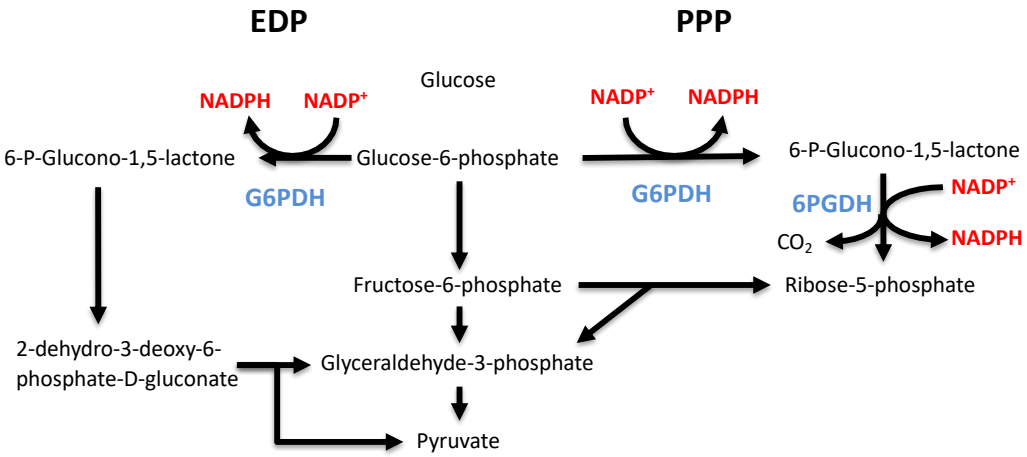

G6PDH: Glucose-6-P + $NADP^+$ → 6-P-D-glucono-1,5-lactone + NADPH + H^+

$\Delta G'^m = -2.3 \pm 2.6$ kJ/mol

6PGDH: 6-P-gluconate + $NADP^+$ → Ribulose 5-P + CO_2 + NADPH + H^+

$\Delta G'^m = -5.9 \pm 6.3$ kJ/mol

Figure 3. NADPH generating reactions systems in bacteria. The reaction Gibbs free energies were obtained from Equilibrator [56].

Isocitrate dehydrogenase: The isocitrate dehydrogenase (EC 1.1.1.42) is part of the TCA cycle and is responsible for catalysing the reaction from isocitrate to α-ketoglutarate, CO_2 and NADPH are released (see **Figure 4**). The formation of α-ketoglutarate has an important link to nitrogen and carbon metabolism. Along with isocitrate lyase, isocitrate dehydrogenase is an important channel between the glyoxylate shunt and the TCA cycle. Therefore, the activity of the isocitrate dehydrogenase has an important input in the control of the metabolic flux through this reactions, especially when using non-fermentative substrates such as acetate and ethanol [47,57].

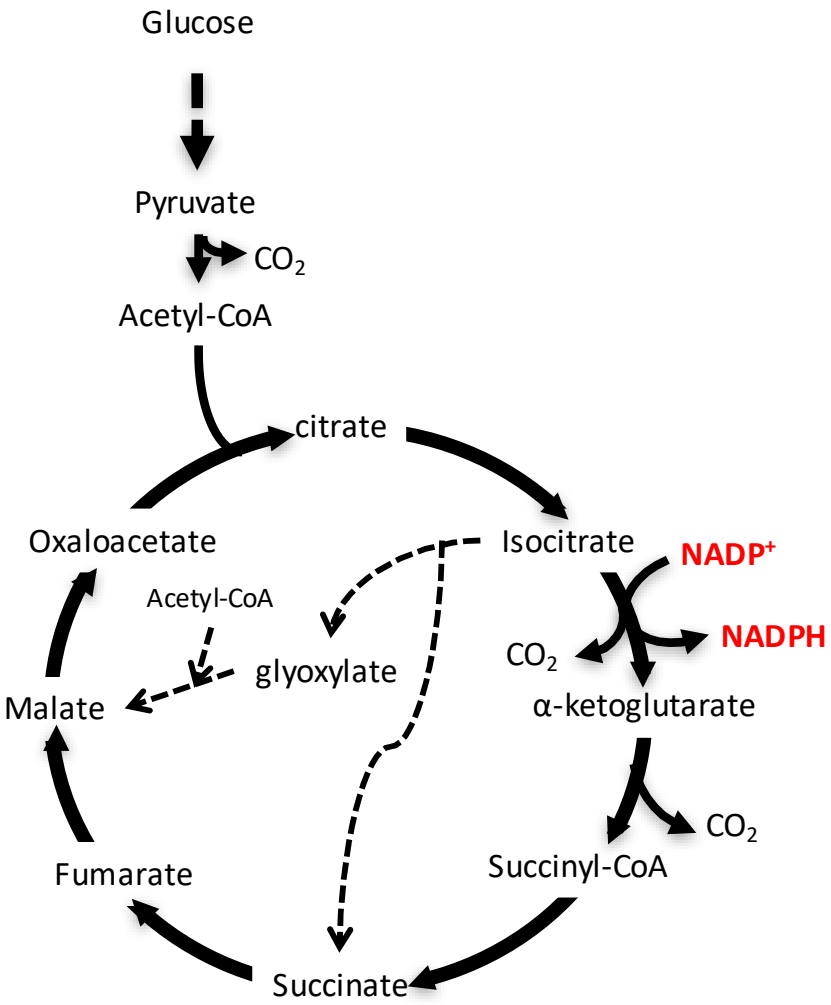

ICDH: Isocitrate + $NADP^+$ → α-ketoglutarate + CO_2 +NADPH + H^+

$\Delta G'^m = -10.7 \pm 6.3$ kJ/mol

Figure 4. Tricarboxylic acid cycle (TCA), highlighting the generation of NADPH. The Gibbs free energy of the reaction was calculated through Equilibrator [56].

Transhydrogenases

E. coli possess two transhydrogenase systems, the soluble transhydrogenase (UdhA) and the membrane bound transhydrogenase (PntAB). Under standard conditions NADH and NADPH have equal energy and transformation would be energy neutral. However do to the different NAD/NADH and NADP/NADPH ratio's in the cell (Table 3) conversion of NADH into NADPH is an energy demanding process.

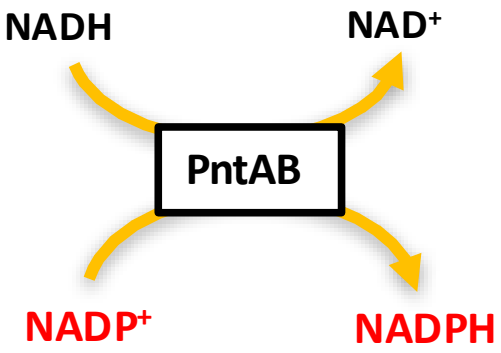

PntAB: $NADH + NADP^+ + H^+ \leftrightarrow NAD^+ + NADPH + H^+$

$\Delta G'^m = 1.0 \pm 0.7$ kJ/mol

Figure 5. The membrane-integral nicotinamide nucleotide transhydrogenase PntAB. The Gibbs free energy of the reaction was obtained through Equilibrator [56].

PntAB: the membrane-integrated nicotinamide nucleotide transhydrogenase PntAB (EC 1.6.1.2) of *E. coli* can use the electrochemical proton gradient across the cytoplasmic membrane to drive the reduction of $NADP^+$ via the oxidation of NADH (see **Figure 5**). The activity of the transhydrogenase PntAB was found to be greater in batch conditions with glucose as substrate (see **Figure 6A**). In this case 35–45% of the NADPH that is required for biosynthesis was produced via PntAB, when no UdhA was active [54]; the pentose phosphate pathway and isocitrate dehydrogenase contributed 35–45% and 20–25%, respectively [54]. In chemostat conditions, the Pentose Phosphate Pathway was found to be the major contributor of NADPH compared to isocitrate dehydrogenase and that from all the fluxes there is a surplus of NADPH (see **Figure 6B**) [58].

UdhA: the energy-independent soluble pyridine nucleotide transhydrogenase UdhA (EC 1.6.1.1) of *E. coli* is responsible for the reoxidation of NADPH. Sauer et al. [54] could observe that the UdhA is necessary for growth in conditions of NADPH in excess, converting NADPH to NADH.

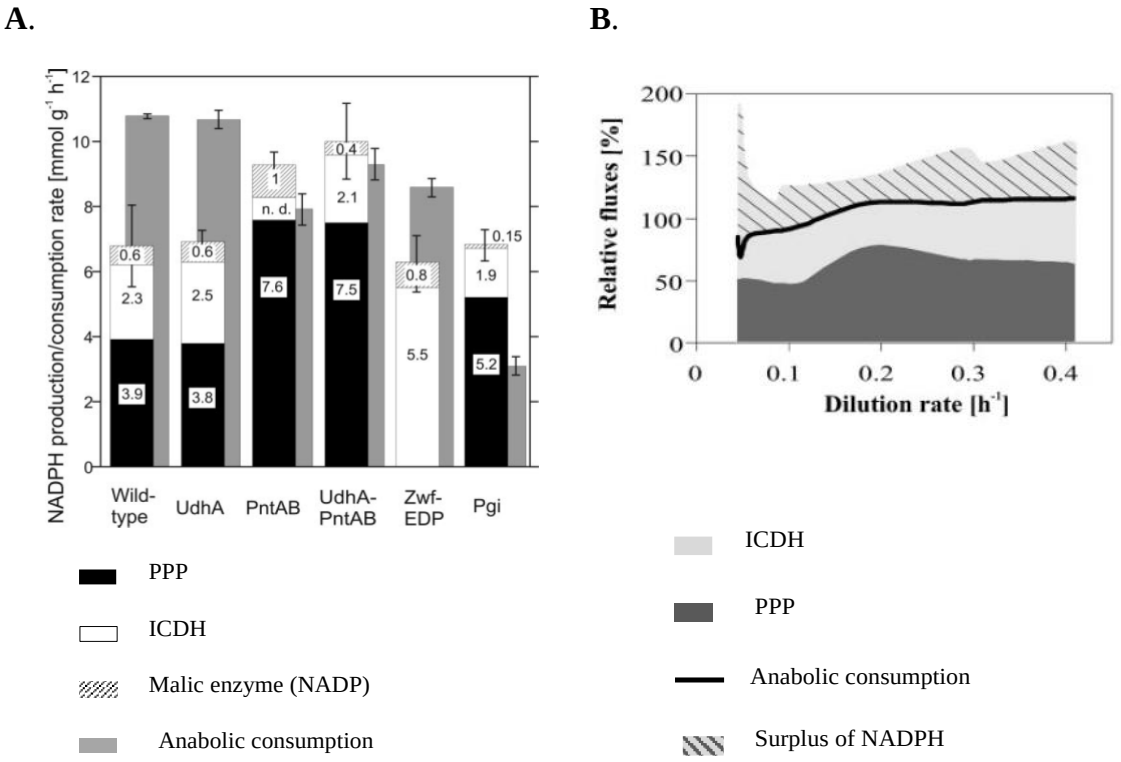

Figure 6. Production and consumption rates of NADPH during batch and chemostat conditions. 6A: Rates in different mutant strains under batch cultivations, figure taken from Canonaco et al. [54]. 6B: NADPH production and consumption rates during chemostat cultivations relative to the glucose uptake rate (taken from Nanchen et al.[58]),

1.6 Approaches to increase NADPH production in *E. coli*

For the formation of polyhydroxybutyrate NADPH is required (second step, starting from the precursor acetyl-CoA). Several strategies have been applied in modified strains of *E. coli* to enhance NADPH formation, especially [31]:

(i) NADP dependent GAPDH (Glyceraldehyde-3-Phosphate dehydrogenase) instead of NAD dependent

(ii) Phosphoglucose isomerase (*pgi*) deletion [59],

(iii) Overexpression of pentose phosphate (PP) pathway enzymes (*zwf*, *gnd*, *talA*, and *tktA*) [13], and

(iv) Overexpression of transhydrogenase (*udha*) [60].

NADP dependent GAPDH: One of the important key nodes in the glycolytic flux is GAPDH (EC 1.2.1.12) that uses NAD^+ as a cofactor. GAPDH is encoded by *gapA* and is known to have higher relative activity compared to other enzymes in the glycolytic pathway [61]. It is a reversible enzyme that can switch direction under an excess of NADH [62,63]. For NADPH dependent producing pathways, Martinez et al. [44] showed the shift of a *gapA* gene to a *gapC* from *Clostridium acetobutylicum* for the synthesis of NADPH molecules instead of NADH. In this study, the mutant strain containing the *gapC* gene presented a higher flux through glycolysis than through the PP pathway since the requirement of NADPH was already alleviated by GAPDH [44]. This line of research was later applied for PHB producing *E. coli* cells. The gene *gapN* from *Streptococcus mutans* was substituted for *gapA*, and a significant increase of PHB accumulation was obtained [64].

***pgi* deletion**: The knock-out of phosphoglucoisomerase (*pgi)* that corresponds to the reaction from glucose-6-phosphate to fructose-6-phosphate, has been a strategy to increase the flux through the PPP [41]. A study performed with modified strains of *E. coli* found that strains lacking the *pgi* gene grow slowly on glucose and are estimated to form an excess of NADPH [65]. This strategy applied for PHB production showed that the cells repressed their growth due to the excess of NADPH, and this excess was somehow alleviated by the PHB pathway [66].

***udhA* overexpression**: In recombinant *E. coli* cells, where the UdhA transhydrogenase was overexpressed, PHB increased from 49 to 66 % of dry cell weight [60]. This result is comparable to observations from Canonaco et al. [54]. The authors did show that the cells were able to restore growth in NADPH excess through the UdhA transhydrogenase**.** The redox alleviation generated by the UdhA allowed the cells to grow and use the available NADPH.

1.7 NADPH consuming product pathway – PHB synthesis

To study the impact of modified redox stoichiometry, sources (discussed above) and sinks, product pathways are varied. As shown in **Figure 1,** the production of PHB was chosen as established product pathway.

The PHB pathway was first studied and described in *Azotobacter beijerinckii* [22] and *Alcaligenes eutrophus* [15,17]. The first step consists of the condensation of two molecules of

acetyl-CoA to generate acetoacetyl-CoA. The second step is the reduction of acetoacetyl-CoA to form 3-hydroxybutyryl-CoA with the oxidation of one molecule of NADPH. The last step is the initiation of the polymerization reaction, where an ester is formed between the monomers of 3-HB [22]. The polymerization involves the enzyme PHA synthase, PHA synthases share a conserved cysteine as a catalytic active site to which the growing PHA chain is covalently attached. The active-site cysteine has been found to constitute a catalytic triad similar to esterases. Several studies have concluded that the CoA generated in the reaction from two acetyl-CoA to acetoacetyl-CoA generates inhibition in the enzyme β-ketothiolase, therefore the activity of the PHB synthase is considered to be controlled by the cellular concentration of CoA [40,67,68].

1.8 Thermodynamics of metabolic pathways

Next to stoichiometric relations, thermodynamic driving forces are crucial for understanding cellular metabolism [69,70]. The study of thermodynamic driving forces in metabolic pathways provides a comprehensive overview of the bottlenecks and constraints. Different computational tools are available for systematic analysis and optimization of metabolic pathways. For example the Equilibrator tool developed by Noor et al. [56] or anNET by Zamboni et al. [71] and others. These tools use thermodynamic information to estimtate the feasibility of pathways, expected metabolite concentrations and (minimal) driving forces of the single reaction steps.

1.9 Scope of the study and outline

Aim of the thesis project is to obtain a comprehensive understanding of redox regulation and enable a defined split between product and biomass synthesis using redox constraints and metabolic regulation.

The regulatory metabolites in the central carbon metabolism and the allocation of cellular resources between the product and biomass formation are studied using theoretical as well as experimental approaches. Especially, flux balance analysis (FBA) is used to predict the metabolic flux using different glycolytic pathways. Additionally, thermodynamic pathway analysis is applied to evaluate the feasibility and expected metabolite concentration range. The

results from the calculation are compared with experimental results from respective mutant strains.

The impact of the precursor acetyl-CoA and the co-factor NADPH and the feasibility of the different pathways for PHB production is presented in **Chapter 2.** In **Chapter 3,** strains with the preferred pathways (replacement of the genes *gapA:gapN* and a knock-out of the gene *zwf*) suggested by the thermodynamic analysis were studied experimentally. The analysis assessed the continuous production of PHB under carbon limited conditions and oxygen-limited conditions. In **Chapter 4** a quantitative analysis of PHB is presented, using labelled ^{13}C-HB as an internal standard for measuring low concentrations of PHB through isotope dilution mass spectrometry (IDMS) and propanolysis extraction.

References

1. Dugar D, Stephanopoulos G. Relative potential of biosynthetic pathways for biofuels and bio-based products. Nat Biotechnol [Internet]. 2011 [cited 2014 Nov 17];29:1074–8. Available from: http://www.ncbi.nlm.nih.gov/pubmed/22158355

2. Tsunekawa H, Azuma S, Okabe M. Acquisition of a sucrose utilization system in Escherichia coli K-12 derivatives and its application to industry . Acquisition of a Sucrose Utilization System in Escherichia coli K-12 Derivatives and Its Application to Industry. 1992;58:2081–8.

3. Adrie J. J. Straathof AB. Potential of commodity chemicals to become bio-based according to maximum yields and petrochemical prices. Biofuels, Bioprod Biorefining. 2017;11:798–810 (2017);

4. McCloskey D, Palsson BØ, Feist AM. Basic and applied uses of genome-scale metabolic network reconstructions of Escherichia coli. Mol Syst Biol [Internet]. 2013 [cited 2015 Mar 27];9:661. Available from: http://www.pubmedcentral.nih.gov/articlerender.fcgi?artid=3658273&tool=pmcentrez&rendertype=abstract

5. Straathof AJJ, Wahl SA, Benjamin KR, Takors R, Wierckx N, Noorman HJ. Grand Research Challenges for Sustainable Industrial Biotechnology. Trends Biotechnol [Internet]. Elsevier Ltd; 2019;37:1042–50. Available from: https://doi.org/10.1016/j.tibtech.2019.04.002

6. Sauer U, Lasko DR, Fiaux J, Hochuli M, Glaser R, Szyperski T, et al. Metabolic flux ratio analysis of genetic and environmental modulations of Escherichia coli central carbon metabolism. J Bacteriol. 1999;181:6679–88.

7. Oldiges M, Lütz S, Pflug S, Schroer K, Stein N, Wiendahl C. Metabolomics: Current state and evolving methodologies and tools. Appl Microbiol Biotechnol. 2007;76:495–511.

8. Heijnen JJ. Stoichiometry and kinetics of microbial growth from a thermodynamic perspective. Basic Biotechnol. Third Ed. 2006.

9. De Kok S, Kozak BU, Pronk JT, Van Maris AJA. Energy coupling in Saccharomyces cerevisiae: Selected opportunities for metabolic engineering. FEMS Yeast Res. 2012;12:387–97.

10. Chen X, Alonso AP, Allen DK, Reed JL, Shachar-Hill Y. Synergy between (13)C-metabolic flux analysis and flux balance analysis for understanding metabolic adaptation to anaerobiosis in E. coli. Metab Eng [Internet]. Elsevier; 2011 [cited 2015 Sep 14];13:38–48. Available from: http://www.ncbi.nlm.nih.gov/pubmed/21129495

11. Willemsen AM, Hendrickx DM, Hoefsloot HCJ, Hendriks MMWB, Wahl SA, Teusink B, et al. Molecular BioSystems balance analysis †. Mol Biosyst [Internet]. Royal Society of Chemistry; 2014;14–6. Available from: http://dx.doi.org/10.1039/C4MB00510D

12. Choi SYL and J. MET ABOLlC ENGINEERING OF ESCHERICHIA COLI FOR THE PRODUCTION OF POLYHYDROXYALKANOATES. Metab Eng. Elsevier; 1998;337–41.

13. Shi H, Nikawa J, Shimizu K. Effect of modifying metabolic network on poly-3-hydroxybutyrate biosynthesis in recombinant Escherichia coli. J Biosci Bioeng. 1999;

14. Lemoigne M. Produits de dehydration et de polymerisation de l'acide ß-oxobutyrique. Bull Soc Chim Biol (Paris). 1926;8:770–8.

15. Lenz RW, Marchessault RH. Bacterial polyesters: Biosynthesis, biodegradable plastics and biotechnology. Biomacromolecules. 2005;6:1–8.

16. Khanna S, Srivastava AK. Recent advances in microbial polyhydroxyalkanoates. Process Biochem [Internet]. 2005 [cited 2014 Jul 14];40:607–19. Available from: http://linkinghub.elsevier.com/retrieve/pii/S0032959204000949

17. Dawes E. Polyhydroxybutyrate: an intriguing biopolymer. Biosci Rep [Internet]. 1988 [cited 2015 Mar 30];8:537–47. Available from: http://link.springer.com/article/10.1007/BF01117332

18. Lee SY. Bacterial Polyhydroxyalkanoates. Biotechnol Bioeng. 1996;49:1–14.

19. Shrivastav A, Kim HY, Kim YR. Advances in the applications of polyhydroxyalkanoate nanoparticles for novel drug delivery system. Biomed Res Int. 2013;2013.

20. Anderson AJ, Dawes EA. Occurrence, metabolism, metabolic role, and industrial uses of bacterial

polyhydroxyalkanoates. Microbiol Rev. 1990;54:450–72.

21. Chen GQ, Jiang XR. Engineering bacteria for enhanced polyhydroxyalkanoates (PHA) biosynthesis. Synth Syst Biotechnol. Elsevier Ltd; 2017;2:192–7.

22. Senior PJ, Dawes EA. The regulation of poly β hydroxybutyrate metabolism in Azotobacter beijerinckii. Biochem J. 1973;134:225–38.

23. Lee SY, Lee KM, Chan HN, Steinbüchel A. Comparison of recombinant Escherichia coli strains for synthesis and accumulation of poly-(3-hydroxybutyric acid) and morphological changes. Biotechnol Bioeng. 1994;44:1337–47.

24. Schubert P, Steinbüchel A, Schlegel HG. Cloning of the Alcaligenes eutrophus genes for synthesis of poly-beta-hydroxybutyric acid (PHB) and synthesis of PHB in Escherichia coli. J Bacteriol. 1988;170:5837–47.

25. Slater S, Gallaher T, Dennis D. Production of poly-(3-hydroxybutyrate-co-3-hydroxyvalerate) in a recombinant Escherichia coli strain. Appl Environ Microbiol. 1992;58:1089–94.

26. Koller M, Braunegg G. Potential and Prospects of Continuous Polyhydroxyalkanoate (PHA) Production. Bioengineering [Internet]. 2015 [cited 2015 Sep 8];2:94–121. Available from: http://www.mdpi.com/2306-5354/2/2/94/

27. Madison LL, Huisman GW. Metabolic engineering of poly(3-hydroxyalkanoates): from DNA to plastic. Microbiol Mol Biol Rev [Internet]. 1999;63:21–53. Available from: http://www.ncbi.nlm.nih.gov/pubmed/10066830%0Ahttp://www.pubmedcentral.nih.gov/articlerender.fcgi?artid=PMC98956

28. Shimizu K. Regulation Systems of Bacteria such as Escherichia coli in Response to Nutrient Limitation and Environmental Stresses. Metabolites [Internet]. 2013 [cited 2015 Jul 30];4:1–35. Available from: http://www.pubmedcentral.nih.gov/articlerender.fcgi?artid=4018673&tool=pmcentrez&rendertype=abstract

29. Lee IY, Kim MK, Park YH, Lee- SY. Regulatory Effects of Cellular Nicotinamide Recombinant Escherichia coli. Biotechnol Bioeng. 1996;52:707–12.

30. Peña C, Castillo T, García A, Millán M, Segura D. Biotechnological strategies to improve production of microbial poly-(3-hydroxybutyrate): A review of recent research work. Microb Biotechnol. 2014;7:278–93.

31. Tyo KEJ, Fischer CR, Simeon F, Stephanopoulos G. Analysis of polyhydroxybutyrate flux

limitations by systematic genetic and metabolic perturbations. Metab Eng [Internet]. Elsevier; 2010 [cited 2014 Nov 19];12:187–95. Available from: http://www.ncbi.nlm.nih.gov/pubmed/19879956

32. Wang F, Lee S. Poly (3-Hydroxybutyrate) Production with High Productivity and High Polymer Content by a Fed-Batch Culture of Alcaligenes latus under Nitrogen Limitation. Appl Environ Microbiol [Internet]. 1997 [cited 2015 Mar 30];63:3703–6. Available from: http://aem.asm.org/content/63/9/3703.short

33. Mahishi LH, Tripathi G, Rawal SK. Poly(3-hydroxybutyrate) (PHB) synthesis by recombinant Escherichia coli harbouring Streptomyces aureofaciens PHB biosynthesis genes: effect of various carbon and nitrogen sources. Microbiol Res. 2003;158:19–27.

34. Taymaz-Nikerel H. Quantitative analysis of relationships between fluxome and metabolome in Escherichia coli. TU Delft - Dep. Biotechnol. - Bioprocess Technol. Gr. 2010.

35. Yamane T. Yield of Poly-0(-)-3-Hydrox ybut yrate from Various Carbon Sources: A Theoretical Study. 1993;41:165–70.

36. Kim BS. Production of poly (3-hydroxybutyrate) from inexpensive substrates. 2000;27:774–7.

37. Silva LF, Taciro MK, Michelin Ramos ME, Carter JM, Pradella JGC, Gomez JGC. Poly-3-hydroxybutyrate (P3HB) production by bacteria from xylose, glucose and sugarcane bagasse hydrolysate. J Ind Microbiol Biotechnol [Internet]. 2004 [cited 2015 May 20];31:245–54. Available from: http://www.ncbi.nlm.nih.gov/pubmed/15221664

38. Sekar K, Tyo KEJ. Regulatory effects on central carbon metabolism from poly-3-hydroxybutryate synthesis. Metab Eng [Internet]. Elsevier; 2015 [cited 2015 Jan 17];28:180–9. Available from: http://linkinghub.elsevier.com/retrieve/pii/S1096717615000051

39. Magdouli S, Brar SK, Blais JF, Tyagi RD. How to direct the fatty acid biosynthesis towards polyhydroxyalkanoates production? Biomass and Bioenergy [Internet]. Elsevier Ltd; 2015;74:268–79. Available from: http://dx.doi.org/10.1016/j.biombioe.2014.12.017

40. Haywood GW, Anderson AJ, Chu L, Dawes EA. The role of NADH- and NADPH-linked acetoacetyl-CoA reductases in the poly-3-hydroxybutyrate synthesizing organism Alcaligenes eutrophus. FEMS Microbiol Lett. 1988;52:259–64.

41. Chemler J a, Fowler ZL, McHugh KP, Koffas M a G. Improving NADPH availability for natural product biosynthesis in Escherichia coli by metabolic engineering. Metab Eng [Internet]. Elsevier; 2010 [cited 2015 Mar 30];12:96–104. Available from: http://www.ncbi.nlm.nih.gov/pubmed/19628048

42. Johannes TW, Woodyer RD, Zhao H. Efficient Regeneration of NADPH Using an Engineered Phosphite Dehydrogenase. 2007;96:18–26.

43. Walton AZ, Stewart JD. Understanding and improving NADPH-dependent reactions by nongrowing Escherichia coli cells. Biotechnol Prog. 2004;20:403–11.

44. Martínez I, Zhu J, Lin H, Bennett GN, San K-Y. Replacing Escherichia coli NAD-dependent glyceraldehyde 3-phosphate dehydrogenase (GAPDH) with a NADP-dependent enzyme from Clostridium acetobutylicum facilitates NADPH dependent pathways. Metab Eng [Internet]. 2008 [cited 2015 Mar 30];10:352–9. Available from: http://www.ncbi.nlm.nih.gov/pubmed/18852061

45. Vemuri GN, Altman E, Sangurdekar DP, Khodursky a B, Eiteman M a. Overflow Metabolism in Escherichia coli during Steady-State Growth : Transcriptional Regulation and Effect of the Redox Ratio Overflow Metabolism in Escherichia coli during Steady-State Growth : Transcriptional Regulation and Effect of the Redox Ratio †. Appl Environ Microbiol [Internet]. 2006;72:3653–61. Available from: http://www.ncbi.nlm.nih.gov/pmc/articles/PMC1472329/pdf/2763-05.pdf

46. van Hoek MJA, Merks RMH. Redox balance is key to explaining full vs. partial switching to low-yield metabolism. BMC Syst Biol [Internet]. BioMed Central Ltd; 2012;6:22. Available from: http://www.biomedcentral.com/1752-0509/6/22

47. Spaans SK, Weusthuis RA, van der Oost J, Kengen SWM. NADPH-generating systems in bacteria and archaea. Front Microbiol. 2015;6:1–27.

48. Pietrocola F, Galluzzi L, Bravo-San Pedro JM, Madeo F, Kroemer G. Acetyl coenzyme A: A central metabolite and second messenger. Cell Metab. 2015;21:805–21.

49. Bruinenberg PM, Van Dijken JP, Scheffers WA. A theoretical analysis of NADPH production and consumption in yeasts. J Gen Microbiol. 1983;129:953–64.

50. Contributors. W. Nicotinamide adenine dinucleotide. 2021.

51. Contributors. W. Nicotinamide adenine dinucleotide phosphate. 2021, January 11.

52. Deamer DW. The first living systems: a bioenergetic perspective. Microbiol Mol Biol Rev [Internet]. 1997;61:239–61. Available from: http://www.ncbi.nlm.nih.gov/pubmed/9184012%0Ahttp://www.pubmedcentral.nih.gov/articlerender.fcgi?artid=PMC232609

53. Lázló N. Csonka and Dan G. Fraenkel. Pathways of NADPH Formation in Escherichia coli. J Biol Chem. 1976;252:3382–91.

54. Sauer U, Canonaco F, Heri S, Perrenoud A, Fischer E. The soluble and membrane-bound transhydrogenases UdhA and PntAB have divergent functions in NADPH metabolism of Escherichia coli. J Biol Chem [Internet]. 2004 [cited 2014 Nov 19];279:6613–9. Available from: http://www.ncbi.nlm.nih.gov/pubmed/14660605

55. Edwards JS, Palsson BO. The Escherichia coli MG1655 in silico metabolic genotype: Its definition, characteristics, and capabilities. Proc Natl Acad Sci U S A [Internet]. 2000 [cited 2015 Mar 30];97:5528–33. Available from: http://www.pnas.org/content/97/10/5528.short

56. Noor E, Bar-Even A, Flamholz A, Lubling Y, Davidi D, Milo R. An integrated open framework for thermodynamics of reactions that combines accuracy and coverage. Bioinformatics. 2012;28:2037–44.

57. Sauer U, Eikmanns BJ. The PEP-pyruvate-oxaloacetate node as the switch point for carbon flux distribution in bacteria. FEMS Microbiol. Rev. 2005. p. 765–94.

58. Nanchen A, Schicker A, Sauer U. Nonlinear dependency of intracellular fluxes on growth rate in miniaturized continuous cultures of Escherichia coli. Appl Environ Microbiol. 2006;72:1164–72.

59. Lim SJ, Jung YM, Shin HD, Lee YH. Amplification of the NADPH-related genes zwf and gnd for the oddball biosynthesis of PHB in an E. coli transformant harboring a cloned phbCAB operon. J Biosci Bioeng. 2002;93:543–9.

60. Sánchez AM, Andrews J, Hussein I, Bennett GN, San KY. Effect of overexpression of a soluble pyridine nucleotide transhydrogenase (UdhA) on the production of poly(3-hydroxybutyrate) in Escherichia coli. Biotechnol Prog. 2006;22:420–5.

61. Cho HS, Seo SW, Kim YM, Jung GY, Park JM. Engineering glyceraldehyde-3-phosphate dehydrogenase for switching control of glycolysis in escherichia coli. Biotechnol Bioeng. 2012;109:2612–9.

62. Seidler NW. GAPDH: Biological Properties and Diversity. Dordrecht: Springer Netherlands; 2013 [cited 2014 Nov 19];985. Available from: http://link.springer.com/10.1007/978-94-007-4716-6

63. Ralser M, Wamelink MM, Kowald A, Gerisch B, Heeren G, Struys EA, et al. Dynamic rerouting of the carbohydrate flux is key to counteracting oxidative stress. J Biol. 2007;6.

64. Centeno-Leija S, Huerta-Beristain G, Giles-Gómez M, Bolivar F, Gosset G, Martinez A. Improving poly-3-hydroxybutyrate production in Escherichia coli by combining the increase in the NADPH pool and acetyl-CoA availability. Antonie Van Leeuwenhoek [Internet]. 2014;105:687–96. Available from: http://link.springer.com/10.1007/s10482-014-0124-5

65. Hanson RL, Rose C, Hanson RL, Rose C. Effects of an insertion mutation in a locus affecting pyridine nucleotide transhydrogenase (pnt :: Tn5) on the growth of Escherichia coli . Effects of an Insertion Mutation in a Locus Affecting Pyridine Nucleotide Transhydrogenase (pnt : : Tn5) on the. 1980;141:401–4.

66. Shimizu MMK· K. Fermentation characteristics and protein expression patterns in a recombinant Escherichia coli mutant lacking phosphoglucose isomerase for poly (3-hydroxybutyrate) production. 2003;244–55.

67. Haywood GW, Anderson AJ, Dawes EA. The importance of PHB-synthase substrate specificity in polyhydroxyalkanoate synthesis by Alcaligenes eutrophus. FEMS Microbiol Lett. 1989;57:1–6.

68. Haywood GW, Anderson AJ, Chu L, Dawes EA. Characterization of two 3-ketothiolases possessing differing substrate specificities in the polyhydroxyalkanoate synthesizing organism Alcaligenes eutrophus. FEMS Microbiol Lett. 1988;52:91–6.

69. Cueto-Rojas HF, van Maris AJA, Wahl SA, Heijnen JJ. Thermodynamics-based design of microbial cell factories for anaerobic product formation. Trends Biotechnol [Internet]. Elsevier Ltd; 2015;33:534–46. Available from: http://dx.doi.org/10.1016/j.tibtech.2015.06.010

70. Noor E, Bar-Even A, Flamholz A, Reznik E, Liebermeister W, Milo R. Pathway Thermodynamics Highlights Kinetic Obstacles in Central Metabolism. PLoS Comput Biol. 2014;10.

71. Zamboni N, Kümmel A, Heinemann M. anNET: A tool for network-embedded thermodynamic analysis of quantitative metabolome data. BMC Bioinformatics. 2008;9:1–11.

Chapter 2.

Microbial synthesis of polyhydroxybutyrate from glucose: a thermodynamic study of different synthesis routes

Mariana I. Velasco Alvarez, Marco Valentim Becker, Karel Olavarria Gamez, Mark van Loosdrecht and S. Aljoscha Wahl

Abstract

Genetically engineered strains have been and are widely used to produce bio-based products. For metabolic engineering, several factors must be considered, including yield but also production rate, which is strongly determined by the available thermodynamic driving force. In this study, different pathways for the formation of polyhydroxybutyrate (PHB) have been compared. The glycolytic pathway stoichiometries considered were: (1) Embden-Meyerhof-Parnas pathway, (2) Entner–Doudoroff pathway, and (3) modified Embden-Meyerhof-Parnas pathway (mEMP). The latter with the substitution of the NAD-dependent glyceraldehyde-3-phosphate dehydrogenase (E.C. 1.2.1.12) with an NADP preferring variant (EC 1.2.1.9) (*gapA*::*gapN*). By a thermodynamic analysis the impact of the pathway stoichiometry on the PHB synthesis from glucose, was determined. The approach considered all the available thermodynamic driving forces for each step. Especially a thermodynamic optimization approach, called Max-min Driving Force (MDF) was applied to identify critical reaction steps and metabolites. The impact of precursors, intermediates, and co-factor ratios was further studied using constraint variations. For all pathways, the formation of acetoacetyl-CoA was a critical step ($\Delta rG'^{\circ}$ = 26 kJ/mol). Nevertheless, the mEMP glycolytic stoichiometry (*gapA*::*gapN* substitution) allowed a higher substrate to product ratio (AcCoA/CoA) which results in a higher flux towards acetoacetyl-CoA. The NADPH dependent reduction of acetoacetyl-CoaA showed a minor effect on the available MDF total pathway driving force.

The importance of thermodynamic analysis to unravel metabolic constraints is illustrated in this study. It disclosed not only the (complex) interconnectivity of different pathway constraints but forms also as a guide to metabolic engineering approaches.

1. Introduction

The design of microbial cell factories has mostly relied on stoichiometric calculations, like flux-balance analysis which include constraints on reaction directions. While very successful in generating a systematic understanding of the (complex) metabolic networks, the approach has limited predictive accuracy with respect to the kinetic feasibility of pathway stoichiometries. Kinetic properties, especially the maximal conversion rate can be linked to thermodynamic properties [1].

Therefore, including thermodynamics to analyze and design metabolic pathways is of interest to improve metabolic routes for (bulk) products [2–4]. Different algorithms have been developed and are available [3,5]. Successful examples of thermodynamics based insights and applications are included in the production of 1,3 propanediol, a non-natural product [6,7].

Such analysis and optimization approaches require thermodynamic data (Δ_fG^0 of formation) for each pathway intermediate. Partly, these values are available from experimental works like Alberty et al. [8]. When no experimental data is available, the Δ_fG^0 can be estimated using the so called group contribution method and its refinements [9–11].

One interesting organic compound to (re)investigate is polyhydroxybutyrate (PHB), which can be used to replace fossil fuel-based plastic. PHB belongs to the family of polyhydroxyalkanoates (PHA), and has properties for different application purposes like films, medical utilities or plastic-like materials [12–14]. Microbial production of this polymer was first reported by Lemoigne and it was characterized as a carbon-reserve for some bacteria [15–18] see **Figure 1**. Since its discovery, different approaches have been applied to produce PHB and improve the yields. In natural producers, non-carbon nutrient limitation has been the most exploited strategy to increase PHB synthesis. In this case, bacteria such as *Cupriavidus necator* (earlier known as *Alcaligenes eutrophus* and *Ralstonia eutropha*) and *Pseudomonas* species [19] have been used.

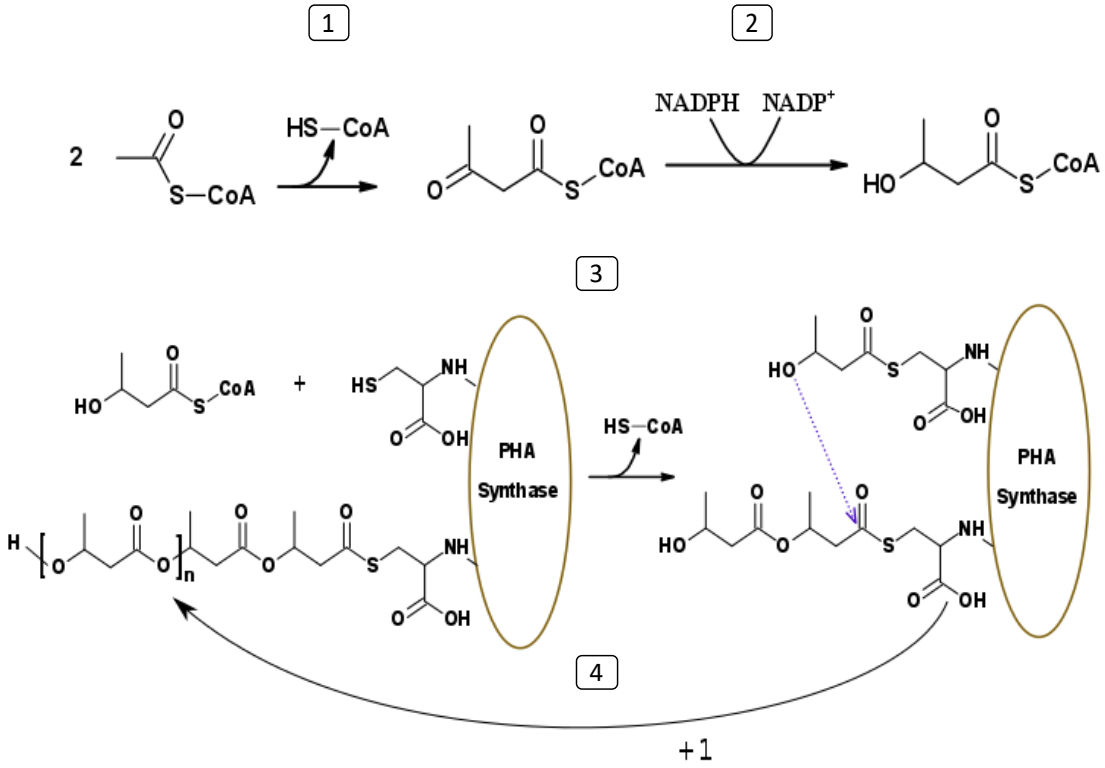

Figure 1. Polyhydroxybutyrate production pathway. (1) From two acetyl-CoA to acetoacetyl-CoA, (2) reduction to 3-hydroxybutyryl-CoA and the polymerization step to PHB, including (3) binding of hydroxybutyryl-CoA to a cysteine residual of the protein PHA synthase, and (4) transfer of the monomer to the polymer chain, leading to an increase in PHB chain length.

Next to the production using natural hosts, there are many studies that increased PHB production using engineered strains, especially *Escherichia coli*. The two main metabolic engineering strategies include: (1) increasing the availability of cofactors and/or precursors: NADPH and/or acetyl-CoA for PHB synthesis and/or (2) increasing the production pathway capacity by overexpression of the respective genes [20–23]. A summary of the most prominent strategies can be found in **Table 1**. The studies include hypotheses about the bottlenecks for PHB production which include: a) Kinetic limitations due to insufficient enzymatic capacity or affinity [24]. b) Competition of cellular pathways for the intermediates acetyl-CoA as well as NADPH resulting in an insufficient availability of these precursors [25–27]). c) Regulation of the polymerization step by possible allosteric regulations [21,23].

Here we focus on the supply of acetyl-CoA and NADPH, both resources required for biosynthesis and PHB production. The supply of both compounds can be engineered by modifications in the glycolytic reactions. Remarkably, the use of one or another glycolytic pathway does not only change the relative amount of acetyl-CoA and NAD(P)H generated but also the free energy conserved as ATP, adding another link between biomass and product formation. Clearly, a change in ATP production additionally has consequences for the thermodynamic driving forces to generate the precursors for PHB accumulation. Surprisingly, the thermodynamic consequences of different glycolytic stoichiometries for the production of PHB have not been reported so far. The most common glycolytic pathways include: 1) the Embden-Meyerhof-Parnas Pathway (EMP), 2) a modified EMP (mEMP), and 3) the Entner–Doudoroff pathway (EDP), which will be compared here using thermodynamic analysis and optimization approaches.

Table 1. Review of selected studies on PHB production that focus on the enhancement of Acetyl-CoA, NADPH, both compounds, or in *Escherichia coli*, *Cupriavidus necator*, and *Saccharomyces cerevisiae*.

Cofactor	Organism	Substrate / limitation	Strategy (main phenotype)	Reference
	E. coli	20 g/L Glucose/ Xylose/ Glycerol 3 mN/L N/C = 0.03 (but also yeast extract added)	An engineered strain using Serine-Deamination (SD) pathway, the Entner-Doudoroff (ED) pathway, and the pyruvate dehydrogenase (PDH) complex led to an increase in acetyl-CoA for PHB accumulation.	[29]
	E. coli	Carbon excess with glucose	The synthesis of PHB is sensible to acetyl-CoA/ CoA ratios, while the ratios of NADPH/NADP showed no significant effect.	[30]
NADPH	*E. coli*	10 g/L glucose N-limited N/C=0.19	The replacement of the native NAD^+-GAPDH activity by the heterologous $NADP^+$-GAPDH activity increased the NADPH/NADH ratio 1.7-fold in recombinant *E. coli* that favored PHB synthesis.	[27]
	E. coli	30 g/L glucose N-limited N/C= 0.014 (5g/L yeast extract)	The overexpression of NAD kinase in *E. coli* was used to enhance the PHB synthesis.	[31]

	C. necator	10-40 g/L glucose, N-excess	PHB productivity increased through feeding with NH_4Cl.	[32]
	E. coli	20 g/L glucose N-limited (not specified)	The soluble pyridine nucleotide transhydrogenase (UdhA) was used to increase NADPH availability and therefore the productivity of PHB.	[33]
	E. coli	review	The enhancing effect of more NADPH is more crucial in recombinant *E. coli* than in natural producers.	[15]
	E. coli & C. necator	20 g/L glucose unknown*	The $NADPH/NADP^+$ ratio was found to be higher when PHB was produced and therefore crucial for PHB synthesis.	[34]
	E. coli	LB medium	Anaerobic growth conditions favored a high $NADH/NAD^+$ ratio, that directly increased the $NADPH/NADP^+$ ratio through the transhydrogenases activity.	[35]
	E. coli	LB medium	*E. coli* mutant lacking phosphoglucose isomerase (*pgi)* led to the overproduction of NADPH which favored PHB production.	[36]
AcCoA & NADPH	*E. coli*	30g/L glycerol	Micro-aerobic fed- batch cultures in recombinant *E. coli arcA* improved PHB production with a reduced production of reactive oxidative species and the use of glycerol as a cheaper alternative to glucose.	[37]
	E. coli	20 g/L glucose +LB	Accumulation of PHB in *E. coli* promotes the expression levels of several enzymes of glycolysis (Fba, TpiA, GpmA, and Eda), to provide more acetyl-CoA and NADPH.	[38]
	E. coli	20 g/L glucose +LB	Redirecting the carbon through the pentose phosphate pathway increased PHB accumulation.	[22]
	S. cerevisiae	20 g/L glucose	Two strategies were tested: (1) NADPH was increased through GAPN dependent enzyme and (2) acetyl-CoA was enhanced through phosphoketolase pathway. The last one resulted in the highest PHB production.	[28]
Other	*E. coli*	30 g/L glucose N-limited	The PHB synthesis is primarily regulated by the expression levels of the product pathway and not by the availability of precursors.	[39]
	E. coli	30 g/L glucose	Under nitrogen or carbon limited conditions, PHB flux is limited by gene copy number of the product pathway.	[24]

*not reported in the materials and methods

2. Theoretical Background and Methods

The Gibbs free energy of a reaction is calculated from the Gibbs free energy of formation of the substrates and products ($\Delta_rG'°$ at standard conditions that are pH 7 at 25 °C) and a correction for the specific conditions (see Eq. (1), with *R*, the ideal gas constant and *T*, the temperature, and the Q_r the reaction quotient [4,40,41]).

$$\Delta_r G^{'} = \Delta_r G^{'\circ} + RT\ln(Q_r) \ldots\ldots\ldots\ldots\ldots\ldots\ldots\ldots\ldots\ldots\ldots\ldots\ldots(1)$$

For many intracellular metabolites the Gibbs free energy of formation has not yet been experimentally determined. For these compounds, the so called group contribution approach, based on functional groups present in the compound [8], was used. This calculation is also implemented in the software tool Equilibrator® [42], which was used for most calculations.

Max-min Driving Force (MDF) optimization for PHB formation

The MDF of a pathway represents the optimal thermodynamic feasibility at physiological conditions (pH 7, 25 °C (298.15 K), pressure is 1 bar, and an ionic strength of 0.1 M) [3]. Especially, the MDF value is obtained from an optimization of the pathway intermediate concentration where the bottleneck reaction(s) driving force is maximized [3]. Provided that the MDF (= min(-Δ_rG')) is positive, the pathway is feasible. The higher the MDF value, the higher fluxes can be expected. Here, the putative driving forces for the PHB formation reactions were calculated for three different pathways: EMP, mEMP and EDP (see **Figure 2)**.

Flux force efficacy for PHB pathway

The flux force efficacy represents a measure for the fraction of a pathway to carry forward and backward flux. The bigger the percentage, the less possible is a backward flux. The Δ_rG' is defined as the driving force and is the value obtained from the pathway analysis (MDF optimization) [3].

$$Flux\ florce\ efficacy = \frac{e^{-\frac{\Delta rG\prime}{RT}} - 1}{e^{-\frac{\Delta rG\prime}{RT}} + 1}$$

3. Results

Three pathways were analysed for engineered *E. coli* PHB production strains: (A) The Embden-Meyerhof-Parnas Pathway (EMP), (B) a modified EMP pathway with a substitution of *gapA* (NAD^+ dependent GAPDH) with *gapN* ($NADP^+$ dependent GAPDH), in the following called mEMP, and (C) the Entner–Doudoroff pathway (EDP) see **Figure 2**.

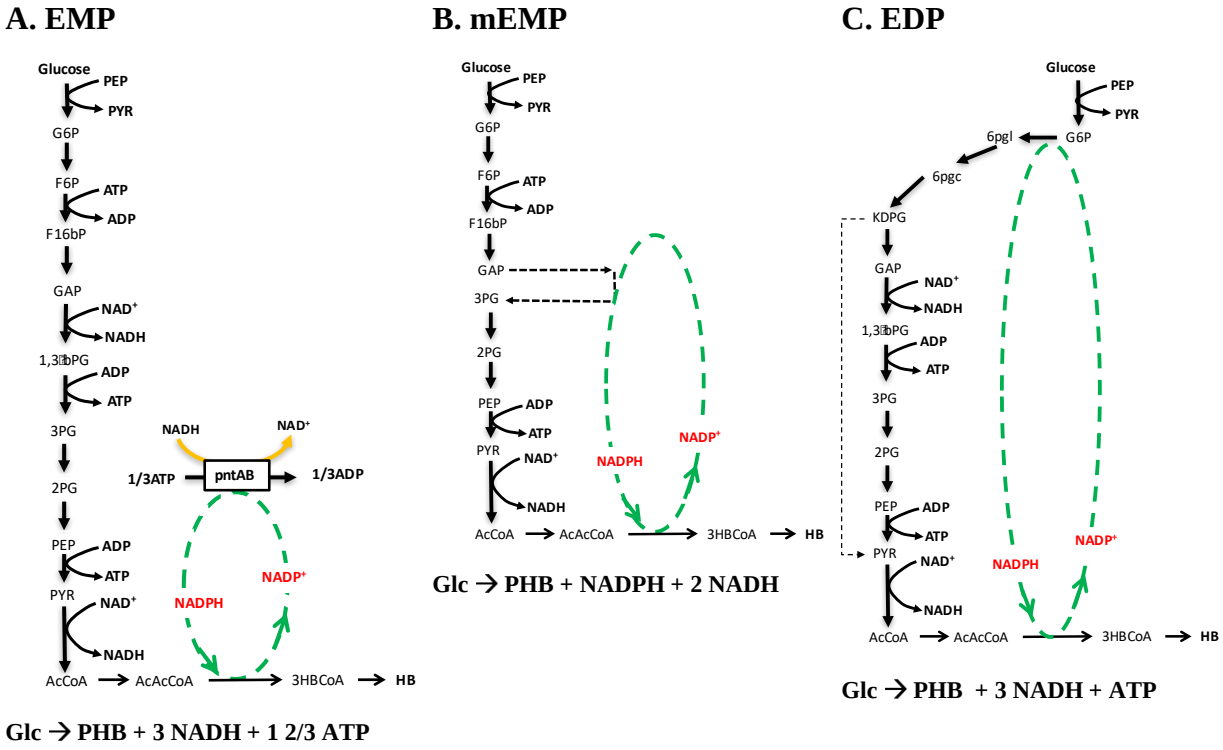

Figure 2. The analyzed metabolic pathway stoichiometries for glucose conversion to hydroxybutyrate. A: EMP, B: mEMP and C: EDP. Glucose is imported by PTS (phosphotransferase system). In the case of EMP, $NADP^+$ is assumed to be regenerated to NADPH using electrons from NADH via the transmembrane transhydrogenase pntAB. The NADPH generating and consuming reactions are highlighted in green.

Each glycolytic pathway generates a different overall stoichiometry with respect to ATP and NAD(P)H (see **Figure 2**) generation. Particularly, the catabolism of glucose to pyruvate results in: For EMP: 2 moles of ATP from substrate level phosphorylation, no (direct) NADPH regeneration, but this is obtained from NADH by the membrane bound transhydrogenase (PntAB). For mEMP: The modified EMP pathway does not generate ATP from substrate level phosphorylation. NADPH is directly generated from glycolysis

with 2 moles of NADPH instead of 2 NADH. For EDP, one mole of ATP is formed by substrate level phosphorylation and one mole of NADPH is generated in the oxidative pentose phosphate pathway, one NADH from GAPDH. These pathways together with PHB synthesis are analyzed with respect to the thermodynamic maximal, minimal driving forces (MDF).

Pathway analysis to PHB

The steps involved in the PHB pathway are described in **Figure 2**. The first reaction involves two molecules of acetyl-CoA to form acetoacetyl-CoA releasing one CoA-SH. This reaction is well known and the $\Delta_rG'°$ has been determined as 26.1 kJ/mol. Such high positive $\Delta G'°$ indicates that a high concentration of acetyl-CoA relative to acetoacetyl-CoA and CoA is required for the pathway direction. At least a ratio of around 2:1 for acetyl-CoA:CoA is required for the reaction to be in equilibrium, when assuming a concentration of acetoacetyl-CoA of 0.108 µM ($0 = 26.1 + RT\,ln\frac{1.08 \cdot 10^{-7} \cdot 0.001}{0.002^2}$). The second step is a reduction reaction, i.e. acetoacetyl-CoA is reduced by NADPH to generate the intermediate 3-hydroxybutyryl-CoA. This reaction is thermodynamically favorable with a $\Delta_rG'°$ of -19.4 kJ/mol.

As shown in Figure 2, the polymerization of 3-hydroxybutyryl-CoA is a two-step reaction. The monomer is first bound to a cysteine of the PHA synthase and then moved to a second binding site within the polymer chain, extending the chain length. This step is basically a re-arrangement of the molecules and no new functional groups are formed. The $\Delta_rG'°$ is close to zero and therefore neglected here [12].

Different approaches were used to obtain the Gibbs energy of formation of a monomer inside the P(3-HB) polymer: a) the group contribution [9] approach and b) using the measured enthalpy of combustion [43] (see **Table 2)**. Values between -278.2 and -286.6 kJ/mol were obtained. In the following calculations, a $\Delta_fG'°$ = -286.6 kJ/mol was used.

Table 2. Comparison of Gibbs free energy of formation of a monomer of PHB as obtained through various methods.

	Group contribution		**Measured**
	$\Delta_f G°$ (kJ/mol)	$\Delta_f G°$(kJ/mol)	$\Delta_f G°$ (kJ/mol)
	Mavrovouniotis [9]	Jankowski [10]	Enthalpy of combustion [43]
(R)-3-Hydroxybutyrate $C_4H_6O_2$	-278.2	-286.6	-280.3*

*The value was obtained from the combustion of a crystalline form of 3-HB, MW=86g/mol.

Table 3. Comparison of the Gibbs free energies at physiological conditions (ionic strength= 0.1 M, pH= 7, T= 25 °C) of reaction (**$\Delta_r G'^m$**) of PHB from glucose through different glycolytic pathways, no optimization performed and without the oxidization of NAD(P)H. Flux Force Efficacy (FFE) and Min-max Driving Force (MDF) for the optimized concentrations of the reactions in the pathway are given (these include respiration in all cases). These values were obtained using the constraints shown in Table 4, A1.

Pathway	**$\Delta_r G'^m$ (kJ/mol)**	**MDF (kJ/mol)**	**FFE (%)**	**Reaction equation**
EMP	-280.7**	7.87	91.98	$C_6H_{12}O_6 + (C_4H_6O_2)_n \rightarrow$ $1.66\ ATP + 3\ NADH + (C_4H_6O_2)_{n+1} + 2CO_2$
mEMP	-450.7**	11.79	98.29	$C_6H_{12}O_6 + (C_4H_6O_2)_n \rightarrow$ $2NADH + NADPH + (C_4H_6O_2)_{n+1} + 2CO_2$
EDP	-365.7**	11.19	97.83	$C_6H_{12}O_6 + (C_4H_6O_2)_n \rightarrow$ $ATP + 3\ NADH + (C_4H_6O_2)_{n+1} + 2CO_2$
with ETC*	-1781.2			$C_6H_{12}O_6 + (C_4H_6O_2)_n + 1.5O_2 \rightarrow$ $(C_4H_6O_2)_{n+1} + 2CO_2$

*A P/O ratio of 2 was considered in all pathways for the electron transport chain (ETC) ATP generation, the ATP formed was then used for maintenance. EMP: NADPH is obtained from NADH via membrane transhydrogenase (PntAB), mEMP: Surplus NADPH is consumed by the ETC.

**The analysis was performed considering no oxygen present and no external electron acceptor present.

Comparing the different pathway stoichiometries, it can be observed that the higher the ATP yield, the lower the released free Gibbs energy. With no ATP from substrate level phosphorylation, the mEMP has the highest available thermodynamic driving force (MDF).

It is also interesting to note that EDP and mEMP have fifteen enzymatic reaction steps, compared to EMP that has seventeen (see Annex 2, Table B1).

Clearly, *in vivo*, ATP generation is required for several processes, including growth and maintenance. In this study, was not considered biomass formation in order to simplify the sinks of NADPH. Nevertheless, the impact of the reduced ATP gain will be limited because there is an electron surplus that can be used in oxidative phosphorylation, delivering sufficient ATP surplus (6 ATP per glucose for mEMP). This surplus ATP is assumed to be balanced (i.e. consumed) by maintenance processes. Consequently, the overall extracellular reaction equation as well as $\Delta_r G'^m$ becomes the same for all pathway stoichiometries (see **Table 3**). On the other hand, with an overall higher available thermodynamic driving force for the product pathway reactions (and less for maintenance) a more beneficial distribution of the Gibbs free energy over the single reactions can be obtained. This is evaluated by optimization of the single reaction thermodynamic driving forces by varying the intracellular concentrations. The limiting step(s) are the ones with the lowest driving forces, after the maximization of the lowest driving force, which is appointed as MDF.

Furthermore, the obtained MDF for every pathway was used to calculate the FFE (Flux Force Efficacy) see **Table 3**. The mEMP and EDP have a higher FFE than EMP. In the case of mEMP and EDP the thermodynamic efficiency is lower since there is more Gibbs free energy dissipated. The EMP pathway has, on the contrary, a lower flux force efficacy and a higher thermodynamic efficiency.

Determining pathway bottlenecks: EMP, mEMP and EDP

Regardless of the used glycolytic stoichiometry, the reaction with the lowest driving force was acetyl-CoA thiolase, 2 acetyl-CoA → acetoacetyl-CoA + CoA (PhaA, see Annex 2, Table B1) but at different values for each pathway. To further study this limitation, a sensitivity analysis was performed through varying the acetyl-CoA/CoA ratio as well as NADPH/$NADP^+$ and the intermediate concentration acetoacetyl-CoA.

Firstly, analyzing the effect of the AcAcCoA concentration, see **Figure 3**, **A1,** and secondly the effect of NADH/NAD^+ ratio, see **Figure 4**, **B1,** and the effect of NADPH/$NADP^+$ ratio, see Figure **4**, **B2.** The boundaries considered for the analysis are displayed in **Table 4** according to the physiological constrains found in *E. coli* cells [44].

Table 4. Values used in the sensitivity analysis of AcCoA/CoA ratios from 1 to $1*10^4$. The values of the boundaries (lower and upper bound) are in M, the studies performed in B1 and B2 were assessed at a fixed NAD(P)H/NAD(P) ratio. **A1**: The analysis studied the effect of different AcCoA/CoA ratios at a fixed AcAcCoA, **B1**: The analysis studied the effect of a fixed NADH/NAD^+ ratio of 3.2 with the same scenario as A1, **B2**: The analysis studied the effect of a fixed NADPH/$NADP^+$ ratio of 57, having the scenario of A1.

Analysis	AcCoA/CoA	AcAcCoA	NADH/NAD	NADPH/NADP
A1	**Ratio range**	**Fixed concentration**	**Boundaries**	**Boundaries**
	1 - 10000	$1.08\ 10^{-7}$	10^{-6} - 0.02	10^{-6} - 0.02
B1	**Ratio range**	**Fixed concentration**	**Fixed ratio**	**Boundaries**
	1 - 10000	$1.08\ 10^{-7}$	3.2*	10^{-6} - 0.02
B2	**Ratio range**	**Fixed concentration**	**Boundaries**	**Fixed ratio**
	1 - 10000	$1.08\ 10^{-7}$	10^{-6} - 0.02	57*

The boundaries of AcCoA/CoA were based on the values reported by Wegen et al. [30] and Bennett et al [45]. The boundaries of the NAD(P)H and NAD(P) were taken from Henry et al. [46].

*Data taken from Bennett et al. [45] from *E. coli* in growing conditions using glucose as substrate.

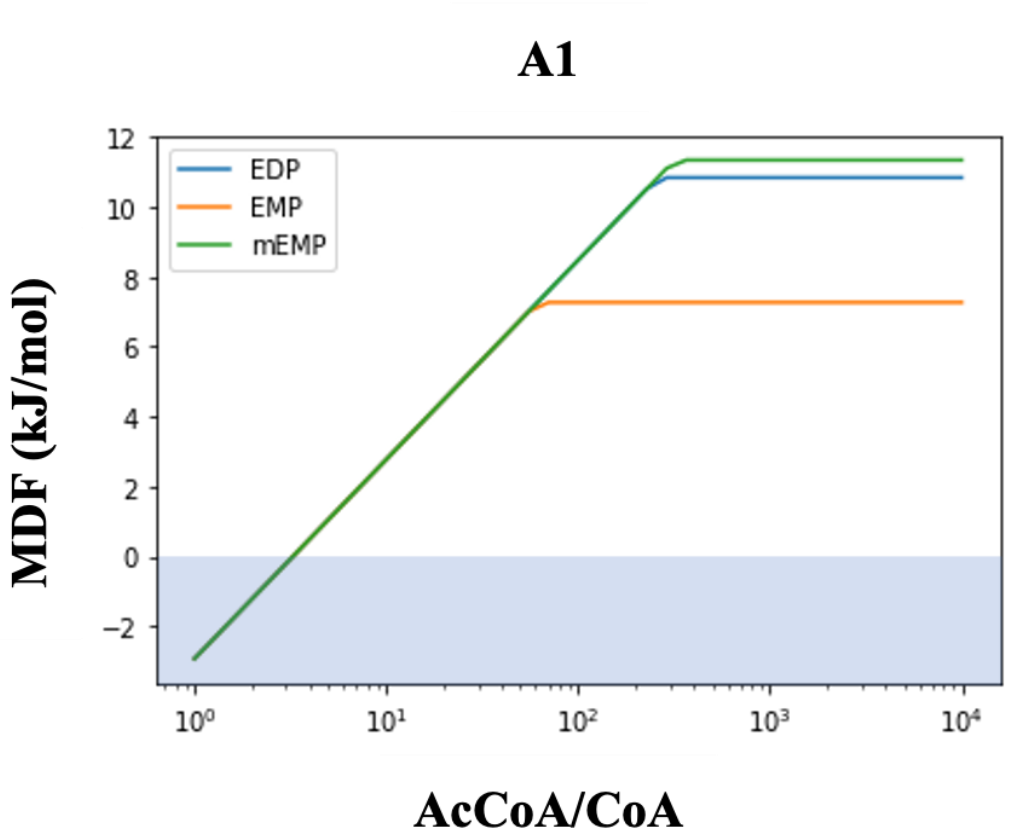

Figure 3. Sensitivity analysis of the obtained MDF as a function of AcCoA/CoA ratios for the different pathways: EMP, mEMP and EDP. The shadowed part is representing the values where the MDF < 0 and therefore the pathways remain unfeasible.

At a AcCoA/CoA ratio higher than 2:1 the MDF becomes feasible (Figure 3). The MDF achieved in the pathways are EMP 7.87 kJ/mol, EDP 11.19 kJ/mol, and for mEMP 11.79 kJ/mol. These MDF were reached at a ratio $<10^3$ which suggests that EDP and mEMP allow a higher driving force, which could indirectly improve the flux towards PHB.

To analyze the impact of the redox co-factor ratios, the calculation of scenario as A1 fixed $NADH/NAD^+$ and $NADPH/NADP^+$ ratios, named scenario B1 and B2 respectively (Table 4, Figure 4). The MDF optimization for B1 resulted in no production (unfeasible MDF < 0) for AcCoA/CoA ratios below 2, the same as in scenario A1. Above a ratio of 2, the EDP and mEMP pathways become feasible, while EMP remains unfeasible. This indicates the dependency of EMP on the $NADH/NAD^+$ ratio for a forward flux. The reaction of glyceraldehyde 3-phosphate (GAP) has a larger constraint in comparison to

acetoacetyl-CoA thiolase EDP and the pathway reaches a maximum MDF of 3.85 kJ/mol and mEMP 11.79 kJ/mol at a ratio of $1 \cdot 10^4$.

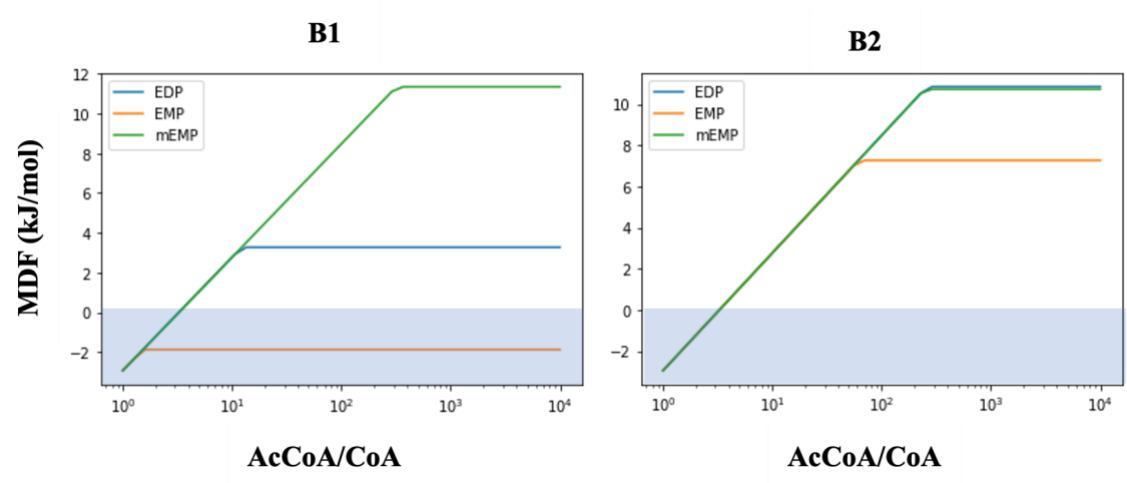

Figure 4. Sensitivity analysis of AcCoA/CoA ratios in the pathways: EMP, mEMP and EDP. B1: Analysis of the effect of AcCoA/CoA ratio with a fixed NADH/NAD$^+$ ratio of 3.2 and a fixed AcAcCoA concentration. B2: Analysis of the effect of AcCoA/CoA ratios with a fixed NADPH/NADP$^+$ ratio of 57 and fixed AcAcCoA concentration. The shadowed part represents the values where the MDF < 0 and therefore the pathways remain unfeasible.

In scenario B2 with fixed NADPH/NADP$^+$ ratio, the MDF follows the trend of scenario A1 (**Figure 4, vs Figure 3, A1**) until a AcCoA/CoA ratio of $1 \cdot 10^3$ is reached. The MDF for EMP reaches 7.87 kJ/mol, while for EDP and mEMP a similar value as in A1, MDF = 11.2 kJ/mol.

This suggests that the in-vivo observed NADPH/NADP$^+$ ratio of 57 would not limit the thermodynamic driving force for PHB production (i.e. the NADPH dependent reaction step from acetoacetyl-CoA to 3-hydroxybutyryl-CoA).

Limitations in the pathways

The acetyl-CoA thiolase (*phaA*) reaction, requires that the AcCoA/CoA ratios remain high so that the reaction is feasible and favor PHB flux.

However, it still should be highlighted that the optimization considered low CoA concentrations down to 10^{-5} M when the maximum MDF is reached, suggesting the relevance of low levels of CoA to favor PHB flux.

The modified EMP glycolysis (mEMP) increases the driving force and consequently, higher AcCoA/CoA ratios can be reached (less ΔG' conserved in ATP) compared to the canonical EMP (**Table 3**). Especially, the free Gibbs energy of the reaction from GAP (present in *E. coli* WT) compared to GAPN (present in *Streptococcus mutans*) is 10 times lower. At the same time, the K_m for GAPN is higher than for GAP, which suggests GAP to be thermodynamic controlled, while for GAPN allosteric mechanism may influence the metabolic flux.

gene	*gapA*
$\Delta_r G'$	-3.6 kJ/mol
$K_{M\ (NAD+)}$	0.045 – 0.19 mM

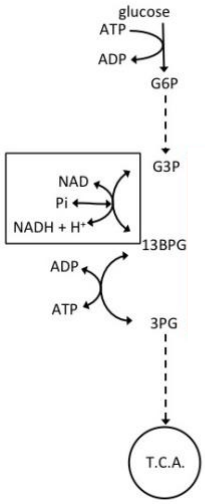

gene	*gapN*
$\Delta_r G'$	-37.8 kJ/mol
$K_{M\ (NADP+)}$	0.046 – 9.2 mM

Figure 5. Reaction(s) and kinetic parameters of GAP and GAPN.

4. Discussion

Thermodynamic metabolic pathway analysis was used to compare different glycolytic pathways (EMP, EDP, mEMP) coupled with PHB production. The results suggest that EDP and mEMP are beneficial to generate a maximal minimal driving force (MDF) and higher flux force efficacies (**Table 3**).

The higher flux force efficacy and MDF originate from a lower ATP yield and consequently more driving force towards higher AcCoA/CoA ratios. The influence of this ratio on the MDF was further analyzed by a parameter sweep, and a log-linear relation was found for a range between 0.1 and 100 for EMP and up to around 250 for mEMP and EDP. Above the ratio of 250, other metabolite (ratios) limit the reachable MDF. For all combinations a minimal AcCoA/CoA ratio of 2 is required to reach a positive MDF and PHB production.

The redox ratios of NADH and NADPH only affected the reachable driving force for specific scenarios. Although NADPH is a cofactor in the PHB pathway, the NADPH/$NADP^+$ ratio did not limit the obtained MDF for most scenarios. Constraining the NADH/NAD^+ ratio, the reachable MDF was reduced for all pathway stoichiometries, with EMP being most affected. Here GAPDH reaches a thermodynamic bottleneck, which is well documented in literature [2,47,48].

The analysis suggests that given a minimal ratio for NADH/NAD as found experimentally should be enough, pointing to AcCoA/CoA as main strategy to enhance PHB production. Several experimental studies focused on increasing acetyl-CoA availability like blocking competing pathways for acetyl-CoA consumption, especially acetate formation [39]. Counterintuitively, such deletion of genes showed no increase in PHB synthesis, suggesting interfering mechanisms. The authors speculated, that enzyme expression was affected by the knock-out of phosphate acetyltransferase and acetate kinase.

Wegen and collaborators [30] assessed the kinetic constraints of PHB formation, where they found that the PHB flux was sensitive to AcCoA/CoA ratios and less sensitive to NADPH/$NADP^+$ ratios. In their study, they observed that an AcCoA/CoA ratio above 4 presented a high response in the PHB flux and that an increase of this ratio was indeed favorable for the PHB flux.
In contrast to these findings, Keith and collaborators [24] reported that the limiting step was the acetoacetyl-CoA reductase, i.e. the reduction of acetoacetyl-CoA to 3-hydroxybutyryl-CoA using NADPH. Nevertheless, the same research group with Tyo and collaborators [39] reported another hypothesis, i.e. that the product pathway expression rather than the cofactor ratios limit PHB formation in *E. coli*. Additionally, under carbon limited conditions they observed excess of intracellular concentration of NADPH and no changes in the acetyl-CoA concentrations, which they interpreted as non-limiting for PHB synthesis. Unfortunately, this hypothesis could not be evaluated thermodynamically, as the respective counterparts, NADP+ and CoA were not measured.

5. Conclusion

The analysis of metabolic pathways through thermodynamics can support to a great extent the modifications and cultivation conditions of the strains studied. Here, the reaction acetoacetyl-CoA thiolase was identified as a crucial bottleneck in the production of PHB from glucose in *E. coli*. This bottleneck (and less the electron carrier aspect) should be carefully considered in future metabolic engineering for PHB production.

The detailed data obtained in the analysis can be found at 4TU ResearchData.
DOI: 10.4121/uuid:18eec7dd-f927-49c3-b917-3b1e5f236786

Acknowledgments

The author would like to acknowledge Sirous Ebrahimi and Stefan van den Berg for assisting the analysis. As well to Hugo-Federico Cueto Rojas for reviewing the chapter.

References

1. van der Meer R, Westerhoff H V., Van Dam K. Linear relation between rate and thermodynamic force in enzyme-catalyzed reactions. Biochim Biophys Acta - Bioenerg. 1980;591:488–93.

2. Kümmel A, Panke S, Heinemann M. Putative regulatory sites unraveled by network-embedded thermodynamic analysis of metabolome data. Mol Syst Biol. 2006;2:1–10.

3. Noor E, Bar-Even A, Flamholz A, Reznik E, Liebermeister W, Milo R. Pathway Thermodynamics Highlights Kinetic Obstacles in Central Metabolism. PLoS Comput Biol. 2014;10.

4. Cueto-Rojas HF, van Maris AJA, Wahl SA, Heijnen JJ. Thermodynamics-based design of microbial cell factories for anaerobic product formation. Trends Biotechnol [Internet]. Elsevier Ltd; 2015;33:534–46. Available from: http://dx.doi.org/10.1016/j.tibtech.2015.06.010

5. Zamboni N, Kümmel A, Heinemann M. anNET: A tool for network-embedded

thermodynamic analysis of quantitative metabolome data. BMC Bioinformatics. 2008;9:1–11.

6. Nakamura CE, Whited GM. Metabolic engineering for the microbial production of 1,3-propanediol. Curr Opin Biotechnol [Internet]. 2003 [cited 2015 Mar 28];14:454–9. Available from: http://linkinghub.elsevier.com/retrieve/pii/S0958166903001265

7. Frazão CJR, Trichez D, Serrano-Bataille H, Dagkesamanskaia A, Topham CM, Walther T, et al. Construction of a synthetic pathway for the production of 1,3-propanediol from glucose. Sci Rep. 2019;9:1–12.

8. Alberty RA. Calculation of standard transformed formation properties of biochemical reactants and standard apparent reduction potentials of half reactions. Arch Biochem Biophys. 1998;358:25–39.

9. Mavrovouniotis ML. Estimation of Standard Gibbs Energy Changes of Biotransformations *. 1991;266:14440–5.

10. Jankowski MD, Henry CS, Broadbelt LJ, Hatzimanikatis V. Group contribution method for thermodynamic analysis of complex metabolic networks. Biophys J [Internet]. 2008 [cited 2015 Jun 19];95:1487–99. Available from: http://www.pubmedcentral.nih.gov/articlerender.fcgi?artid=2479599&tool=pmcentrez&rendertype=abstract

11. Noor E, Bar-Even A, Flamholz A, Lubling Y, Davidi D, Milo R. An integrated open framework for thermodynamics of reactions that combines accuracy and coverage. Bioinformatics. 2012;28:2037–44.

12. Dawes E. Polyhydroxybutyrate: an intriguing biopolymer. Biosci Rep [Internet]. 1988 [cited 2015 Mar 30];8:537–47. Available from: http://link.springer.com/article/10.1007/BF01117332

13. Lu J, Tappel RC, Nomura CT. Mini-Review: Biosynthesis of Poly(hydroxyalkanoates). Polym Rev [Internet]. 2009 [cited 2014 Nov 19];49:226–48. Available from: http://www.tandfonline.com/doi/abs/10.1080/15583720903048243

14. Rehm BH a. Bacterial polymers: biosynthesis, modifications and applications. Nat Rev Microbiol [Internet]. Nature Publishing Group; 2010 [cited 2014 Jul 10];8:578–92.

Available from: http://www.ncbi.nlm.nih.gov/pubmed/20581859

15. Choi SYL and J. MET ABOLlC ENGINEERING OF ESCHERICHIA COLI FOR THE PRODUCTION OF POLYHYDROXYALKANOATES. Metab Eng. Elsevier; 1998;337–41.

16. Lenz RW, Marchessault RH. Bacterial polyesters: Biosynthesis, biodegradable plastics and biotechnology. Biomacromolecules. 2005;6:1–8.

17. North P, Zealand N. Bernd HA Rehm Polyhydroxyalkanoates Introduction. 2018;

18. Martínez-García E, Aparicio T, de Lorenzo V, Nikel PI. New transposon tools tailored for metabolic engineering of gram-negative microbial cell factories. Front Bioeng Biotechnol [Internet]. 2014 [cited 2015 Nov 29];2:46. Available from: http://www.pubmedcentral.nih.gov/articlerender.fcgi?artid=4211546&tool=pmcentrez&rendertype=abstract

19. Wang F, Lee S. Poly (3-Hydroxybutyrate) Production with High Productivity and High Polymer Content by a Fed-Batch Culture of Alcaligenes latus under Nitrogen Limitation. Appl Environ Microbiol [Internet]. 1997 [cited 2015 Mar 30];63:3703–6. Available from: http://aem.asm.org/content/63/9/3703.short

20. Taguchi S, Doi Y. Evolution of polyhydroxyalkanoate (PHA) production system by “enzyme evolution”: successful case studies of directed evolution. Macromol Biosci [Internet]. 2004 [cited 2015 Mar 30];4:146–56. Available from: http://www.ncbi.nlm.nih.gov/pubmed/15468204

21. Kusaka S, Abe H, Lee SY, Doi Y. Molecular mass of poly[(R)-3-hydroxybutyric acid] produced in a recombinant Escherichia coli. Appl Microbiol Biotechnol. 1997;47:140–3.

22. Shi H, Nikawa J, Shimizu K. Effect of modifying metabolic network on poly-3-hydroxybutyrate biosynthesis in recombinant Escherichia coli. J Biosci Bioeng. 1999;

23. Kawaguchi Y, Doi Y. Kinetics and Mechanism of Synthesis and Degradation of Poly(3-hydroxybutyrate) in Alcaligenes eutrophus. Macromolecules. 1992;25:2324–9.

24. Sekar K, Tyo KEJ. Regulatory effects on central carbon metabolism from poly-3-

hydroxybutryate synthesis. Metab Eng [Internet]. Elsevier; 2015 [cited 2015 Jan 17];28:180–9. Available from: http://linkinghub.elsevier.com/retrieve/pii/S1096717615000051

25. Perez-Zabaleta M, Sjöberg G, Guevara-Martínez M, Jarmander J, Gustavsson M, Quillaguamán J, et al. Increasing the production of (R)-3-hydroxybutyrate in recombinant Escherichia coli by improved cofactor supply. Microb Cell Fact. BioMed Central; 2016;15:1–10.

26. Chemler J a, Fowler ZL, McHugh KP, Koffas M a G. Improving NADPH availability for natural product biosynthesis in Escherichia coli by metabolic engineering. Metab Eng [Internet]. Elsevier; 2010 [cited 2015 Mar 30];12:96–104. Available from: http://www.ncbi.nlm.nih.gov/pubmed/19628048

27. Centeno-Leija S, Huerta-Beristain G, Giles-Gómez M, Bolivar F, Gosset G, Martinez A. Improving poly-3-hydroxybutyrate production in Escherichia coli by combining the increase in the NADPH pool and acetyl-CoA availability. Antonie Van Leeuwenhoek [Internet]. 2014;105:687–96. Available from: http://link.springer.com/10.1007/s10482-014-0124-5

28. Kocharin K, Chen Y, Siewers V, Nielsen J. Engineering of acetyl-CoA metabolism for the improved production of polyhydroxybutyrate in Saccharomyces cerevisiae. AMB Express [Internet]. AMB Express; 2012;2:1. Available from: AMB Express

29. Zhang Y, Lin Z, Liu Q, Li Y, Wang Z, Ma H, et al. Engineering of Serine-Deamination pathway, Entner-Doudoroff pathway and pyruvate dehydrogenase complex to improve poly(3-hydroxybutyrate) production in Escherichia coli. Microb Cell Fact [Internet]. 2014 [cited 2015 Sep 7];13:172. Available from: http://www.pubmedcentral.nih.gov/articlerender.fcgi?artid=4279783&tool=pmcentrez&rendertype=abstract

30. Van Wegen RJ, Lee SY, Middelberg APJ. Metabolic and kinetic analysis of poly(3-Hydroxybutyrate) production by recombinant Escherichia coli. Biotechnol Bioeng. 2001;74:70–80.

31. Li Z-J, Cai L, Wu Q, Chen G-Q. Overexpression of NAD kinase in recombinant Escherichia coli harboring the phbCAB operon improves poly(3-hydroxybutyrate)

production. Appl Microbiol Biotechnol [Internet]. 2009 [cited 2014 Nov 19];83:939–47. Available from: http://www.ncbi.nlm.nih.gov/pubmed/19357844

32. Yeo JS, Park JY, Yeom SH, Yoo YJ. Enhancement of poly-3-hydroxybutyrate (PHB) productivity by the two-stage supplementation of carbon sources and continuous feeding of NH4Cl. Biotechnol Bioprocess Eng. 2008;13:14–24.

33. Sánchez AM, Andrews J, Hussein I, Bennett GN, San KY. Effect of overexpression of a soluble pyridine nucleotide transhydrogenase (UdhA) on the production of poly(3-hydroxybutyrate) in Escherichia coli. Biotechnol Prog. 2006;22:420–5.

34. Lee IY, Kim MK, Park YH, Lee- SY. Regulatory Effects of Cellular Nicotinamide Recombinant Escherichia coli. Biotechnol Bioeng. 1996;52:707–12.

35. Carlson R, Wlaschin A, Srienc F. Kinetic Studies and Biochemical Pathway Analysis of Anaerobic Poly- (R) -3-Hydroxybutyric Acid Synthesis in Escherichia coli. Society. 2005;

36. Shimizu MMK· K. Fermentation characteristics and protein expression patterns in a recombinant Escherichia coli mutant lacking phosphoglucose isomerase for poly (3-hydroxybutyrate) production. 2003;244–55.

37. Nikel PI, Pettinari MJ, Galvagno M a, Méndez BS. Poly(3-hydroxybutyrate) synthesis from glycerol by a recombinant Escherichia coli arcA mutant in fed-batch microaerobic cultures. Appl Microbiol Biotechnol [Internet]. 2008 [cited 2014 Nov 19];77:1337–43. Available from: http://www.ncbi.nlm.nih.gov/pubmed/18034236

38. Han M, Yoon S, Lee S. Proteome analysis of metabolically engineeredEscherichia coli producing poly (3-Hydroxybutyrate). J Bacteriol [Internet]. 2001 [cited 2015 Mar 30];183:301–8. Available from: http://jb.asm.org/content/183/1/301.short

39. Tyo KEJ, Fischer CR, Simeon F, Stephanopoulos G. Analysis of polyhydroxybutyrate flux limitations by systematic genetic and metabolic perturbations. Metab Eng [Internet]. Elsevier; 2010 [cited 2014 Nov 19];12:187–95. Available from: http://www.ncbi.nlm.nih.gov/pubmed/19879956

40. Canelas B, Pierick A, Ras C, Seifar RM, Dam JC Van, Gulik WM Van, et al.

Quantitative Evaluation of Intracellular Metabolite Extraction Techniques for Yeast Metabolomics. 2009;81:7379–89.

41. Jol SJ, Kümmel A, Hatzimanikatis V, Beard DA, Heinemann M. Thermodynamic calculations for biochemical transport and reaction processes in metabolic networks. Biophys J. 2010;99:3139–44.

42. Elad Noor1. HSH, ´ ttir2., Ron Milo1*, Ronan M. T. Fleming2 3*, 1Plant. Consistent Estimation of Gibbs Energy Using Component Contributions. J Theor Appl Inf Technol. 2015;78:53–64.

43. Lebedev BK, Kiparisova EG, Vasil VG. Thermodynamics of depolymerization of biotechnological poly[(R)-3-hydroxybutyrate] with formation of (R,R,R)-4,8,12-trimethyl-1,5,9-trioxadodeca-2,6,lO-trione and of its polymerization with ring-opening to highly isotactic poly[(R)-3-hydroxybutyrate] from. 1996;576.

44. Asplund-Samuelsson J, Janasch M, Hudson EP. Thermodynamic analysis of computed pathways integrated into the metabolic networks of E. coli and Synechocystis reveals contrasting expansion potential. Metab Eng [Internet]. Elsevier Inc.; 2018;45:223–36. Available from: https://doi.org/10.1016/j.ymben.2017.12.011

45. Bennett BD, Kimball EH, Gao M, Osterhout R, Van Dien SJ, Rabinowitz JD. Absolute metabolite concentrations and implied enzyme active site occupancy in Escherichia coli. Nat Chem Biol [Internet]. 2009 [cited 2015 Sep 14];5:593–9. Available from: http://www.pubmedcentral.nih.gov/articlerender.fcgi?artid=2754216&tool=pmcentrez&rendertype=abstract

46. Henry CS, Broadbelt LJ, Hatzimanikatis V. Thermodynamics-based metabolic flux analysis. Biophys J. 2007;92:1792–805.

47. Canelas AB, Ras C, ten Pierick A, van Gulik WM, Heijnen JJ. An in vivo data-driven framework for classification and quantification of enzyme kinetics and determination of apparent thermodynamic data. Metab Eng. 2011;13:294–306.

48. Molenaar D, Van Berlo R, De Ridder D, Teusink B. Shifts in growth strategies reflect tradeoffs in cellular economics. Mol Syst Biol [Internet]. Nature Publishing

Group; 2009;5:1–10. Available from: http://dx.doi.org/10.1038/msb.2009.82

1. Annex

1.1 Gibbs free Energy calculations

For the PHB production pathway, the Gibbs free energies for the two reactions converting acetyl-CoA into a monomer unit (3-HBCoA) are represented by eq. 2 and eq. 3.

$$\Delta_r G_1 = \Delta_r G_1^{\circ} + RT \ln \frac{[AcAcCoA][CoA]}{[AcCoA]^2} \quad \text{.....(2)}$$

$$\Delta_r G_2 = \Delta_r G_2^{\circ} + RT \ln \frac{[3-HBCoA][NADP^+]}{[AcAcCoA][NADPH]} \quad \text{.....(3)}$$

For the formation of the PHB polymer, a thiol ester (-CoA) is changed to an ester group. The thioester bond (R–S–CO–R') (containing a sulfur and a carboxyl group) contains approximately a Gibbs free energy of about 40 kJ/mol [3].

Table A1. Free Gibbs energy of every compound and the step reactions from one to three represented in Figure 1. The $\Delta_f G'^m$ counts for standard conditions at pH 7.5, ionic strength of 0.1 and $\Delta_r G'^m$ accounts for a concentration of 0.1 mM.

			Formation	**Reaction**
			$\Delta_f G'^m$ (kJ/mol)	**$\Delta_r G'^m$ (kJ/mol)**
1	**Acetoacetyl-CoA formation**	No	pH=7.5	
	Acetyl-CoA(aq)	2	-1855.6	
	Acetoacetyl-CoA(aq)	1	-1888.8	
	CoA(aq)	1	-1796.3	26.1
2	**Monomer formation**			
	Acetoacetyl-CoA(aq)	1	-1888.8	
	(R)-3-Hydroxybutanoyl-CoA(aq)	1	-1843.1	
	NADPH(aq)	1	-2024.7	
	$NADP^+$(aq)	1	-2089.8	-19.4
3	**Dimer formation (esterification**			
	(R)-3-Hydroxybutanoyl-CoA(aq)	2	-1843.1	
	CoA(aq)	2	-1796.3	
	Dimer P(3HB)	1	-259.3	
	H_2O	1	-157.6	-8.2

Table A2. Calculation of the Gibbs energy of the formation of the monomer, dimer and trimer of PHB from contribution groups.

Group	ΔG'°(kJ/mol)	No. P(3-HB)		
		monomer	dimer	trimer
origin	-98.742	1	1	1
,-CH3	33.054	1	2	3
>CH2	7.113	1	2	3
>CH-	-20.083	1	2	3
,-OH(secondary)	-133.888	1	1	1
,-CO-O-	-307.942	1	1	2
,-CO-S-	-47.279	0	1	1
	sum	-286.604	-547.686	-835.545

*****Estimated through Jankowski

2. Annex

Table B1. Gibbs free energy and fluxes data of the pathways at the maximum MDF reached in every pathway EMP (7.87 kJ/mol), EDP (11.19 kJ/mol), and mEMP (11.79 kJ/mol).

		Reaction	Flux	Physiological $\Delta_r G^m$	Optimized $\Delta_r G'$
EDP	PTS	D-Glucose + Phosphpenolpyruvate <=> D-Glucose 6-phosphate + Pyruvate	2	-44.043	-34.676
	G6PD	D-Glucose 6-phosphate + NADP+ = 6-phospho-D-glucono-1,5-lactone + NADPH	2	-4.023	-9.764
	PGLS	6-phospho-D-glucono-1,5-lactone + H2O <=> 6-Phospho-D-gluconate	2	-22.205	-16.896
	edd	6-Phospho-D-gluconate <=> 2-Dehydro-3-deoxy-6-phospho-D-gluconate + H2O	2	-42.989	-44.145
	eda	2-Dehydro-3-deoxy-6-phospho-D-gluconate <=> Pyruvate + D-Glyceraldehyde 3-phosphate	2	-0.797	-9.764
	GAP	Pi + NAD+ + D-Glyceraldehyde 3-phosphate <=> NADH + 1,3-Bisphosphoglycerate	2	22.38	-9.764
	PGK	ADP + 1,3-Bisphosphoglycerate <=> ATP + D-Glycerate-3-phosphate	2	-18.525	-9.764
	PGAM	D-Glycerate-3-phosphate <=> D-Glycerate-2-phosphate	2	4.205	-9.764
	ENO	D-Glycerate-2-phosphate <=> Phosphoenolpyruvate + H2O	2	-4.078	-9.764
	PDHA	Pyruvate + CoA + NAD+ <=> Acetyl-CoA + CO2 + NADH	4	-35.637	-30.295
	phaA	Acetyl-CoA + Acetyl-CoA <=> Acetoacetyl-CoA + CoA	2	25.561	-28.189
	phaB	Acetoacetyl-CoA + NADPH <=> (R)-3-Hydroxybutanoyl-CoA + NADP+	2	-18.094	-9.764
	phaC	(R)-3-Hydroxybutanoyl-CoA + (R)-3-Hydroxybutanoyl-CoA + H2O <=> (R)-3-((R)-3-Hydroxybutanoyloxy)butanoate + CoA + CoA	1	-25.462	-9.764
	NADH16/ ADK1	O2 + 2 NADH + 2 ADP + 2 Pi <=> 2 NAD+ + 2 ATP + 4 H2O	3	-355.349	-310.91
	ATPM	ATP + H2O <=> ADP + Pi	8	-42.886	-42.644
EMP	PTS	D-Glucose + Phosphpenolpyruvate <=> D-Glucose 6-phosphate + Pyruvate	2	-44.043	-29.037
	PGI	D-Glucose 6-phosphate <=> D-Fructose 6-phosphate	2	2.529	-6.789
	FBP	ATP + D-Fructose 6-phosphate <=> ADP + Fructose-1,6-bisphosphate	2	-14.675	-7.645
	FBA	Fructose-1,6-bisphosphate <=> Glycerone phosphate + D-Glyceraldehyde 3-phosphate	2	2.89	-6.789
	TPI	Glycerone phosphate <=> D-Glyceraldehyde 3-phosphate	2	5.459	-6.789
	GAP	Pi + NAD+ + D-Glyceraldehyde 3-phosphate <=> NADH + 1,3-Bisphosphoglycerate	4	22.38	-6.789
	PGK	ADP + 1,3-Bisphosphoglycerate <=> ATP + D-Glycerate-3-phosphate	4	-18.525	-6.789
	PGAM	D-Glycerate-3-phosphate <=> D-Glycerate-2-phosphate	4	4.205	-6.789
	ENO	D-Glycerate-2-phosphate <=> Phosphoenolpyruvate + H2O	4	-4.078	-6.789
	PYK	ADP + Phosphoenolpyruvate <=> Pyruvate + ATP	2		-6.789
	PDHA	Pyruvate + CoA + NAD+ <=> Acetyl-CoA + CO2 + NADH	4	-35.637	-35.892
	phaA	Acetyl-CoA + Acetyl-CoA <=> Acetoacetyl-CoA + CoA	2	25.561	-28.204
	phaB	Acetoacetyl-CoA + NADPH <=> (R)-3-Hydroxybutanoyl-CoA + NADP+	2	-18.094	-6.789
	phaC	(R)-3-Hydroxybutanoyl-CoA + (R)-3-Hydroxybutanoyl-CoA + H2O <=> (R)-3-((R)-3-Hydroxybutanoyloxy)butanoate + CoA + CoA	1	-25.462	-17.73
	NADH16/ ADK1	O2 + 2 NADH + 2 ADP + 2 Pi <=> 2 NAD+ + 2 ATP + 4 H2O	3	-355.349	-311.025
	ATPM	ATP + H2O <=> ADP + Pi	8	-42.886	-42.434
	pntAB	NADP + NADH + ATP + H2O <=> NADPH + NAD+ + ADP + Pi	2	-42.907	-22.1
mEMP	PTS	D-Glucose + Phosphpenolpyruvate <=> D-Glucose 6-phosphate + Pyruvate	2	-44.043	-34.002
	PGI	D-Glucose 6-phosphate <=> D-Fructose 6-phosphate	2	2.529	-11.790
	FBP	ATP + D-Fructose 6-phosphate <=> ADP + Fructose-1,6-bisphosphate	2	-14.675	-11.790
	FBA	Fructose-1,6-bisphosphate <=> Glycerone phosphate + D-Glyceraldehyde 3-phosphate	2	2.890	-11.790
	TPI	Glycerone phosphate <=> D-Glyceraldehyde 3-phosphate	2	5.459	-11.790
	GAPN	D-Glyceraldehyde 3-phosphate + NADP + H2O <=> D-Glycerate-3-phosphate + NADPH	4	-39.051	-11.790
	PGAM	D-Glycerate-3-phosphate <=> D-Glycerate-2-phosphate	4	4.205	-11.790
	ENO	D-Glycerate-2-phosphate <=> Phosphoenolpyruvate + H2O	4	-4.078	-11.790
	PYK	ADP + Phosphoenolpyruvate <=> Pyruvate + ATP	2	-27.293	-11.790
	PDHA	Pyruvate + CoA + NAD+ <=> Acetyl-CoA + CO2 + NADH	4	-35.637	-11.989
	phaA	Acetyl-CoA + Acetyl-CoA <=> Acetoacetyl-CoA + CoA	2	25.561	-28.224
	phaB	Acetoacetyl-CoA + NADPH <=> (R)-3-Hydroxybutanoyl-CoA + NADP+	2	-18.094	-11.790
	phaC	(R)-3-Hydroxybutanoyl-CoA + (R)-3-Hydroxybutanoyl-CoA + H2O <=> (R)-3-((R)-3-Hydroxybutanoyloxy)butanoate + CoA + CoA	1	-25.462	-13.311
	NADH16/ ADK1	3 O2 + 4 NADH + 4 ADP + 4 Pi + 2 NADPH <=> 4 NAD+ + 2 NADP + 4 ATP + 10 H2O	1	-383.925	-42.361
	ATPM	ATP + H2O <=> ADP + Pi	4	-42.886	-386.754

Table B2. Concentration and boundaries presented in M of the compounds in the pathways EMP, EDP, and mEMP, lb=lower bound, ub= upper bound.

Compound	EMP			EDP			mEMP		
	Concentration	lb	ub	Concentration	lb	ub	Concentration	lb	ub
H_2O	1.00E+00	1.00E+00	1.00E+00	1.00E+00	1.00E+00	1.00E+00	1.00E+00	1.00E+00	1.00E+00
ATP	5.00E-03	5.00E-03	5.00E-03	5.00E-03	5.00E-03	5.00E-03	5.00E-03	5.00E-03	5.00E-03
O_2	2.73E-04	2.73E-04	2.73E-04	2.73E-04	2.73E-04	2.73E-04	2.73E-04	2.73E-04	2.73E-04
NADP	2.00E-02	1.00E-06	2.00E-02	2.00E-02	1.00E-06	2.00E-02	2.00E-02	1.00E-06	2.00E-02
NADPH	2.00E-02	1.00E-06	2.00E-02	2.00E-02	1.00E-06	2.00E-02	2.00E-02	1.00E-06	2.00E-02
ADP	5.00E-04	5.00E-04	5.00E-04	5.00E-04	5.00E-04	5.00E-04	5.00E-04	5.00E-04	5.00E-04
NAD	2.00E-02	1.00E-06	2.00E-02	2.00E-02	1.00E-06	2.00E-02	2.00E-02	1.00E-06	2.00E-02
Pi	1.00E-02	1.00E-02	1.00E-02	1.00E-02	1.00E-02	1.00E-02	1.00E-02	1.00E-02	1.00E-02
NADH	1.00E-06	1.00E-06	2.00E-02	1.00E-06	1.00E-06	2.00E-02	1.99E-03	1.00E-06	2.00E-02
CoA	1.00E-05	*	*	1.00E-05	*	*	1.00E-05	*	*
CO_2	1.00E-05	1.00E-05	1.00E-05	1.00E-05	1.00E-05	1.00E-05	1.00E-05	1.00E-05	1.00E-05
AcCoA	1.00E-03	1.00E-07	1.00E-03	1.00E-03	1.00E-07	1.00E-03	1.00E-03	1.00E-07	5.30E-03
AcAcCoA	**1.08E-07**	**1.08E-07**	**1.08E-07**	**1.08E-07**	**1.08E-07**	**1.08E-07**	**1.08E-07**	**1.08E-07**	**1.08E-07**
Pyr	1.99E-04	1.00E-06	1.00E-02	1.96E-05	1.00E-06	1.00E-02	4.19E-05	1.00E-06	1.00E-02
Gluc	1.00E-02	1.00E-06	1.00E-02	1.00E-02	1.00E-06	1.00E-02	1.00E-02	1.00E-06	1.00E-02
G6P	1.00E-02	1.00E-06	1.00E-02	1.00E-02	1.00E-06	1.00E-02	1.00E-02	1.00E-06	1.00E-02
F6P	1.77E-04	1.00E-06	1.00E-02	na	na	na	2.72E-05	1.00E-06	1.00E-02
GAP	5.08E-05	1.00E-06	1.00E-02	1.00E-02	1.00E-06	1.00E-02	1.00E-06	1.00E-06	1.00E-02
13-bPG	4.55E-04	1.00E-06	1.00E-02	2.90E-03	1.00E-06	1.00E-02	na	na	na
DHAP	8.40E-03	1.00E-06	1.00E-02	na	na	na	1.41E-03	1.00E-06	1.00E-02
F16bP	1.00E-02	1.00E-06	1.00E-02	na	na	na	7.01E-04	1.00E-06	1.00E-02
6PGC	na	na	na	1.00E-02	1.00E-06	1.00E-02	na	na	na
6PGL	na	na	na	6.64E-04	1.00E-06	1.00E-02	na	na	na
KDPG	na	na	na	1.00E-02	1.00E-06	1.00E-02	na	na	na
3PG	4.55E-04	1.00E-06	1.00E-02	6.35E-03	1.00E-06	1.00E-02	1.00E-02	1.00E-06	1.00E-02
2PG	4.06E-06	1.00E-06	1.00E-02	1.52E-05	1.00E-06	1.00E-02	1.92E-05	1.00E-06	1.00E-02
PEP	1.00E-06	1.00E-06	1.00E-02	1.00E-06	1.00E-06	1.00E-02	1.00E-06	1.00E-06	1.00E-02
3-HB-CoA	6.48E-03	1.00E-06	1.00E-02	1.65E-03	1.00E-06	1.00E-02	6.68E-03	1.00E-06	1.00E-02
P(3-HB)	1.00E+00	1.00E+00	1.00E+00	1.00E+00	1.00E+00	1.00E+00	1.00E+00	1.00E+00	1.00E+00

na= not applicable

In bold is highlighted the AcAcCoA concentration which remained fixed through all the analysis (A1, B1 and B2).

*CoA values are fixed to the ratio of AcCoA/CoA desired from 1 to 10^4.

Chapter 3.

Simultaneous growth and PHB production in *E. coli* by engineering NADPH supply during continuous cultivation

Mariana I. Velasco Alvarez, Karel Olavarria Gamez, Hector Sangüesa Ferrer, Mark C.M. van Loosdrecht and S. Aljoscha Wahl

Abstract

Strain engineering for the production of biobased products has been widely applied during the last decades. Though systematic approaches are applied, there are still gaps in the understanding to rationally engineer cellular metabolism efficiently. Crucial for the understanding of cellular metabolism is the influence of co-factors. Here we studied the impact of co-factors on a very well-known product pathway, i.e. the production of Poly-3-hydroxybutyrate (PHB). Especially, substrate limiting chemostat conditions were applied to analyze the impact of different engineering strategies on metabolism, i.e. product formation and growth. Biomass growth (anabolism) and PHB production both require NADPH as co-factor. Here we investigated the influence of the substitution of *gapA* for *gapN* in glycolysis, altering the co-factor substrate from NAD^+ to $NADP^+$. This shift was found to enable a higher thermodynamic driving force for the product pathway compared to canonical glycolysis. A modified *E. coli* strain (K-12 MG1655 Δ*zwf gapA*::$gapN^{S.mutans}$) was constructed and the genes encoding for *phaCAB* genes from *Cupriavidus necator* were introduced. The reference strain (*E. coli* K-12 MG1655, with the PHB plasmid), showed no PHB production at any of the employed dilution rates. In contrast, PHB accumulation was observed in the Δ*zwf gapA*::$gapN^{S.mutans}$ strain. Under fully aerobic conditions the PHB titer was less than 1 % (based on biomass dry weight), oxygen limited conditions resulted in a PHB content of 7 %. While the $NADPH/NADP^+$ ratio was sufficiently high to generate thermodynamic driving force for PHB formation, the acetyl-CoA/CoA ratio was found too low for a high product flux.

1. Introduction

The use of bacteria for the production of biobased chemicals requires that metabolism is reprogrammed and optimized for the desired product. Many product pathways rely on redox reactions, linking the product pathway to central carbon metabolism [1]. Several products like lycopene, polyhydroxyalkanoates, 1,3-propanediol or ε-caprolactone require reducing equivalents from NADPH which are also required for biomass synthesis. Therefore, a balance between growth and the flux into the production pathway should be achieved for optimal performance [2].

Suggested strategies for enhanced NADPH supply include: (a) knock-out of phosphoglucose isomerase (*pgi*) to enforce metabolic flux through the oxidative branch of the pentose-phosphate pathway [3], (b) overexpression of soluble pyridine nucleotide transhydrogenase (UdhA) to increase the conversion of NADH to NADPH [4] and (c) replacing *gapA* (encoding for the phosphorylating NAD^+ dependent glyceraldehyde-3-phosphate dehydrogenase (E.C. 1.2.1.12)) by *gapN* (encoding for a non-phosphorylating NADP-dependent glyceraldehyde-3-phosphate dehydrogenase (E.C. 1.2.1.9)) [2].

The latter strategy was studied by Martinez and co-workers [5] and Centeno-Leija and co-workers [6] where the *gapN* genes of *Clostridium acetobutylicum* and *Streptococcus mutans* were introduced in *E. coli* cells. The *gapA*::*gapN* replacement implies the generation of two NADPH instead of two NADH from glycolysis which resulted in higher yields for the products lycopene and polyhydroxybutyrate.

PHB is an interesting product pathway to study the impact of redox cofactor engineering. Firstly, the pathway is well-known and can be expressed well in *E. coli*. Especially using the pathway genes from *Cupriavidus necator* (*phaCAB* genes [7,8]). Secondly, the product can be quantified precisely and the PHB content directly reflects the ratio between product formation and biomass synthesis. .

Additionally, there is still potential to increase volumetric productivities as well as yields for PHB production. Currently, the common bioprocess operation mode for PHB synthesis is fed-batch using nitrogen limitation [9]. While nitrogen limitation creates conditions for metabolic overflow that also favors PHB accumulation, it creates limitations for the protein synthesis, affecting the enzymatic capacity of the producing cells [10]. Next to this biological drawback, the fed-batch process conditions limit the

productivity (volume of product per unit of time) by: (1) time between batches (cleaning and start-up) and (2) not exploiting the full mass transfer capacities of the reactors for most of the production time.

Here we propose to overcome these limitations by (1) engineer cells, i.e. introducing a coupling between biomass and PHB formation and an efficient utilization of the carbon and electron source, (2) apply chemostat conditions to operate continuously at the (maximal) bioreactor capacity with respect to volume and oxygen transfer.

To achieve the coupling (1) the aforementioned shift in glycolysis *gapA*::*gapN* was applied. Additionally, the gene glucose 6-phopshate dehydrogenase (*zwf*) was knocked-out to further constrain the NADPH balance, i.e. force the incoming glucose through the EMP pathway [11].

Table 1. Comparison of characterized *E. coli* and *S. cerevisiae* mutant strains containing the PHB pathway. All data originate from batch cultivations using glucose as substrate (carbon excess).

Strain genotype	**μ_{max}(h^{-1})**	**%PHB (g_{PHB}/g_{CDW})**	**Reference**
E. coli K12 MG1655 Δ*gapA::gapN*/pTrc*gapN*	0.4	64	[6]
S. cerevisiae MATa SUC2 MAL2-8c ura3-52 his3-D1::gapN	0.27-0.28	0.1	[12]
E. coli DF11/pAeKG1	na	10.71	[3]
E. coli GJT001 (pUDHA)	na	66	[4]
*E. coli XL1-Blue(pSYL107)**	na	77	[13]

na= not available

*Cultivation in fed batch and oxygen limited conditions.

PHB is a reduced product, and can act as internal electron acceptor. To enforce the product synthesis, the external electron acceptor can be limited, such that internal ones are used. This strategy can enhance the flux towards PHB. However, some drawbacks of such approach are the reduced ATP production, and the formation of fermentation products (i.e. competing internal acceptors) to counterbalance ATP shortage. Here, oxygen limitation was evaluated as a strategy to obtain PHB formation in chemostat conditions with an engineered *E. coli* strain [14].

2. Materials and Methods

2.1 Molecular Biology Approaches

All constructed strains were derived from *E. coli* K-12 MG1655 (F- lambda- ilvG- rfb-50 rph-1). This parental strain was obtained from the Coli Genetic Stock Center (Yale, USA). The description and characteristics of its genome were obtained from Blattner et. al [15].

Two chromosomal modifications were introduced: (1) substitution of gene *gapA* (encoding for the NAD-depending phosphorylating glyceraldehyde-3-phosphate dehydrogenase; E.C. 1.2.1.12) by the gene *gapN* from *Streptoccocus mutans* (encoding for the NADP-preferring non-phosphorylating glyceraldehyde-3-phosphate dehydrogenase, E.C. 1.2.1.9) and (2) the deletion of the gene *zwf*, encoding for the glucose-6-phosphate dehydrogenase (E.C. 1.1.1.49).

In addition, the resultant strain and the parental strain were transformed with the plasmid pBBRMCS2-phaCAB, bearing the genes encoding for the thiolase (E.C. 2.3.1.9), acetoacetyl-CoA reductase (E.C. 1.1.1.36) and the PHB synthase (E.C. 2.3.1.B2) from *Cupriavidus necator*. The main characteristics of the parental and the constructed strains are summarized in the Table 3.

To substitute the *gapA* by *gapN*, the method developed by Wanner and Datsenko [16] was applied with some modifications, explained as follows. The *gapN* gene ("GeneID:1028095", protein_id="NP_721104.1") was amplified from isolated colonies of *Streptoccus mutans* (*Streptococcus mutans* UA159**,** NCBI Reference Sequence: NC_004350.2, kindly donated by Dr. Maria Regina Lorenzetti Simionato from Universidade de São Paulo, Brazil), using the primers SmutGAPNXbacrt and SmutGAPNKpncrt. The obtained PCR product and the plasmid pTrc99A (Pharmacia) were restricted with the enzymes *KpnI* and *Xba*I (New England Biolabs), and ligated with T4 DNA Ligase (Thermo Scientific), following the instructions of the manufacturer to obtain the plasmid named ptrcGANP. In a second stage, the cassette FRT-Kan^{R}-FRT was amplified from the plasmid pKD13 using the primers upFRTpkd13 and downFRTpkd13 (see **Annex A**) which added restriction sites for the enzyme *Sal*I. Both the PCR product and the plasmid ptrcGANP were restricted with the enzyme *SalI* and ligated (T4 DNA ligase) to obtain the plasmid ptrcGANP-FRT-KanR-FRT. In a third stage, a linear DNA molecule was obtained, by PCR, using the plasmid ptrcGANP-FRT-KanR-FRT as the

template and the primers WDGANPxGAPfw3 and WDGANPxGAPrv3. The obtained PCR product was purified and treated with *DpnI*, according with the instructions of the manufacturer, to eliminate traces of the plasmidial template. The treated linear DNA molecule was introduced, by electroporation, in cells of *E. coli* MG1655 previously transformed with the plasmid pKD46, grown at 30 °C and treated with L-arabinose as previously described [16]. The recombinant cells were selected by their ability to growth in plates of LB-Kanamycin and the presence of the expected modification was verified by PCR and sequencing. Before the deletion of the *zwf* gene, the kanamycin resistant marker flanked by the FRT sequences was removed by the introduction of the helper plasmid pCP20, bearing the gene encoding for a DNA flipase [16]. This helper plasmid was cured growing the cells at 37 °C. The sensitivity of the resultant strain to ampicillin, chloramphenicol and kanamycin was verified by negative selection.

For the further deletion of the *zwf* gene, a chromosomal fragment of the strain *E. coli* JW1841-1 F- (*Δ(araD-araB)567, ΔlacZ4787(::rrnB-3), λ-, Δzwf-777::kan, rph-1, Δ(rhaD-rhaB)568, hsdR514*) embracing the substitution of *zwf* by the cassette FRT-Kan^R-FRT was amplified by PCR using genomic DNA from *E. coli* JW1841-1 as template and the primers UPEcolizwf and DWEcolizwf. The obtained PCR product was introduced in the strain previously obtained and the recombinant colonies were selected using the same procedure explained above. The kanamycin resistance gene was also removed as previously explained before the transformation with the plasmid pBBRMCS2-phaCAB. This latter plasmid was also introduced in the parental strain *E. coli* MG1655. The resultant strains, after the transformation with the plasmid pBBRMCS2-phaCAB, were denominated K12+pPHB and K12GAPNΔzwf+pPHB.

Table 3. *Escherichia coli* strains used in this study.

Name	Genotype	Description	Source
K12	MG1655 (F-, λ-, rph-1)	Parental strain	CGSC #7740*
K12+pPHB	K12 + pBBRMCS2-phaCAB	Parental strain transformed with the plasmid pBBRMCS2-*phaCAB***	This study
K12GAPN+pPHB	K12GAPN+ pBBRMCS2-phaCAB	K12GAPN transformed with the plasmid pBBRMCS2-*phaCAB*	This study
K12GAPNΔzwf+pPHB	K12GAPNΔzwf + pBBRMCS2-phaCAB	K12GAPNΔzwf transformed with the plasmid pBBRMCS2-*phaCAB*	This study

*CGSC: The Coli Genetic Stock Center, University of Yale, CT, USA

**The plasmid pBBRMCS2-*phaCAB* carries the *phaCAB* genes from *Cupriavidus necator*, including the native promoter.

2.2 Enzyme activity measurements

The cell-free extracts were prepared as previously reported [17]. Briefly, broth samples from the batch or the continuous cultures were centrifuged at 4000 g during 10 minutes at 4 °C. The pellets were washed once with Buffer A (50 mM Tris-HCl pH 8.0, 5 mM MgCl2, 5 mM NaCl, 5 mM β-mercaptoethanol, 10% v/v glycerol) and the cellular suspension was centrifuged again using the same conditions. The washed pellets were re-suspended in 10 mL of Buffer A complemented with 2 mM D/L-Dithiothreitol and cOmplete Proteases Inhibition Cocktail™ (Roche, Switzerland) following the instructions of the manufacturer. The re-suspended pellets were sonicated on ice to minimize protein denaturation. Sonicated samples were centrifuged at 10000 g at 4 °C for 30 minutes to separate soluble proteins from cell debris. The obtained supernatants were considered cell-free extracts. Total protein content in the cell-free extracts was quantified using the method described by Bradford [18]. Solutions of bovine serum albumin (Sigma-Aldrich, U.S.A.) at known concentrations were used as standards. The reaction buffer was Buffer A with ad hoc modifications, depending on the assay. The NAD-GAP activity was directly measured with slight modifications of the method reported by Fillinger and co-workers: 50 mM sodium phosphate (pH 7.0), 20 mM sodium arsenate, 4 mM glyceraldehyde-3-phosphate and 2 mM NAD [19]. The NADP-GANP activity was directly measured with the method reported by Marchal and Branlant [20] with small modifications: 50 mM Tris (pH 8.5), 5 mM β-mercaptoethanol, 0.5 mM NADP, 1 mM glyceraldehyde-3-phosphate. All the enzymatic assays were performed at 37°C, following the production of NAD(P)H spectrophotometrically at 340 nm, using a microplate reader (Sinergy HTX, Biotek, USA).

2.3 Media and pre-culture conditions

In all cases, the inoculum was prepared from isolated colonies obtained from stocks stored at -80 °C. Experiments for strain characterizations were performed using mineral medium as reported by Taymaz-Nikerel et al.[21] containing 5 g/L $(NH_4)_2SO_4$, 2 g/L KH_2PO_4; 0.5 g/L MgSO4; 0.5 g/L NaCl; 2 g/L NH_4Cl; 0.001 g/L Thiamine, 2 mL of trace

elements as described by Verduyn and co-workers [22]. Glucose (10 g/L) was employed as the sole carbon source. Kanamycin (50 µg/mL) was added as selection marker during the study of strains transformed with the plasmid pBBRMCS2-phaCAB. The precultures and batch cultures were incubated in a rotary shaker at 37 °C and 200 r.p.m. (Sartorius Stedim Biotech S.A., France).

2.4 Bioreactor cultivation medium and chemostat conditions

Carbon and/or oxygen limited continuous cultures were performed using a minimal medium as described by Taymaz-Nikerel et al. [21]. The medium consisted of 5 g/L $(NH_4)_2SO_4$, 2 g/L KH_2PO_4; 0.5 g/L MgSO4; 0.5 g/L NaCl; 2 g/L NH_4Cl; 0.001 g/L Thiamine, 2 mL of trace elements as described by Verduyn and co-workers [22], and 0.2 mL silicone-based antifoaming agent (Antifoam C, silicon oil-based, Sigma, Kanagawa, Japan). The carbon source was 20 g/L glucose. The medium was sterilized through filtration (0.02 µM pore size capsule filter, Sartorius, Göttingen, Germany). A bioreactor with a vessel of 1.5 L working volume (Applikon Biotechnology B.V., Delft, The Netherlands) was used. The cultivations were controlled using a Sartorius ©BIOSTAT B Plus Twin setup. The broth volume was controlled at 1 L using a level sensor attenuated outflow pump. The culture pH was controlled at 7.0 by addition of 2 M KOH and 2 M H_2SO_4. Antifoam (Antifoam C, silicon oil-based, Sigma, Kanagawa, Japan) was added for 2 s (2s/h that is approximately 200 µL/h) every hour and stirring was kept constant at 700 r.p.m. The oxygen availability was adjusted by modifying the in-gas composition (mix of air and nitrogen gas). The temperature was set to 37 °C and controlled by a thermal tubing system.

2.5 On-line measurements

The volume fractions of CO_2 and O_2 of the bioreactor off-gas and in the pressurized air were measured with a mixed CO_2 (infrared) and O_2 (paramagnetic) gas analyzer (NGA 2000, Rosemount Analytical, Hasselroth, Germany). The temperature, pH, feed weight, CO_2 and O_2 in the off-gas and pressurized air, were monitored and registered with a MFCS/W in 2.1 software (Sartorius Stedim Biotech S.A.,France).
To estimate the maximum growth rate in the strains studied (K12GAPNΔzwf+pPHB and K12+pPHB), the CO_2 data in the batch phase was subtracted.

2.6 Broth and intracellular measurements

2.6.1 Cell dry weight (CDW) and optical density

The biomass concentration (dry weight) was measured using a gravimetrical method: 5 mL of broth were withdrawn and filtered using a pore size paper filter (Supor-450, 0.22 µm, 47 mm, Pall Corporation). The filtrate was then dried at 70 °C during 48 h and weighted.

To estimate the growth rate in shake flask cultivations, optical density samples were measured using a spectrophotometer (Biochrom Libra S12 Visible, Cambridge, UK) at 600 nm.

2.6.2 Extracellular measurements

To measure the extracellular concentrations of glucose, ethanol, lactate, succinate and acetate, 1 mL broth was withdrawn from the bioreactor. The samples were filtrated using a 0.22 µm Durapore PVDF membrane filter and measured using HPLC (Waters 515 using a BioRad HPX-87H 300 * 7.8 mm column with a Guard column BioRad Cation-H refill cartridge 30* 4.6 mm). The eluent contained 1.5 mmol/L H_3PO_4 in Milli-Q water (~70 °C) and the flow was set to 0.6 mL/min. As detector, a refractometer (Waters 2414, MA, USA) and an U.V. detector (Waters 2489 at 210 nm) were used. The injection was 10 µL (Waters 717, MA,USA) at 15 °C.

2.6.3 PHB quantification

PHB was quantified using a previously described method [23]. Briefly, samples of 1 mL of broth were taken from the cultures in bioreactor or shaking flasks. The samples were centrifuged for 5 min at 10621g at room temperature. The supernatants were discarded and 500 µL Milli Q water was added together with 200 µL of internal standard (13C-PHB containing cell extract) and the pellet was re-suspended. The solution was then transferred into GC vials and these samples were kept at -80 °C for at least 20 minutes. The frozen samples were freeze-dried overnight using a Mini-Lyotrap Freeze Dryer (Edwards Modulyo, Sussex, UK). Propanolysis of the dried sample was performed by adding 100 µL of 3:7 HCl:1-propanol and 50 µL dichloroethane, short vortexing and

incubation for 2 hours at 100 ºC (vortexing every half hour). Then, the liquid was transferred to glass tubes containing 150 µL of 1,2 dichlorethane. 300 µL Milli Q water was added and the tubes were centrifuged for 1 min at 10621 g. 200 µL of the lower organic phase was transferred to new glass tubes, shortly vortexed and centrifuged for 1 min at 10621 g. From this organic phase 120 µL were transferred into an insert and placed back in a vial suitable for gas chromatography (GC). The samples were measured on a 7890A GC coupled to a 5975C Quadrupole MSD (both from Agilent, Santa Clara, CA, USA). The spectra were evaluated using Mass Hunter Quantitative Analysis for MS (version B.07.00; Agilent).

2.7 Intracellular Metabolite analysis

Rapid sampling was performed to measure total broth metabolite concentrations using a system described earlier [24]. Broth samples of 1 mL were taken from the reactor within a time of 0.5 s into a tube containing 5 mL of quenching solution of methanol at -40 °C. Then the sample was weighted and mixed with the fully labeled internal standard directly. The exact weight of the samples was quantified using a precise balance, measuring before and after sampling. The samples were stored in a -80 °C freezer until further processing as previously described [21].

The intracellular metabolite concentrations were assessed through isotope dilution mass spectrometry (IDMS) [25]. Amino acids were derivatized using a mixture of acetonitrile and N-methyl-N-(tert- butyldimethylsilyl) trifluoroacetamide (MTBSTFA, Thermo Scientific) and quantified through a 7890A GC (Agilent, Santa Clara, CA, USA) instrument coupled to a 5975C MSD single quadrupole mass spectrometer (Agilent, Santa Clara, CA, USA) as described by Jonge et al. [26]. Nucleotides and coenzymes were measured through LC-MS (HPLC: Alliance HT pump 2795 (Waters, USA), MS: Quattro Ultima Pt triple quadrupole mass spectrometers (Waters, UK)), as reported by Wahl et al. [25]. The metabolites of glycolysis, TCA cycle and PPP were derivatized using a mixture of O-methoxyamine hydrochloride (MOX, purum, Sigma- Aldrich, Buchs, Switzerland) and pyridine (HPLC grade 99.9 %, Sigma-Aldrich, Buchs, Switzerland) for the first phase and N-Methyl-N-trimethylsilyltrifuoroacteamide-Trimethylchlorosilane (MSTFA-TMCS (Thermo Scientific, Bellafonte, PA, USA)) for

the second phase. Consequently the derivatized samples were analyzed through GC-MS as described by Mashego et al. [27].

The NAD(P)H/NAD(P) ratios were determined using (pseudo) equilibrium reactions [28,29]. The [NADPH/$NADP^+$] ratio was estimated through the reaction Glutamate Dehydrogenase (GDH) NADPH-dependent that forms glutamate from α-ketoglutarate. The equilibrium constant (Keq) is equal to 1.5x 10^{-7} for a pH 7 [30]. An ammonia concentration of 5 mM was assumed for all conditions around the values measured by Wang et al. at pH 7 in *E. coli* WT [31].

$$\frac{[\mathrm{NADPH}]}{[\mathrm{NADP^+}]} = \mathrm{K_{eq}} \cdot \frac{[\mathrm{L-glutamate}]}{[\mathrm{NH_3}][\alpha-\mathrm{KG}]}$$

The [NADH/NAD^+] ratio was calculated using the equilibrium reaction Mannitol-1-phosphate dehydrogenase (M1PDH) that reduces fructose-6-phosphate to mannitol-1-phosphate [32]. The equilibrium constant (Keq) is equal to 7.9x 10^{-3} for a pH 7 as reported by Nikerel et al. [32].

$$\frac{[\mathrm{NADH}]}{[\mathrm{NAD^+}]} = \mathrm{K_{eq}} \cdot \frac{[\mathrm{F6P}]}{[\mathrm{M1P}]}$$

2.8 In silico modelling and simulations

Flux balance analysis (FBA) was performed using COBRA toolbox (2019) package, running in MATLAB 2017b [33]. The metabolic model was based on the available *Escherichia coli* network based on the "Ecolicore" model that contains 97 based reactions and 3 reactions were added [34] (see Annex B1). The final model contained the PHB pathway and the switch from *gapA* to *gapN*.

3. Results

3.1 Physiology: Impact of the redox cofactor engineering during batch growth

The batch (maximum) growth rates of the strains K12+pPHB and K12GAPNΔzwf+pPHB were determined from aerobic batch experiments using glucose as the sole carbon source (**Table 4**.). As positive controls, the wild type strain K12 was grown under the same conditions. There is a small influence of the plasmid, i.e. the

growth rate of plasmid carrying *E. coli* were 7 % lower. The maximum growth rate of K12GANPΔzwf was 0.25 h^{-1}. This growth rate is higher than the growth rate of 0.11 h^{-1} observed for another K12 where the *gap* gene was substituted by the *ganp* gene from *S. mutans* but *zwf* was not removed [35]. The reduced growth rate in comparison with WT observed by Centeno-Leija and co-workers was attributed to a kinetic limitation provoked by the poor performance of the enzyme encoded by *ganp*. When increasing the expression using a plasmid carrying another copy of the *ganp* gene the growth rate increased to 0.44 h^{-1} [35]. Similarly, [5] observed a growth rate of 0.38 h^{-1} using a comparable strain with *gap* knocked-out and plasmid based expression of *ganp* [5].

Table 4. Batch growth rates (μ_{max}) using mineral medium with glucose as the sole carbon source under fully aerobic conditions (BR: bioreactor, SF: shake flask vessel).

Strain	μ_{max} (h^{-1})	Strain	μ_{max} (h^{-1})
K12	0.71[a]	**K12+pPHB**	0.64[a]
K12GAPN	0.25[b]	**K12GAPN+pPHB**	0.27[b]
K12GAPNΔzwf	0.25[b]	**K12GAPNΔzwf+pPHB**	0.22[a]

[a]bioreactor (measured by CO_2 in the off-gas)

[b]shake flask vessel

3.2 Physiology: carbon limited conditions under aerobic conditions

In contrast to batch conditions, steady-state, chemostat cultivations allow to vary the process conditions with respect to growth rate by limiting the substrate supply rate(s). Flux balance analyses were performed to design cultivation conditions enforcing simultaneous growth and PHB production in the mutant strain K12GAPNΔzwf+pPHB (see network of most relevant reactions in **Figure 1)**. The flux under continuous cultivation conditions was predicted through FBA simulations by fixing the biomass formation rate and minimizing the glucose uptake rate setting a lower boundary in the uptake rate. The simulations were optimized only for ATP for maintenance.

The impact of reactions involving NADP(H), the transhydrogenase UdhA and isocitrate lyase were studied. Isocitrate lyase was expected to play a role as it allows for a bypass of isocitrate dehydrogenase which is $NADP^+$ dependent. Especially, carbon could be oxidized via the glyoxylate shunt without NADPH regeneration, lowering the “pressure” to produce PHB.

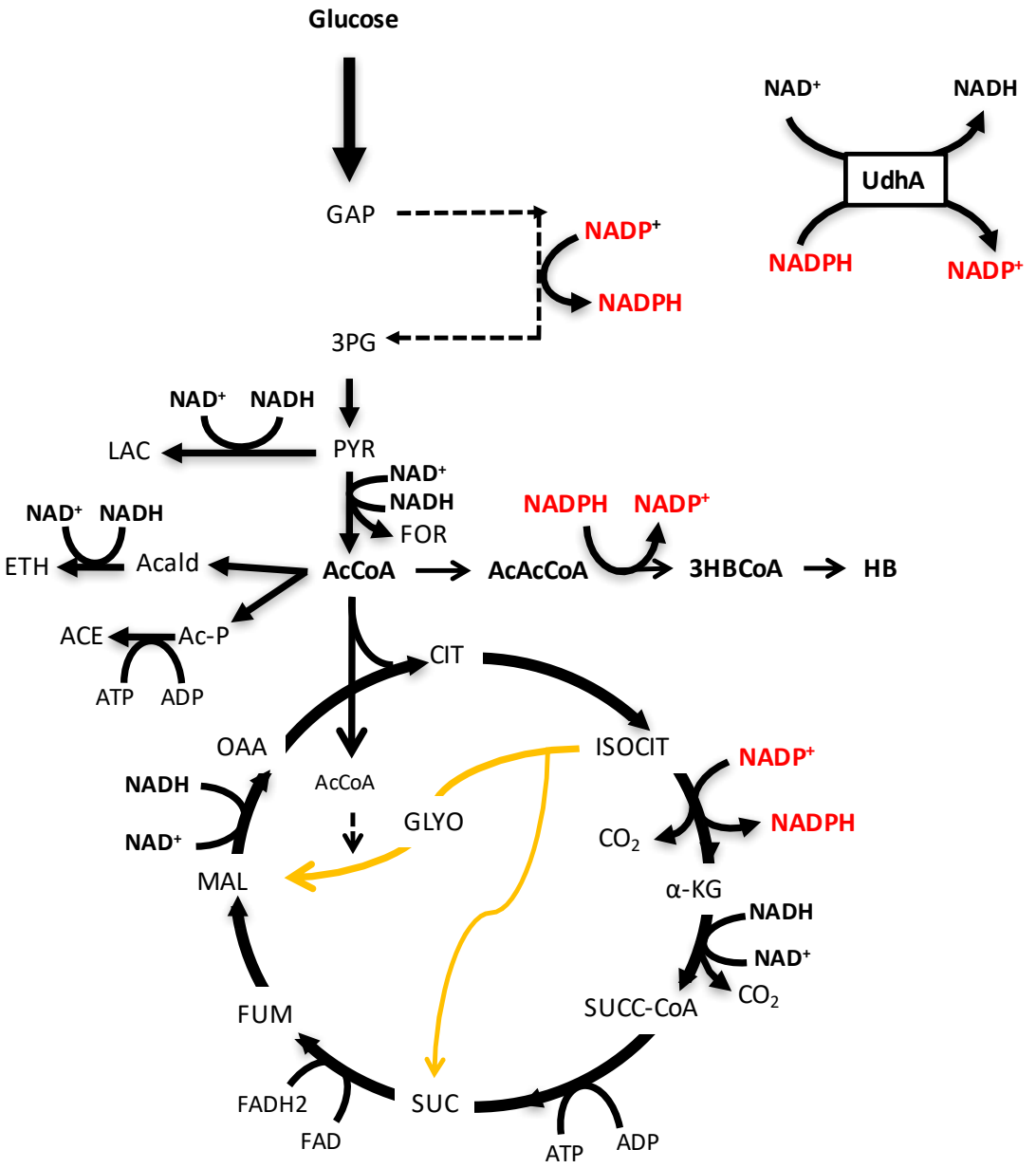

Figure 1. Metabolic network model for K12GAPNΔzwf+pPHB including most reactions (full set of reactions can be found in Appendix A1). Yellow lines indicate the reactions catalyzed by isocitrate lyase and malate synthase. The black dashed line indicates the reaction catalyzed by the NADP-preferring non-phosphorylating glyceraldehyde-3-phosphate dehydrogenase.

The activity of the soluble transhydrogenase UdhA is known to have a major role when NADPH is in excess [36]. Furthermore, Heinemann et al. [37] found that the soluble transhydrogenase is far from equilibrium *in vivo* and directed towards the formation of NADH from NADPH. As a result, it is regulated by the reaction GAPD in glycolysis to

form 1,3 bisphosphoglycerate (1,3BPG) from glyceraldehyde-3-phosphate (GAP) through the reduction of NAD^+. A NADH/NAD ratio larger than 0.018 is suggested to stop the reaction GAPD.

In the strain K12GAPNΔzwf+pPHB the GAPD is replaced by GAPN that is dependent on $NADP^+$ instead of NAD^+. This shift might allow a higher activity of the soluble transhydrogenase UdhA, as NADH is no longer produced in glycolysis.

Consequently, the effect of the reaction of the soluble transhydrogenase was studied in the strain K12GAPNΔzwf+pPHB through a sensitivity analysis.

3.2.1 Flux Balance and Sensitivity Analysis under aerobic conditions

The *in silico* simulations were performed with the following constraints:

a) Isocitrate lyase (ICL) scenarios: Three different scenarios for the activity of ICL were analyzed: 1) High: An upper limit of 0.928 mmol/g/h as found by Sauer et al. [36], 2) a medium boundary of: 0.5 mmol/g/h, and 3) no flux through the ICL.

b) Soluble transhydrogenase (UdhA) variation: The maximum flux was varied between 0 and 3.8 mmol/gCDW/h. The set maximum has been observed for an *E. coli* Δpgi growing on glucose [36]. In this strain, all catabolic flux is forced through the oxidative branch of the pentose phosphate pathway resulting in a high production of NADPH. Surplus NADPH reducing equivalents are assumed to be transferred to NADH by the soluble transhydrogenase [36].

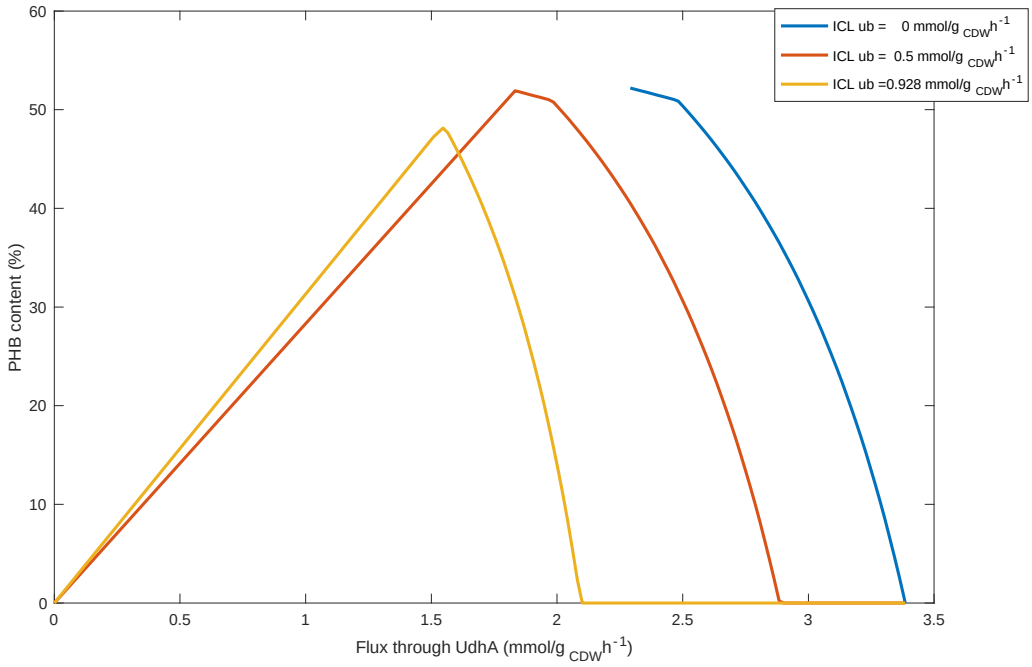

Figure 2. *In silico* prediction of PHB production in the strain K12GAPNΔzwf+pPHB as a function of transhydrogenase (UdhA) at a fixed dilution rate of 0.1 h^{-1}. The flux for different constraints for isocitrate lyase (ICL) fluxes 0.5 and 0.928 mmol/g_{CDW}/h were analyzed. The flux optimization was performed using maximization maintenance (ATP sink). A lower boundary for oxygen uptake of 4.6 mmol/g_{CDW}/h and a lower boundary for glucose uptake of 2.4 mmol/g_{CDW}/h was considered for aerobic conditions.

The *in silico* analysis shows a strong dependence of PHB production to UdhA as well as ICL. A minimal flux through the ICL (0.5 and 0.928 mmol/g_{CDW}/h) achieves a considerable amount of PHB in UdhA ranges between 1 and 2 mmol/g_{CDW}/h (see **Figure 2**). Therefore, the strain K12GAPNΔzwf+pPHB would be able to produce PHB experimentally at a flux of UdhA above 1.5 mmol/g_{CDW}/h .

When there is no flux through ICL, no solution can be found for ranges of UdhA between 0 and 2.5 mmol/g/h. At low UdhA flux, not enough ATP can be generated for growth and maintenance. The modified glycolysis generates NADPH which has to be converted to NADH for energy generation in respiration, which here is limited by the UdhA boundary. This means that only at a high flux through the UdhA the cells would be able to grow in a high titer of NADPH (generated by glycolysis and TCA cycle).

3.2.2 Aerobic Steady-state cultivations

Following the predictions from FBA, chemostat cultivations were performed under different conditions, using carbon limitation and variations in oxygen supply (see **Table 5,** fully aerobic).

Depending on the *in vivo* intracellular fluxes of UdhA and ICL, PHB accumulation was expected. To explore the flux space, experiments at different growth rates are performed, changing the impact of the putative constraints of UdhA and ICL (data not shown). Here two dilution rates (growth rate) were tested: 0.05 and 0.1 h^{-1}. The change in dilution rate not only increased the uptake rate, but also the ratio between the main cellular processes, growth, maintenance and product formation were influenced (Table 5).

Table 5. Reconciled specific rates q_i under carbon limitation at two different dilution rates (D= 0.05 and 0.1 h^{-1}). qS: specific glucose consumption rate (mmol/g_{CDW}/h). The Yields of the fermentation products are expressed in mmol/mmolS. Y_{Ace}=acetate yield, Y_{Lac}=lactate yield, Y_{PHB}= polyhydroxybutyrate yield, and Yield of biomass $Y_{(x/s)}$ (g_{CDW}/g_S).

Strain	D (h^{-1})	qO_2/qS	-qS	Y_{Ace}	Y_{lac}	Y_{PHB}	Y (gCDW/gS)
*K12	0.05	2.566	0.768	b.d.l.	b.d.l.	-	0.434
	0.1	2.244	1.359	b.d.l.	b.d.l.	-	0.471
K12+pPHB	0.04	3.276 ± 0.098	0.738 ± 0.019	0.0015 ± 0.0001	0.0379 ± 0.0022	b.d.l.	0.320 ± 0.004
	0.08	2.880 ± 0.098	1.269 ± 0.061	0.0015 ± 0.0001	0.0556 ± 0.0041	b.d.l.	0.344 ± 0.014
K12GAPNΔzwf+ pPHB	0.047	3.355 ± 0.021	0.830 ± 0.007	0.0087 ± 0.0004	0.0078 ± 0.0004	b.d.l.	0.308
	0.093	3.089 ± 0.006	1.506 ± 0.014	0.0078 ± 0.0002	0.0053 ± 0.0001	0.0001 ± 0.0001	0.360 ± 0.004

*The data used for K12 was taken from Taymaz-Nikerel and co-workers [38]. The factor to convert from Cmol of biomass to gCDW was 24.56 gCDW/Cmol.

b.d.l.: below detection level

Aerobic PHB production was observed for the strain K12GAPNΔzwf+pPHB. This strain also displayed a higher glucose uptake rate compared to K12 and K12+pPHB. This could be a result of the modified stoichiometry, specifically lower ATP yield and NADPH instead of NADH production in lower glycolysis. A higher flux is required to obtain the same amounts of ATP, which also leads to surplus NADPH surplus enforcing PHB production. At the same time, very low rates (yields) of fermentation products were observed (**Table 5)** for all strains (no overflow metabolism) [39].

The results suggest that (1) to some extent PHB production under carbon limited conditions can be enforced by increasing NADPH production, (2) there must be another

sink for NADPH, resp. the used constraints were not reached experimentally. Therefore, the redox balance was further constrained by reducing the oxygen supply**.**

3.3 Flux balance analysis under oxygen limited conditions in engineered E. coli

To analyze the impact of the O_2 uptake rate on the PHB production rate, simulations were performed varying the biomass specific O_2 uptake rate between 6 (fully aerobic) and 0 mol_{O2}/mol_S (fully anaerobic). There is significant sensitivity with respect to the oxygen uptake rate (**Figure. 3**). Experimentally, variations in the O_2 supply were implemented by changing the in-gas composition. The simulation of the strain K12+pPHB showed no PHB production under aerobic or oxygen limited conditions.

The experimental data and the FBA prediction agree qualitatively (**Figure 3**), although there is experimental data missing in the region from 2 to 2.5 O_2/S, which requires future verification. Nevertheless, the FBA prediction maximum and observed maximal PHB yield were obtained at a comparable O_2/S ratio. The predicted yield was six times higher than the maximum experimentally observed. The mismatch can be explained by further differences in the experimental and optimized flux distributions. Especially, in the FBA calculation, less carbon is entering biomass formation. Furthermore, no by-products like acetate were predicted (see Annex B).

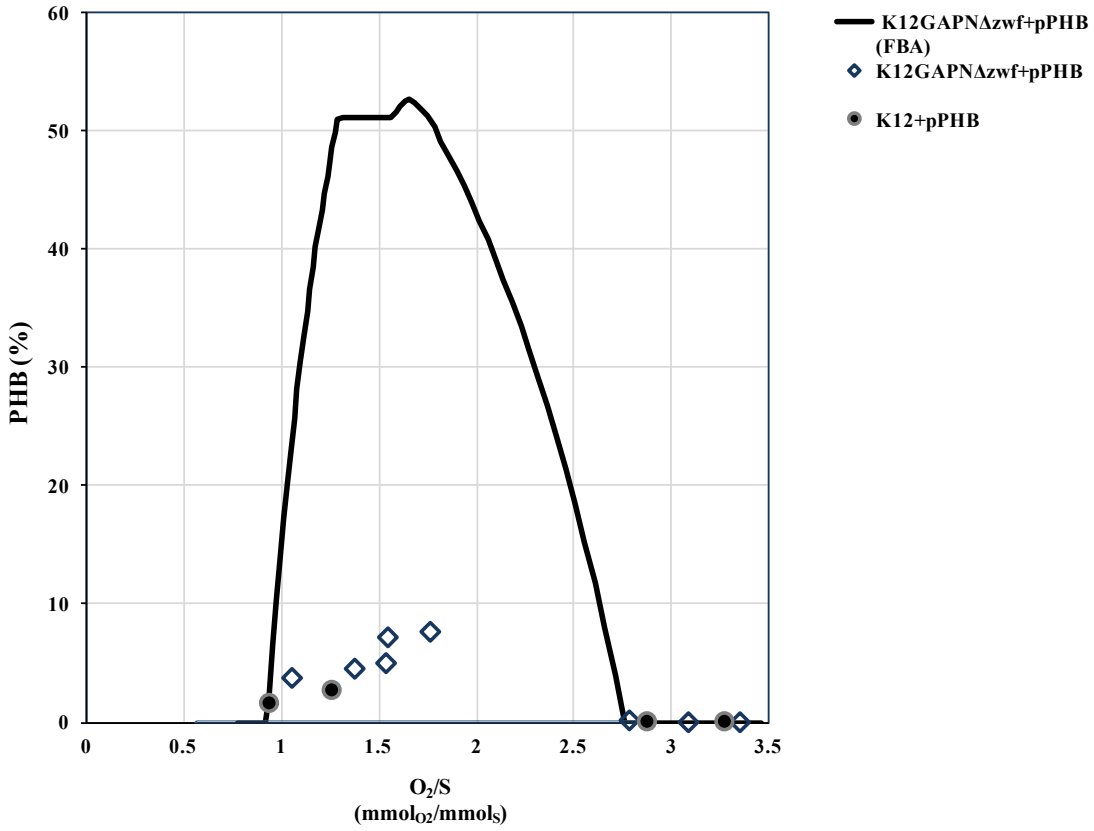

Figure 3. Measured vs. predicted PHB content (g_{PHB}/g_{CDW}) at different oxygen to substrate ratios (shown as qO_2/qS ratio) at a growth rate of 0.1 h^{-1}. For the FBA prediction, the ATP for maintenance was optimized (reaction mATP) and following upper boundaries were set for acetate production 2.5 $mmol/g_{CDW}/h$, for ICL 3.5 $mmol/g_{CDW}/h$, and UdhA 3.8 $mmol/g_{CDW}/h$.

Comparable to the prediction, no PHB formation was observed under fully aerobic conditions (right side of the graph, 3.2 O_2/S). With decreasing oxygen supply, PHB accumulation increases until about 1.7 O_2/S. At this state there is also a bump that is related to a change in the qS which not uniformly drops at a ratio of 1.3 O_2/S. Alternatively the qS remains constant and then drops at a ratio of 1 O_2/S. At lower O_2/S supply, the yield decreases again, as expected more fermentation products were observed (**Table 6**.).

3.3.1 Oxygen limited steady state cultivations

Comparing the two different glycolysis strains, it was oberserved that lactate production decreased for strain K12GAPNΔzwf+pPHB (nearly absent), while for K12+pPHB a yield of 0.506 $mmol_{Lac}/mmol_S$ was obtained (see **Table 6**). Also other fermentation products were produced at higher rates (yields) by K12+pPHB strain, except ethanol production which was three-fold lower.

Table 6. Comparison of the fermentation product yields ($mmol_i/mmol_S$) during steady state oxygen limited chemostat (D= 0.1 h^{-1}) for the strains K12+pPHB and K12GAPNΔzwf+pPHB (measured at a similar O_2/S ratio of approximately 1.5 ($mmol_{O2}/mmol_S$)). Lac: Lactate, Eth: ethanol, Glyc: glycerol, Suc: succinate, PHB: polyhydroxybutyrate, X: biomass.

Strain	qO_2/qS	Y_{Ace}	Y_{Lac}	Y_{Eth}	Y_{Glyc}	Y_{Succ}	Y_{PHB}	Y_X (gCDW/gS)
K12+pPHB	1.258 ± 0.021	0.2932 ± 0.1041	0.5059 ± 0.1746	0.0067 ± 0.0257	0.1434 ± 0.049	0.3012 ± 0.0907	0.0045 ± 0.0001	0.081 ± 0.231
K12GAPNΔzwf+pPHB	1.543 ± 0.009	0.3857 ± 0.0076	b.d.l.	0.3284 ± 0.0097	0.172 ± 0.0035	0.004 ± 0.0001	0.0276 ± 0.0005	0.168 ± 0.001

b.d.l.: below detection level

The main difference between the different strains are the glycolytic cofactor dependencies, i.e. NAD(P)H produced which lead to changes of production yields of certain fermentation products (Table 6). A common indicator of carbon excess is the formation of acetate which was produced by all the strains as a result of oxygen limitation.

When the system is aerobic, the tricarboxylic acid cycle (TCA) will be active and produce NADH and FADH to be later respired in the electron transport chain that will generate ATP. In contrast, in oxygen limited conditions fumarate reductase is active and α-ketoglutarate dehydrogenase is repressed which leads to a reduced activity of the oxidative reactions of the TCA cycle. Acetyl-CoA can be formed from pyruvate by pyruvate formate lyase (PFL). For the strain K12GAPNΔzwf+pPHB, acetyl-CoA was preferred against lactate (Figure 4), which was mainly converted to acetate and ethanol and to some extent succinate, formate and PHB [40]. For the strain K12+pPHB, lactate and succinate had a higher yield of 0.5 and 0.3 respectively (Table 6).

3.4 Metabolome response: the effect of the gapA::gapN replacement on the aerobic metabolome

3.4.1 Impact on the metabolites of central carbon metabolism under aerobic conditions

In order to assess the changes performed in central carbon metabolism of the strain K12GAPNΔzwf+pPHB, the strain was compared to the strain K12+pPHB. The comparison was performed at a dilution rate of 0.1 h^{-1} (see **Figure 4**).

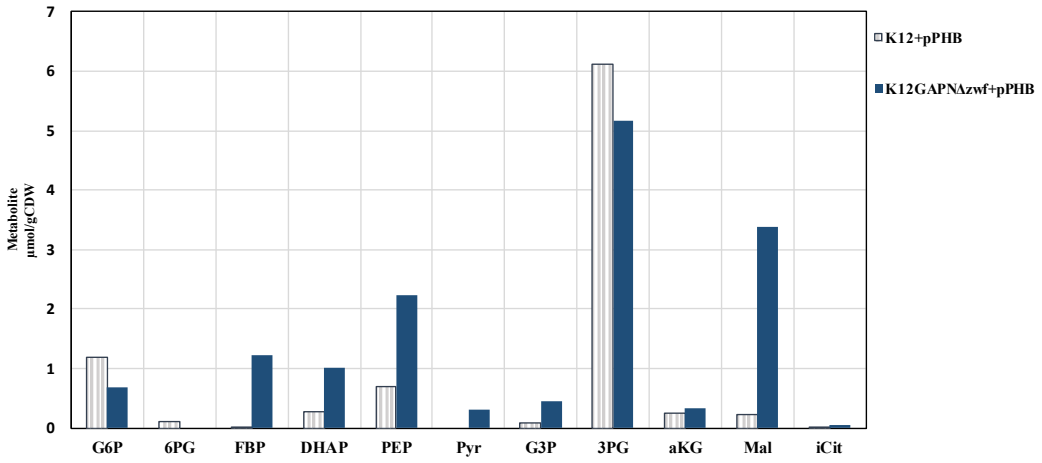

Figure 4. Comparison of the metabolites concentration of the modified strains K12+pPHB and K12GAPNΔzwf+pPHB at an approximate dilution rate of 0.1 h^{-1}, under fully aerobic conditions.

Most of the metabolites in K12GAPNΔzwf+pPHB showed a higher concentration compared to strain K12+pPHB, except for G6P (Glucose-6-phosphate) and 3PG (Glycerol-3-phosphate). As a result of the knockout of *zwf* in K12GAPNΔzwf+pPHB, no 6PG (6-phosphogluconate) was detected. Moreover, the strain K12GAPNΔzwf+pPHB showed a small increase in pyruvate concentration and then malate appears to accumulate.

3.4.2 Concentration of product pathway precursors

Theoretical, network based thermodynamics suggest that the driving force for the PHB product pathway critically depends on the precursor ratios, i.e. AcCoA/CoA as well as NADPH/NADP. While AcCoA and CoA can be measured directly, NAD(P)H/NAD(P) are not stable during sample processing. These ratios were therefore determined from equilibrium reactions [28,32]. For the different strains and condtitions, similar

[NADH]/[NAD^+] ratios were found under fully aerobic conditions, and lower for K12GAPNΔzwf+pPHB under oxygen limited conditions (Table 7). The ratio of [NADPH/$NADP^+$] remained in a comparable range in all the strains.

Table 7. Estimation of the [NADH]/[NAD^+] and [NADPH]/[$NADP^+$] ratios in the different strains at a dilution rate of 0.1 h^{-1} under aerobic and oxygen limited conditions. AEC (Adenalyte energy charge) was determined under aerobic conditions.

	[NADH]/[NAD^+]		**[NADPH]/[$NADP^+$]**		**AEC**	
	Aerobic	Oxygen limited	Aerobic	Oxygen limited	Aerobic	Oxygen limited
K12*	0.021 ± 0.002	na	1.108 ± 0.135	na	0.80 ± 0.0	na
K12+pPHB	0.024 ± 0.001	1.21 ± 0.001	1.037 ± 0.041	0.485 ± 0.243	0.789 ± 0.008	na
K12GAPNΔzwf +pPHB	0.022 ± 0.003	0.029 ± 0.005	0.939 ± 0.348	0.873 ± 0.287	0.792 ± 0.019	na

na = not available, *values taken from Nikerel et al. [41].

Additionally, in the analysis of metabolite data, Acetyl-CoA and CoA were measured. The AcCoA/CoA together with the NADPH/$NADP^+$ ratio are important factors to analyze regarding the effect on PHB production as stated in in the thermodynamic study performed in **Chapter 2.** In such study was found that above a AcCoA/CoA ratio of 2 the pathway was feasible towards PHB, this is in agreement with the metabolome measurement results. Experimentally at a AcCoA/CoA ratio of 2.7 (see **Figure 5.**) the maximum PHB was attained in the strain K12GAPNΔzwf+pPHB. Thus, the oxygen limited conditions lead to an increase of the AcCoA/CoA ratio compared to the aerobic conditions. On the other hand, the NADPH/$NADP^+$ ratio stayed within a stable range until PHB % dropped at the same point (O_2/S =1.3) as the AcCoA/CoA ratio. Therefore, a strong linear correlation between AcCoA/CoA and PHB production was observed with a R^2 of 0.918, while the NADPH/$NADP^+$ ratio showed no significant correlation with a R^2 0.0026.

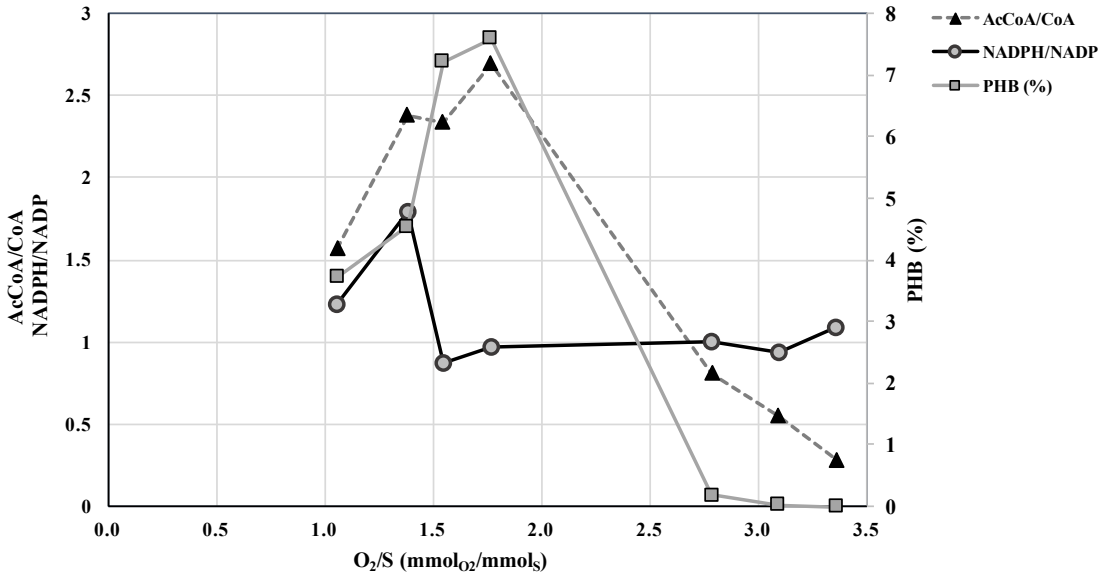

Figure 5. Measured NADPH/NADP$^+$ and AcCoA/CoA ratios during a transition from aerobic (right side, high O_2/S) to oxygen limited conditions in the strain K12GAPNΔzwf+pPHB. The ratio of NADPH/NADP$^+$ was calculated from an assumed equilibrium reaction (Gdh).

3.4.3 Impact of oxygen-limited conditions on the metabolome

The metabolites involved in glycolysis were affected by the redox state of the cells as a consequence of the reducing power produced in the form of NAD(P)H. To show this possible relocation of metabolites the profile of every qO_2/qS ratio was analyzed in the aerobic and oxygen limited condition (see **Figure 6**). Metabolite concentrations increasing with oxygen availability were 3PG (3-phosphoglycerate), PEP (Phosphoenolpyruvate), Tre (Trehalose) and UDP-Glc (UDP-Glucose).

In addition, the accumulation of some metabolites from the TCA, such as malate and citrate can be observed. On the other hand, all the metabolites from the non-oxidative branch of the PPP remained low as a result of the knock-out of the *zwf* gene.

In the strain K12GAPNΔzwf+pPHB shows a small increase in pyruvate concentration and then malate appears to accumulate. The raw data with the standard errors can be found in **Annex D**.

The amino acid profile of the strain K12GAPNΔzwf+pPHB for every O_2/S was studied and arranged according to the metabolites each amino acid is derived from (see **Annex E**). The group of amino acids that are NADPH dependent for their synthesis are Val

(Valine), Pro (Proline), Thr (Threonine), Asp (Asparagine), Tyr (Tyrosine), Trp (Tryptophan), Lys (Lysine) and Glu (Glutamate) [42]. From this group, the ones that showed higher concentrations are Val, Glu, Lys and Asp. The amino acids derived from pyruvate (Ala, Val and Leu) showed up at a higher concentration than other amino acids, yet at a steady range. Interestingly, the amino acid Gly (Glycine) which is derived from 3PG prevails at higher concentrations than the other amino acids from 3PG, this agrees with the attained yield of this metabolite under aerobic conditions. The amino acids Glu and Gln, which are derived from α-KG and therefore closely linked to the TCA, emerged in higher yields than the amino acids from OAA (oxaloacetate). Glutamate is especially predominant at the highest O_2/S (fully aerobic conditions) and then decreased at the lowest O_2/S. However, in wild type *E. coli,* large concentrations of glutamate have been found [21]. This trend from large to low concentrations goes in hand to the O_2/S in all the amino acids profile. Yet, the enhancement of NADPH/NADP ratio was not found to have an effect on the amino acids dependent on NADPH.

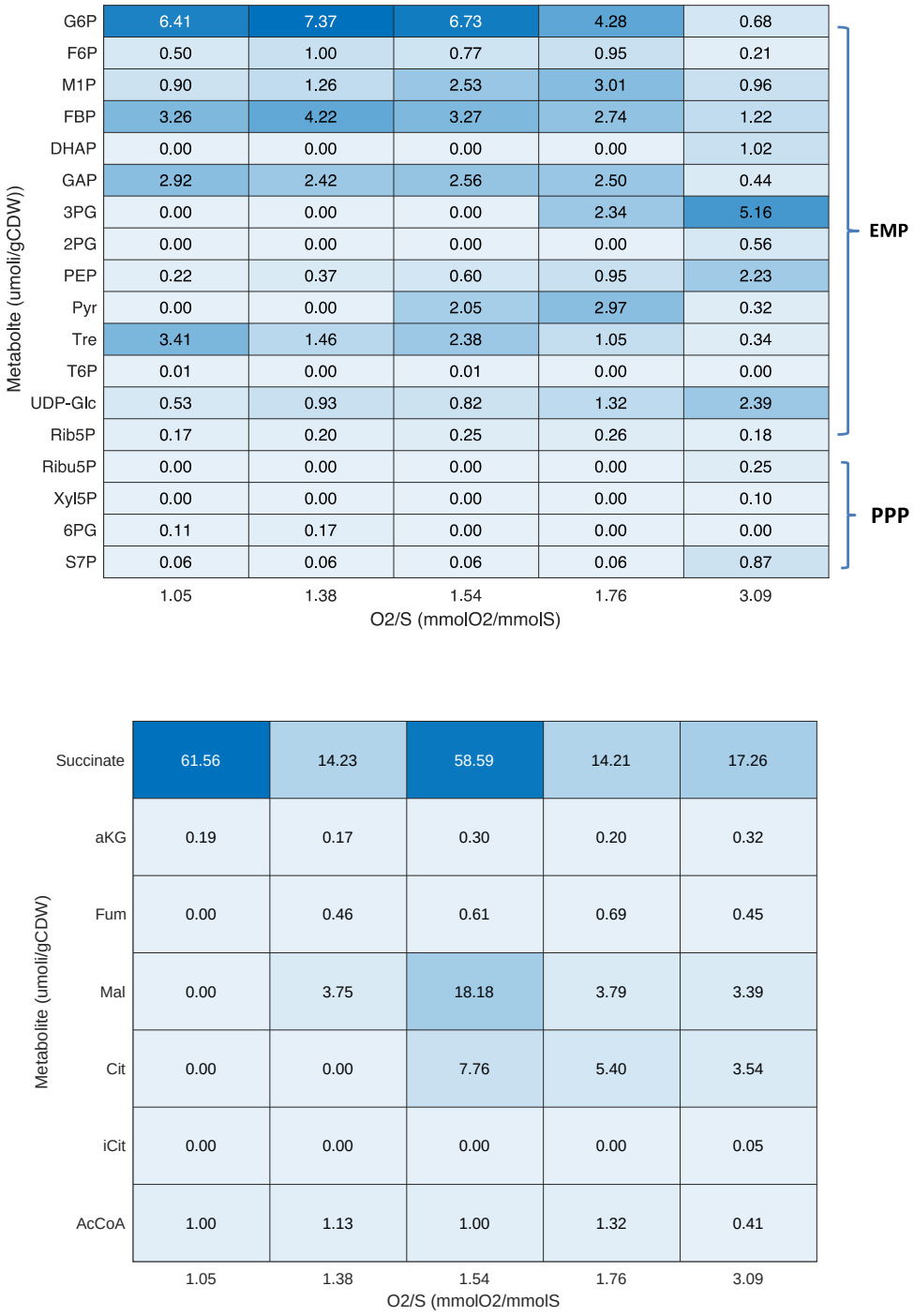

Figure 6. Heatmap of the concentration of metabolites during the transition from fully aerobic to oxygen limited conditions in the strain K12GAPNΔzwf+pPHB at a D= 0.1 h. The upper graph represents metabolites from the EMP (Embden-Meyerhof-Parnas) and PPP (Pentose Phosphate Pathway). The bottom graph represents the metabolites from the TCA (Tricarboxylic acid) cycle. Aerobic: O_2/S =3.09 at D= 0.1 h^{-1}. Oxygen limited: data of O_2/S from 1.05 to 1.76 $^{-1}$.

4. Discussion

4.1 Impact on physiology and metabolism of the substitution of gapA::gapN

The enginnered strain K12GAPNΔzwf+pPHB was designed to enhance the availability of NADPH for biomass synthesis and PHB production in the cells.
In silico analysis showed a high sensitivity of PHB production with respect to the flux through ICL and UdhA. A maximum accumulation of 53% PHB was predicted with no flux through the ICL and a low flux through the UdhA. It is well known that the UdhA plays a significant role in the reoxidation of NADPH when this appears in excess in the cells [4,36,43]. This possible scenario was tested experimentally under carbon limitation and fully aerobic conditions. A very low PHB yield was observed under these conditions in the strain K12+pPHB and K12GAPNΔzwf+pPHB respectively. The glyoxylate shunt has been found to be repressed in *E. coli* under growth in glucose aerobic conditions [44], therefore a low or absent flux through the ICL, and a considerable activity of UdhA (higher than 1 mmol/g_{CDW}/h) corresponds the experimental data obtained at aerobic conditions at a D =0.1 h^{-1}.
Traditionally, PHB formation has been described as a product from overflow metabolism under growth limiting conditions. However, Lee et al. [45] showed experimentally that *E. coli* transformed with the PHB genes from *C. necator* was able to produce PHB in a batch and fed-batch culture without nutrient limitation. Until now, other limitations than carbon have shown to favor PHB formation [46]. Still, the strain K12GAPNΔzwf+pPHB showed the possibility to form PHB in small amounts. Strain K12+pPHB did produce PHB in batch cultures but not under aerobic chemostat conditions.

4.2 Effect on the oxygen limitation on the redox state of the cells and the possibility to direct electrons to PHB formation

To enforce more carbon towards PHB, oxygen limiting conditions were evaluated in this study. Strain K12GAPNΔzwf+pPHB showed that at lower oxygen concentration some PHB could be formed in a higher percentage (7.6 % PHB) than under aerobic conditions and (0.2 % PHB). In comparison to the strain K12+pPHB no PHB was formed under aerobic conditions and a small percentage was achieved under oxygen limitation (2.7 % PHB). The reason for the difference likely results from the shift in glycolysis for

the NADPH production in the strain K12GAPNΔzwf+pPHB. The replacement of *gapA* to *gapN*, was earlier predicted to generate more thermodynamic driving force for the PHB pathway (**Chapter 2**). Also, FBA predicted PHB production under oxygen limited conditions. Comparting the prediction with experimental data, the expected trends were reproduced qualitatively (the model predicted a higher PHB content). The discrepancy from the model might be a result of the re-oxidation of NADPH through other metabolic NADPH dependent reactions, and from up or down regulation of certain genes to adjust to the modifications performed in the cell [47]. Especially, earlier studies showed that NADH-quinone oxidoreductase subunit F (*nuoF*) can evolve and lead to a NADH:ubiquinone oxidoreductase that also accepts electrons directly from NADPH. When the cells were under redox stress, that is more molecules of NADPH were produced the cells were able to have a fast adaptive evolution to cope with stress [48]. Including this scenario in the FBA prediction, the predicted PHB content is lower (around 13 %) and very close to the experimental results.

Experimentally, a change in redox cofactor in glycolysis induced changes in the fermentation products formed to alleviate redox stress, more prominently under oxygen limited conditions in chemostat. The specific glucose uptake rate of the strains under study showed a different behavior. Under anaerobic conditions, Yang et al. [49] reported a value of 3.55 mmol/g_{CDW}/h in *E. coli* GJT001 (WT). The result is comparable to what was obtained in this study 3.03 mmol/g_{CDW}/h in the strain K12GAPNΔzwf+pPHB at oxygen limited conditions.

Next to PHB accumulation, the profile of fermentation products changed to alleviate redox stress. Especially, K12GANPΔzwf+pPHB produced more acetate and ethanol, but less lactate compared to K12+pPHB. Oxygen limited conditions generated a higher ratio of NADH/NAD^+ that resulted in the production of fermentation products. In the strain K12+pPHB 2 NADH are produced, whereas in K12GAPNΔzwf+pPHB 2 NADPH are produced in glycolysis (glucose to pyruvate). The strain K12+pPHB (only PHB genes) formed lactate as major fermentation by-product, followed by formate and succinate [14,50]. In K12GAPNΔzwf+pPHB lactate was not formed as a fermentation by-product under oxygen limited conditions, but instead acetate, formate and ethanol (see **Table 6.**).

4.3 Metabolites profile under aerobic and oxygen limited conditions

The strain K12GAPNΔzwf+pPHB was designed to synthesize more NADPH than required for biosynthetic demands (about 15.8–17.3 mmol of NADPH per gram of cells) [36]. The results showed that the cells were able to shift the overproduction of the NADPH reducing equivalents in the synthesis of PHB. Despite the overproduction of NADPH there was no increase in NADPH/$NADP^+$ ratios, even at lower oxygen availability. This indicates a strong regulation of the NADPH load in the cells and likely that the NADPH concentration is not directly influencing the carbon flux towards PHB.

Earlier studies reported NADPH/$NADP^+$ ratios in a range of 1.05-58.82, and 0.03-0.27 for NADH/NAD^+ [51]. This corresponds to the data obtained in our study through the equilibrium reactions. The ratios of NADH/NAD^+ in the strain K12+pPHB increased under oxygen-limited conditions from 0.02 to 1.2, this increment goes in agreement with the results obtained by Graef et al. [14]. Conversely, the ratio of NADPH/$NADP^+$ stays within a range of 1. A similar NADPH/$NADP^+$ ratio (approximately 1.2) has been observed in an engineered strain *E. coli* (GJT001) for PHB production [4] in aerobic conditions and grown in glucose. This implies that the control of NADPH oxidation does not seem to be a burden under aerobic and oxygen limited conditions.
Wegen et al. [13] suggested that the flux towards PHB is strongly influenced by the AcCoA/CoA ratio, which also is in line with a thermodynamic analysis of the PHB production pathway (see **Chapter 2**.). Here, we also observed a correlation between PHB content and the AcCoA/CoA ratio in experiments with the strain K12GAPNΔzwf+pPHB.

The importance of acetyl-CoA has been addressed in some studies as a precursor that does not represent a limitation in PHB formation, with the argument that production of acetate was observed in *E. coli* when PHB is produced and therefore was present in excess [4]. However, there was no clear explanation regarding the influence of acetyl-CoA in PHB formation [2]. Moreover, there is no detailed information regarding the AcCoA/CoA ratio other than concentrations which might be too ambiguous to provide a conclusion.

The strain K12GAPNΔzwf+pPHB furthermore produces a lower amount of NADH and ATP through substrate level phosphorylation. Nevertheless, the adenylate energy charge (AEC) was within the range of values found in non-modified K12 [52]. During growth *E. coli* has an adenylate energy charge around 0.8 [52], which is a value close to the one

obtained in the strains in this study. Therefore, in our chemostat cultivations, there was no obvious energy limitation as reported in other studies performed with a strain of *E. coli* with the substitution of *gapA::gapN* [35]. Likely the difference is due to the growth under carbon limitation in a chemostat in our study versus growth in a batch cultivation by Centeno Leija et al. [6].

From the experimental observations and simulations, the TCA cycle plays an important role in the availability of acetyl-CoA and PHB production. Under oxygen limiting conditions, the flux of the TCA cycle decreases, this results in a build-up of acetyl-CoA/CoA ratio that led to by-product formation and some PHB formation as assessed in the thermodynamic study (**Chapter 2**.).

Furthermore, glycolysis appears to have a higher concentration of pyruvate under oxygen limited conditions, as a result of accumulated metabolites and less flux through the TCA cycle. The precursor of acetyl-CoA, pyruvate, appeared with the highest concentration at a range of 1.7-1.5 of O_2/S ratio, where a higher PHB yield was obtained. This confirms the metabolite profile that support PHB formation.

5. Conclusion

Genetic engineering could be used to modify specific steps to tailor the redox metabolites to favor the formation of desired compounds. To fulfill the metabolic demands for cell metabolism, modifications in glycolysis is a proposed approach to create an increased flux towards PHB formation. In this study, we studied the impact of NADPH enhancement in *E. coli* for stimulating PHB formation. The results demonstrated the adaptability of the cells under redox stress conditions, and that other parameters have to be taken into account for optimizing PHB formation. Especially maximizing the AcCoA/CoA ratio is needed for an effective production of PHB and potentially also other reduced industrial products derived from acetyl-CoA.

References

1. Perez-Zabaleta M, Sjöberg G, Guevara-Martínez M, Jarmander J, Gustavsson M, Quillaguamán J, et al. Increasing the production of (R)-3-hydroxybutyrate in recombinant Escherichia coli by improved cofactor supply. Microb Cell Fact. BioMed Central; 2016;15:1–10.

2. Tyo KEJ, Fischer CR, Simeon F, Stephanopoulos G. Analysis of polyhydroxybutyrate flux limitations by systematic genetic and metabolic perturbations. Metab Eng [Internet]. Elsevier; 2010 [cited 2014 Nov 19];12:187–95. Available from: http://www.ncbi.nlm.nih.gov/pubmed/19879956

3. Shimizu MMK· K. Fermentation characteristics and protein expression patterns in a recombinant Escherichia coli mutant lacking phosphoglucose isomerase for poly (3-hydroxybutyrate) production. 2003;244–55.

4. Sánchez AM, Andrews J, Hussein I, Bennett GN, San KY. Effect of overexpression of a soluble pyridine nucleotide transhydrogenase (UdhA) on the production of poly(3-hydroxybutyrate) in Escherichia coli. Biotechnol Prog. 2006;22:420–5.

5. Martínez I, Zhu J, Lin H, Bennett GN, San K-Y. Replacing Escherichia coli NAD-dependent glyceraldehyde 3-phosphate dehydrogenase (GAPDH) with a NADP-dependent enzyme from Clostridium acetobutylicum facilitates NADPH dependent pathways. Metab Eng [Internet]. 2008 [cited 2015 Mar 30];10:352–9. Available from: http://www.ncbi.nlm.nih.gov/pubmed/18852061

6. Centeno-Leija S, Huerta-Beristain G, Giles-Gómez M, Bolivar F, Gosset G, Martinez A. Improving poly-3-hydroxybutyrate production in Escherichia coli by combining the increase in the NADPH pool and acetyl-CoA availability. Antonie Van Leeuwenhoek [Internet]. 2014;105:687–96. Available from: http://link.springer.com/10.1007/s10482-014-0124-5

7. Shi H, Nikawa J, Shimizu K. Effect of modifying metabolic network on poly-3-hydroxybutyrate biosynthesis in recombinant Escherichia coli. J Biosci Bioeng. 1999;

8. Choi SYL and J. MET ABOLlC ENGINEERING OF ESCHERICHIA COLI FOR THE PRODUCTION OF POLYHYDROXYALKANOATES. Metab Eng. Elsevier; 1998;337–41.

9. Koller M, Braunegg G. Potential and Prospects of Continuous Polyhydroxyalkanoate (PHA) Production. Bioengineering [Internet]. 2015 [cited 2015 Sep 8];2:94–121. Available from: http://www.mdpi.com/2306-5354/2/2/94/

10. Reitzer L. Nitrogen Assimilation and Global Regulation in Escherichia coli . Annu Rev Microbiol. 2003;57:155–76.

11. Nicolas C, Kiefer P, Letisse F, Krömer J, Massou S, Soucaille P, et al. Response of the central metabolism of Escherichia coli to modified expression of the gene encoding the glucose-6-phosphate dehydrogenase. FEBS Lett [Internet]. 2007 [cited 2014 Nov 9];581:3771–6. Available from: http://www.ncbi.nlm.nih.gov/pubmed/17631881

12. Kocharin K, Siewers V, Nielsen J. Improved polyhydroxybutyrate production by Saccharomyces cerevisiae through the use of the phosphoketolase pathway. Biotechnol Bioeng. 2013;110:2216–24.

13. Van Wegen RJ, Lee SY, Middelberg APJ. Metabolic and kinetic analysis of poly(3-Hydroxybutyrate) production by recombinant Escherichia coli. Biotechnol Bioeng. 2001;74:70–80.

14. Graef MR De, Alexeeva S, Snoep JL, Mattos MJT De. The Steady-State Internal Redox State (NADH / NAD) Reflects the External Redox State and Is Correlated with Catabolic Adaptation in Escherichia coli. J Bacteriol. 1999;181:2351–7.

15. Blattner FR, Plunkett G, Bloch CA, Perna NT, Burland V, Riley M, et al. The complete genome sequence of Escherichia coli K-12. Science (80-). 1997;277:1453–62.

16. Datsenko KA, Wanner BL. One-step inactivation of chromosomal genes in Escherichia coli K-12 using PCR products. 2000;2000.

17. Olavarria K, Fina A, Velasco MI, van Loosdrecht MCM, Wahl SA. Metabolism of sucrose in a non-fermentative Escherichia coli under oxygen limitation. Appl Microbiol Biotechnol. Applied Microbiology and Biotechnology; 2019;103:6245–56.

18. Bradford MM 1976. A rapid and sensitive method for the quantitation of microgram quantities of protein utilizing the principle of protein-dye binding. Anal Biochem. 1975;72:248–54.

19. Fillinger S, Boschi-Muller S, Azza S, Dervyn E, Branlant G, Aymerich S. Two glyceraldehyde-3-phosphate dehydrogenases with opposite physiological roles in a nonphotosynthetic bacterium. J Biol Chem. 2000;275:14031–7.

20. Marchal S, Branlant G. Characterization of the amino acids involved in substrate specificity of nonphosphorylating glyceraldehyde-3-phosphate dehydrogenase from Streptococcus mutans. J Biol Chem. 2002;277:39235–42.

21. Taymaz-Nikerel H, de Mey M, Ras C, ten Pierick A, Seifar RM, van Dam JC, et al. Development and application of a differential method for reliable metabolome analysis in Escherichia coli. Anal Biochem [Internet]. Elsevier Inc.; 2009 [cited 2014 Nov 19];386:9–19. Available from: http://www.ncbi.nlm.nih.gov/pubmed/19084496

22. Verduyn C, Postma E, Scheffers WA, Van Dijken JP. Effect of benzoic acid on metabolic fluxes in yeasts: A continuous-culture study on the regulation of respiration and alcoholic fermentation. Yeast. 1992;8:501–17.

23. Velasco Alvarez MI, Ten Pierick A, van Dam PTN, Maleki Seifar R, van Loosdrecht MCM, Wahl SA. Microscale quantitative analysis of polyhydroxybutyrate in prokaryotes using IDMS. Metabolites. 2017;7:1–8.

24. Wu L, Mashego MR, van Dam JC, Proell AM, Vinke JL, Ras C, et al. Quantitative analysis of the microbial metabolome by isotope dilution mass spectrometry using uniformly 13C-labeled cell extracts as internal standards. Anal Biochem [Internet]. 2005 [cited 2015 Aug 20];336:164–71. Available from: http://www.ncbi.nlm.nih.gov/pubmed/15620880

25. Wahl SA, Seifar RM, ten Pierick A, Ras C, van Dam JC, Heijnen JJ, et al. Quantitative Metabolomics Using ID-MS. Methods Mol Biol [Internet]. 2014. p. 91–105. Available from: http://link.springer.com/10.1007/978-1-4939-1170-7_6

26. de Jonge LP, Buijs NAA, ten Pierick A, Deshmukh A, Zhao Z, Kiel JAKW, et al. Scale-down of penicillin production in Penicillium chrysogenum. Biotechnol J. 2011;6:944–58.

27. Mashego MR, Wu L, Van Dam JC, Ras C, Vinke JL, Van Winden WA, et al. MIRACLE: mass isotopomer ratio analysis of U-13C-labeled extracts. A new method for accurate quantification of changes in concentrations of intracellular metabolites. Biotechnol Bioeng [Internet]. 2004;85:620–8. Available from: https://doi.org/10.1002/bit.10907

28. Canelas B, Pierick A, Ras C, Seifar RM, Dam JC Van, Gulik WM Van, et al. Quantitative Evaluation of Intracellular Metabolite Extraction Techniques for Yeast Metabolomics. 2009;81:7379–89.

29. Cueto-Rojas HF, Seifar RM, Pierick A Ten, Heijnen SJ, Wahl A. Accurate measurement of the in vivo ammonium concentration in Saccharomyces cerevisiae. Metabolites. 2016;6.

30. Noor E, Bar-Even A, Flamholz A, Reznik E, Liebermeister W, Milo R. Pathway Thermodynamics Highlights Kinetic Obstacles in Central Metabolism. PLoS Comput Biol. 2014;10.

31. Wang L, Lai L, Ouyang Q, Tang C. Flux balance analysis of ammonia assimilation network in E. coli predicts preferred regulation point. PLoS One. 2011;6.

32. Taymaz-Nikerel H. Quantitative analysis of relationships between fluxome and metabolome in Escherichia coli. TU Delft - Dep. Biotechnol. - Bioprocess Technol. Gr. 2010.

33. Schellenberger J, Que R, Fleming RMT, Thiele I, Orth JD, Feist AM, et al. Quantitative prediction of cellular metabolism with constraint-based models: The COBRA Toolbox v2.0. Nat Protoc. 2011;6:1290–307.

34. Edwards JS, Palsson BO. The Escherichia coli MG1655 in silico metabolic genotype: Its definition, characteristics, and capabilities. Proc Natl Acad Sci U S A [Internet]. 2000 [cited 2015 Mar 30];97:5528–33. Available from: http://www.pnas.org/content/97/10/5528.short

35. Centeno-Leija S, Utrilla J, Flores N, Rodriguez A, Gosset G, Martinez A. Metabolic and transcriptional response of Escherichia coli with a NADP+-dependent glyceraldehyde 3-phosphate dehydrogenase from Streptococcus mutans. Antonie Van Leeuwenhoek [Internet]. 2013;104:913–24. Available from: http://link.springer.com/10.1007/s10482-013-0010-6

36. Sauer U, Canonaco F, Heri S, Perrenoud A, Fischer E. The soluble and membrane-bound transhydrogenases UdhA and PntAB have divergent functions in NADPH metabolism of Escherichia coli. J Biol Chem [Internet]. 2004 [cited 2014 Nov 19];279:6613–9. Available from: http://www.ncbi.nlm.nih.gov/pubmed/14660605

37. Kümmel A, Panke S, Heinemann M. Putative regulatory sites unraveled by network-embedded thermodynamic analysis of metabolome data. Mol Syst Biol. 2006;2:1–10.

38. Taymaz-Nikerel H, Borujeni AE, Verheijen PJT, Heijnen JJ, van Gulik WM. Genome-derived minimal metabolic models for Escherichia coli MG1655 with estimated in vivo respiratory ATP stoichiometry. Biotechnol Bioeng. 2010;107:369–81.

39. Verhagen KJ, van Gulik WM, Wahl SA. Dynamics in redox metabolism, from stoichiometry towards kinetics. Curr Opin Biotechnol [Internet]. Elsevier Ltd; 2020;64:116–23. Available from: https://doi.org/10.1016/j.copbio.2020.01.002

40. Shalel-Levanon S, San KY, Bennett GN. Effect of ArcA and FNR on the expression of genes related to the oxygen regulation and the glycolysis pathway in Escherichia coli under microaerobic growth conditions. Biotechnol Bioeng. 2005;92:147–59.

41. Taymaz-Nikerel H, De Mey M, Baart G, Maertens J, Heijnen JJ, van Gulik W. Changes in substrate availability in Escherichia coli lead to rapid metabolite, flux and growth rate

responses. Metab Eng [Internet]. Elsevier; 2013 [cited 2014 Nov 12];16:115–29. Available from: http://www.ncbi.nlm.nih.gov/pubmed/23370343

42. Akashi H, Gojobori T. Metabolic efficiency and amino acid composition in the proteomes of Escherichia coli and Bacillus subtilis. Proc Natl Acad Sci U S A. 2002;99:3695–700.

43. Canonaco F, Hess TA, Heri S, Wang T, Szyperski T, Sauer U. Metabolic £ ux response to phosphoglucose isomerase knock-out in Escherichia coli and impact of overexpression of the soluble transhydrogenase UdhA. 2001;204:247–52.

44. Carlson R, Srienc F. Fundamental Escherichia coli biochemical pathways for biomass and energy production: identification of reactions. Biotechnol Bioeng [Internet]. 2004 [cited 2015 Apr 23];85:1–19. Available from: http://www.ncbi.nlm.nih.gov/pubmed/14705007

45. Lee SY, Chang HN. Effect of complex nitrogen source on the synthesis and accumulation of poly(3-hydroxybutyric acid) by recombinant Escherichia coli in flask and fed-batch cultures. J Environ Polym Degrad. 1994;2:169–76.

46. Du, GC; Chen, J; Yu, J; Lun S. Continuous production of poly-3-hydrobutyrate by Ralstonia eutropha in a two-stage culture system. J Biotechnol. 2001;88, 59-65.:59–65.

47. Seo JH, Lee WH, Chin YW, Han NS, Kim MD. Enhanced production of GDP-l-fucose by overexpression of NADPH regenerator in recombinant Escherichia coli. Appl Microbiol Biotechnol. 2011;91:967–76.

48. Auriol C, Bestel-Corre G, Claude J-B, Soucaille P, Meynial-Salles I. Stress-induced evolution of Escherichia coli points to original concepts in respiratory cofactor selectivity. Proc Natl Acad Sci U S A. 2011;108:1278–83.

49. Yang YT, San KY, Bennett GN. Redistribution of metabolic fluxes in Escherichia coli with fermentative lactate dehydrogenase overexpression and deletion. Metab Eng. 1999;1:141–52.

50. Sekar K, Tyo KEJ. Regulatory effects on central carbon metabolism from poly-3-hydroxybutryate synthesis. Metab Eng [Internet]. Elsevier; 2015 [cited 2015 Jan 17];28:180–9. Available from: http://linkinghub.elsevier.com/retrieve/pii/S1096717615000051

51. Spaans SK, Weusthuis RA, van der Oost J, Kengen SWM. NADPH-generating systems in bacteria and archaea. Front Microbiol. 2015;6:1–27.

52. Chapman AG, Fall L, Atkinson DE. Adenylate energy charge in Escherichia coli during growth and starvation. J Bacteriol. 1971;108:1072–86.

Annex A.

Table A1. List of primers used to construct the *Escherichia coli* strain K12GAPNΔzwf+pPHB

Primer	Sequence
SmutGAPNXbacrt	5'-ggttaatctagacaactactacaactgacagatg-3'
SmutGAPNKpncrt	5'-attcaaggtaccatgacaaaacaatataaaaattatgtc-3'
upFRTpkd13	5'-gatccgtcgacctgcagttcg-3'
downFRTpkd13	5'-agtaatGTCGACgtgtaggctggagctgcttc-3'
WDGANPxGAPfw3	5'-cttttattcactaacaaatagctggtggaatatatgacaaaacaatataaaaattatgtc-3'
WDGANPxGAPrv3	5'-gaccgaagtcgctctttttagatcacagtgtcatctcaacaaacagccaagcttgcatgc-3'
UPEcolizwf	5'-tatcagttttgccgcactttgc-3'
DWEcolizwf	5'-cgcctgtaaccggagctcatag-3'

Table A2. Results from the enzymatic assays performed to verify the effect of the performed genetic manipulations.

Strain	Assay	grown in LB (U/mg[#])	grown in MMG (U/mg[#])
K12	NAD-GAP	0.032 ± 0.001	0.69 ± 0.03
	NADP-GANP	b.d.l.	b.d.l.
	NADP-G6PDH	0.005 ± 0.001	0.09 ± 0.01
K12GAPN	NAD-GAP	b.d.l.	b.d.l.
	NADP-GANP	0.014 ± 0.002	0.14 ± 0.03
	NADP-G6PDH	0.006 ± 0.001	0.05 ± 0.02
K12GAPNΔzwf	NAD-GAP	b.d.l.	b.d.l.
	NADP-GANP	0.016 ± 0.001	0.14 ± 0.02
	NADP-G6PDH	b.d.l.	b.d.l.

[#]1 U = 1 μmol/min; mg refers to mg of total protein

NAD-GAP: NAD-dependent phosphorylating glyceraldehyde-3-phosphate dehydrogenase

NADP-GANP: NADP-dependent non-phosphorylating glyceraldehyde-3-phosphate dehydrogenase

NADP-G6PDH: NADP-dependent glucose-6-phosphate dehydrogenase

b.d.l.: below detection level

Annex B.

Table B1. Flux Balance Analysis model used in CobraToolbox

The reactions in the model 'Ecolicore' with the added reactions are listed:

1	ACALD	acetaldehyde dehydrogenase (acetylating)	acald[c] + coa[c] + nad[c] <=> accoa[c] + h[c] + nadh[c]
2	ACALDt	acetaldehyde reversible transport	acald[e] <=> acald[c]
3	ACKr	acetate kinase	ac[c] + atp[c] <=> actp[c] + adp[c]
4	ACONTa	aconitase (half-reaction A, Citrate hydro-lyase)	cit[c] <=> acon_C[c] + h2o[c]
5	ACONTb	aconitase (half-reaction B, Isocitrate hydro-lyase)	acon_C[c] + h2o[c] <=> icit[c]
6	ACt2r	acetate reversible transport via proton symport	ac[e] + h[e] <=> ac[c] + h[c]
7	ADK1	adenylate kinase	amp[c] + atp[c] <=> 2 adp[c]
8	AKGDH	2-Oxoglutarate dehydrogenase	akg[c] + coa[c] + nad[c] -> co2[c] + nadh[c] + succoa[c]
9	AKGt2r	2-oxoglutarate reversible transport via symport	akg[e] + h[e] <=> akg[c] + h[c]
10	ALCD2x	alcohol dehydrogenase (ethanol)	etoh[c] + nad[c] <=> acald[c] + h[c] + nadh[c]
11	ATPM	ATP maintenance requirement	atp[c] + h2o[c] -> adp[c] + h[c] + pi[c]
12	Biomass_Ecoli_core_w_GAM	Biomass Objective Function with GAM	1.496 3pg[c] + 3.7478 accoa[c] + 59.81 atp[c] + 0.361 e4p[c] + 0.0709 f6p[c] + 0.129 g3p[c] + 0.205 g6p[c] + 0.2557 gln_L[c] + 4.9414 glu_L[c] + 59.81 h2o[c] + 3.547 nad[c] + 13.0279 nadph[c] + 1.7867 oaa[c] + 0.5191 pep[c] + 2.8328 pyr[c] + 0.8977 r5p[c] -> 59.81 adp[c] + 4.1182 akg[c] + 3.7478 coa[c] + 59.81 h[c] + 3.547 nadh[c] + 13.0279 nadp[c] + 59.81 pi[c]
13	CO2t	CO2 transporter via diffusion	co2[e] <=> co2[c]
14	CS	citrate synthase	accoa[c] + h2o[c] + oaa[c] -> cit[c] + coa[c] + h[c]
15	CYTBD	cytochrome oxidase bd (ubiquinol-8: 2 protons)	2 h[c] + 0.5 o2[c] + q8h2[c] -> h2o[c] + 2 h[e] + q8[c]
16	D_LACt2	D-lactate transport via proton symport	h[e] + lac_D[e] <=> h[c] + lac_D[c]
17	ENO	enolase	2pg[c] <=> h2o[c] + pep[c]
18	EX_ac(e)	Acetate exchange	ac[e] ->
19	EX_acald(e)	Acetaldehyde exchange	acald[e] ->
20	EX_akg(e)	2-Oxoglutarate exchange	akg[e] ->
21	EX_co2(e)	CO2 exchange	co2[e] <=>
22	EX_etoh(e)	Ethanol exchange	etoh[e] ->
23	EX_for(e)	Formate exchange	for[e] ->
24	EX_fru(e)	D-Fructose exchange	fru[e] ->
25	EX_fum(e)	Fumarate exchange	fum[e] ->
26	EX_glc(e)	D-Glucose exchange	glc_D[e] <=>
27	EX_gln_L(e)	L-Glutamine exchange	gln_L[e] ->
28	EX_glu_L(e)	L-Glutamate exchange	glu_L[e] ->
29	EX_h(e)	H+ exchange	h[e] <=>
30	EX_h2o(e)	H2O exchange	h2o[e] <=>

31	EX_lac_D(e)	D-Lactate exchange	lac_D[e] ->
32	EX_mal_L(e)	L-Malate exchange	mal_L[e] ->
33	EX_nh4(e)	Ammonium exchange	nh4[e] <=>
34	EX_o2(e)	O2 exchange	o2[e] <=>
35	EX_pi(e)	Phosphate exchange	pi[e] <=>
36	EX_pyr(e)	Pyruvate exchange	pyr[e] ->
37	EX_succ(e)	Succinate exchange	succ[e] ->
38	FBA	fructose-bisphosphate aldolase	fdp[c] <=> dhap[c] + g3p[c]
39	FBP	fructose-bisphosphatase	fdp[c] + h2o[c] -> f6p[c] + pi[c]
40	FORt2	formate transport via proton symport (uptake only)	for[e] + h[e] -> for[c] + h[c]
41	FORti	formate transport via diffusion	for[c] -> for[e]
42	FRD7	fumarate reductase	fum[c] + q8h2[c] -> q8[c] + succ[c]
43	FRUpts2	Fructose transport via PEP:Pyr PTS (f6p generating)	fru[e] + pep[c] -> f6p[c] + pyr[c]
44	FUM	fumarase	fum[c] + h2o[c] <=> mal_L[c]
45	FUMt2_2	Fumarate transport via proton symport (2 H)	fum[e] + 2 h[e] -> fum[c] + 2 h[c]
46	G6PDH2r	glucose 6-phosphate dehydrogenase	g6p[c] + nadp[c] <=> 6pgl[c] + h[c] + nadph[c]
47	GAPD	glyceraldehyde-3-phosphate dehydrogenase	g3p[c] + nad[c] + pi[c] <=> 13dpg[c] + h[c] + nadh[c]
48	GLCpts	D-glucose transport via PEP:Pyr PTS	glc_D[e] + pep[c] -> g6p[c] + pyr[c]
49	GLNS	glutamine synthetase	atp[c] + glu_L[c] + nh4[c] -> adp[c] + gln_L[c] + h[c] + pi[c]
50	GLNabc	L-glutamine transport via ABC system	atp[c] + gln_L[e] + h2o[c] -> adp[c] + gln_L[c] + h[c] + pi[c]
51	GLUDy	glutamate dehydrogenase (NADP)	glu_L[c] + h2o[c] + nadp[c] <=> akg[c] + h[c] + nadph[c] + nh4[c]
52	GLUN	glutaminase	gln_L[c] + h2o[c] -> glu_L[c] + nh4[c]
53	GLUSy	glutamate synthase (NADPH)	akg[c] + gln_L[c] + h[c] + nadph[c] -> 2 glu_L[c] + nadp[c]
54	GLUt2r	L-glutamate transport via proton symport, reversible (periplasm)	glu_L[e] + h[e] <=> glu_L[c] + h[c]
55	GND	phosphogluconate dehydrogenase	6pgc[c] + nadp[c] -> co2[c] + nadph[c] + ru5p_D[c]
56	H2Ot	H2O transport via diffusion	h2o[e] <=> h2o[c]
57	ICDHyr	isocitrate dehydrogenase (NADP)	icit[c] + nadp[c] <=> akg[c] + co2[c] + nadph[c]
58	ICL	Isocitrate lyase	icit[c] -> glx[c] + succ[c]
59	LDH_D	D lactate dehydrogenase	lac_D[c] + nad[c] <=> h[c] + nadh[c] + pyr[c]
60	MALS	malate synthase	accoa[c] + glx[c] + h2o[c] -> coa[c] + h[c] + mal_L[c]
61	MALt2_2	Malate transport via proton symport (2 H)	2 h[e] + mal_L[e] -> 2 h[c] + mal_L[c]
62	MDH	malate dehydrogenase	mal_L[c] + nad[c] <=> h[c] + nadh[c] + oaa[c]
63	ME1	malic enzyme (NAD)	mal_L[c] + nad[c] -> co2[c] + nadh[c] + pyr[c]
64	ME2	malic enzyme (NADP)	mal_L[c] + nadp[c] -> co2[c] + nadph[c] + pyr[c]
65	NADH16	NADH dehydrogenase (ubiquinone-8 & 3 protons)	4 h[c] + nadh[c] + q8[c] -> 3 h[e] + nad[c] + q8h2[c]
66	NADTRHD	NAD transhydrogenase	nad[c] + nadph[c] -> nadh[c] + nadp[c]

67	NH4t	ammonia reversible transport	nh4[e] <=> nh4[c]
68	O2t	o2 transport via diffusion	o2[e] <=> o2[c]
69	PDH	pyruvate dehydrogenase	coa[c] + nad[c] + pyr[c] -> accoa[c] + co2[c] + nadh[c]
70	PFK	phosphofructokinase	atp[c] + f6p[c] -> adp[c] + fdp[c] + h[c]
71	PFL	pyruvate formate lyase	coa[c] + pyr[c] -> accoa[c] + for[c]
72	PGI	glucose-6-phosphate isomerase	g6p[c] <=> f6p[c]
73	PGK	phosphoglycerate kinase	3pg[c] + atp[c] <=> 13dpg[c] + adp[c]
74	PGM	phosphoglycerate mutase	2pg[c] <=> 3pg[c]
75	PIt2r	phosphate reversible transport via proton symport	h[e] + pi[e] <=> h[c] + pi[c]
76	PPC	phosphoenolpyruvate carboxylase	co2[c] + h2o[c] + pep[c] -> h[c] + oaa[c] + pi[c]
77	PPCK	phosphoenolpyruvate carboxykinase	atp[c] + oaa[c] -> adp[c] + co2[c] + pep[c]
78	PPS	phosphoenolpyruvate synthase	atp[c] + h2o[c] + pyr[c] -> amp[c] + 2 h[c] + pep[c] + pi[c]
79	PTAr	phosphotransacetylase	accoa[c] + pi[c] <=> actp[c] + coa[c]
80	PYK	pyruvate kinase	adp[c] + h[c] + pep[c] -> atp[c] + pyr[c]
81	PYRt2r	pyruvate reversible transport via proton symport	h[e] + pyr[e] <=> h[c] + pyr[c]
82	RPE	ribulose 5-phosphate 3-epimerase	ru5p_D[c] <=> xu5p_D[c]
83	RPI	ribose-5-phosphate isomerase	r5p[c] <=> ru5p_D[c]
84	SUCCt2_2	succinate transport via proton symport (2 H)	2 h[e] + succ[e] -> 2 h[c] + succ[c]
85	SUCCt3	succinate transport out via proton antiport	h[e] + succ[c] -> h[c] + succ[e]
86	SUCDi	succinate dehydrogenase (irreversible)	q8[c] + succ[c] -> fum[c] + q8h2[c]
87	SUCOAS	succinyl-CoA synthetase (ADP-forming)	atp[c] + coa[c] + succ[c] <=> adp[c] + pi[c] + succoa[c]
88	TALA	transaldolase	g3p[c] + s7p[c] <=> e4p[c] + f6p[c]
89	THD2	NAD(P) transhydrogenase	2 h[e] + nadh[c] + nadp[c] -> 2 h[c] + nad[c] + nadph[c]
90	TKT1	transketolase	r5p[c] + xu5p_D[c] <=> g3p[c] + s7p[c]
91	TKT2	transketolase	e4p[c] + xu5p_D[c] <=> f6p[c] + g3p[c]
92	TPI	triose-phosphate isomerase	dhap[c] <=> g3p[c]
93	PGL	6-phosphogluconolactonase	6pgl[c] + h2o[c] -> 6pgc[c]
94	ATPS4r	ATP synthase (four protons for one ATP)	adp[c] + 3 h[e] + pi[c] <=> atp[c] + h2o[c] + 2 h[c]
95	ETOHt2r	ETOHt2r	etoh[c] -> etoh[e]
96	ED1	6-phosphogluconate dehydratase	6pgc[c] -> h2o[c] + KDPG[c]
97	ED2	2-dehydro-3-deoxy-phosphogluconate aldolase	KDPG[c] -> g3p[c] + pyr[c]
98	sintPHB	PHB synthesis	2 accoa[c] + h[c] + nadph[c] -> 2 coa[c] + nadp[c] + HB[c]
99	GAPN	glyceraldehyde-3-phosphate dehydrogenase (NADP-dependent)	g3p[c] + h2o[c] + nadp[c] -> 3pg[c] + 2 h[c] + nadph[c]
100	EX_HB[c]	PHB exchange	HB[c] ->

Annex C. Specific rates of the strains studied K12+pPHB and K12GAPNΔzwf+pPHB.

Table C1. Reconciled specific uptake and secretion rates q_i of the strain K12+pPHB at steady state aerobic carbon limited and oxygen limited chemostat cultivations. Specific uptake rates are expressed per gram of cell dry weight (mmol/g_{CDW}h), Yield of biomass $Y_{(x/s)}$ in g_{CDW}/gs and O_2/S ratios (mmolO_2/mmols); q_{Glc}=glucose consumption rate, q_{Ace}=acetate production rate, q_{O2}= oxygen consumption rate and q_{CO2}=carbon dioxide production rate, q_{Lac}=lactate production rate, q_{Eth}= ethanol production rate, q_{Gly}= glycerol production rate, q_{For}=formate production rate, q_{Succ}=succinate production rate, q_{PHB}=polyhydroxybutyrate production rate.

	Aerobic		Oxygen Limited		
μ (h^{-1})	0.04	0.08	0.04	0.05	0.09
O_2/S	3.276	2.880	3.276	0.939	1.259
OTR	14.074 ± 0.021	22.829 ± 0.132	14.678 ± 0.017	4.107 ± 0.020	8.452 ± 0.050
$-q_{O2}$	2.419 ± 0.036	3.656 ± 0.039	2.557 ± 0.035	2.755 ± 0.042	7.986 ± 0.050
q_{CO2}	2.584 ± 0.035	3.992 ± 0.039	2.738 ± 0.035	2.261 ± 0.044	6.936 ± 0.050
q_X	1.731 ± 0.122	3.196 ± 0.464	1.807 ± 0.086	1.994 ± 0.051	3.754 ± 1.796
$-q_{Glc}$	0.738 ± 0.037	1.269 ± 0.130	0.781 ± 0.026	2.933 ± 0.053	6.345 ± 2.195
q_{Ace}	0.001 ± 0.000	0.002 ± 0.000	0.001 ± 0.000	1.412 ± 0.071	1.860 ± 0.785
q_{Lac}	0.028 ± 0.002	0.071 ± 0.007	0.027 ± 0.002	1.413 ± 0.045	3.210 ± 1.363
q_{Eth}	0.002 ± 0.002	0.051 ± 0.006	0.014 ± 0.005	0.177 ± 0.032	0.425 ± 0.201
q_{Glyc}	0.001 ± 0.000	0.005 ± 0.001	0.002 ± 0.000	0.538 ± 0.033	0.910 ± 0.380
q_{For}	0.000 ± 0.000	0.024 ± 0.003	0.006 ± 0.000	1.600 ± 0.053	2.690 ± 1.128
q_{Succ}	0.005 ± 0.000	0.018 ± 0.003	0.005 ± 0.000	0.669 ± 0.149	1.911 ± 0.803
q_{PHB}	nd	nd	nd	0.009 ± 0.000	0.029 ± 0.000
RQ	1.068 ± 0.007	1.092 ± 0.007	1.071 ± 0.007	0.821 ± 0.015	0.869 ± 0.007
$Y_{(X/S)}$	0.320 ± 0.004	0.344 ± 0.014	0.316 ± 0.002	0.093 ± 0.001	0.081 ± 0.231

nd = not detected

The oxygen uptake rates and CO_2 production were recalculated through carbon and electron balance, the original off-gas data was inaccurate.

Table C2. Reconciled specific uptake and secretion rates q_i of the strain K12GAPNΔzwf+pPHB at steady state carbon limited and oxygen limited chemostat. Specific uptake rates are expressed per gram of cell dry weight (mmol/g_{CDW}/h), Yield of biomass $Y_{(x/s)}$ in g_{CDW}/g_S and O_2/S ratios ($mmolO_2$/mmols); q_{Glc}=glucose consumption rate, q_{Ace}=acetate production rate, q_{O2}= oxygen consumption rate and q_{CO2}=carbon dioxide production rate, q_{Lac}=lactate production rate, q_{Eth}= ethanol production rate, q_{Gly}= glycerol production rate, q_{For}=formate production rate, q_{Succ}=succinate production rate, q_{PHB}=polyhydroxybutyrate production rate.

	Aerobic						
μ (h^{-1})	0.047	0.093	0.197	0.100	0.100	0.100	0.100
q_{O2} /q_S	3.355	3.089	2.782	1.763	1.543	1.378	1.053
OTR	16.241 ± 0.022	28.534 ± 0.013	53.393 ± 0.269	11.777 ± 0.025	8.332 ± 0.023	5.375 ± 0.035	2.515 ± 0.044
-q_{O2}	2.784 ± 0.034	4.652 ± 0.060	8.257 ± 0.388	4.762 ± 0.099	4.681 ± 0.097	3.537 ± 0.107	2.639 ± 0.113
q_{CO2}	2.985 ± 0.033	5.013 ± 0.059	9.048 ± 0.378	5.308 ± 0.104	6.247 ± 0.128	4.265 ± 0.125	2.910 ± 0.122
q_X	1.876 ± 0.031	3.919 ± 0.068	7.742 ± 0.604	3.442 ± 0.117	3.742 ± 0.106	3.701 ± 0.182	3.668 ± 0.126
-q_{Glc}	0.830 ± 0.007	1.506 ± 0.014	2.968 ± 0.114	2.701 ± 0.031	3.034 ± 0.071	2.567 ± 0.060	2.506 ± 0.039
q_{Ace}	0.007 ± 0.001	0.012 ± 0.001	0.021 ± 0.002	1.042 ± 0.029	1.253 ± 0.137	1.416 ± 0.116	1.726 ± 0.072
q_{Lac}	0.007 ± 0.001	0.008 ± 0.000	0.192 ± 0.013	nd	nd	nd	nd
q_{Eth}	0.028 ± 0.006	nd	0.088 ± 0.035	0.887 ± 0.040	1.499 ± 0.103	0.879 ± 0.067	0.684 ± 0.026
q_{Glyc}	nd	nd	0.008 ± 0.001	0.465 ± 0.013	0.428 ± 0.038	0.394 ± 0.031	0.458 ± 0.020
q_{For}	0.003 ± 0.001	0.012 ± 0.001	0.040 ± 0.003	1.865 ± 0.055	1.071 ± 0.160	1.437 ± 0.127	1.989 ± 0.096
q_{Succ}	0.007 ± 0.001	0.011 ± 0.000	0.037 ± 0.004	0.011 ± 0.001	0.012 ± 0.003	0.009 ± 0.000	0.030 ± 0.007
q_{PHB}	0.000 ± 0.000	0.000 ± 0.000	0.004 ± 0.002	0.075 ± 0.002	0.077 ± 0.002	0.048 ± 0.002	0.039 ± 0.001
RQ	1.072 ± 0.006	1.078 ± 0.009	1.096 ± 0.036	1.115 ± 0.015	1.335 ± 0.015	1.206 ± 0.019	1.103 ± 0.024
$Y_{(X/S)}$	0.308 ± 0.000	0.355 ± 0.000	0.356 ± 0.008	0.174 ± 0.001	0.168 ± 0.001	0.197 ± 0.003	0.200 ± 0.001

nd=not detected

Annex D. Intracellular metabolites

The tables presented from the matbolite data obtained in μmol/g_{cdw} at different dilution rates and O_2/S ratios (mmolO_2/mmols);

Glycolysis, TCA, Pentose Phosphate pathway

Table D1. Central metabolites in the total broth of the strain K12+pPHB expressed in μmol/g_{cdw}.

	Aerobic		Oxygen Limited	
μ (h^{-1})	0.04	0.08	0.04	0.05
O_2/S	3.554	2.880	3.276	0.939
FBP	0.0004 ± 0.000	0.0002 ± 0.000	0.00004 ± 0.000	0.439 ± 0.258
PEP	0.103 ± 0.009	0.697 ± 0.220	1.134 ± 0.400	2.381 ± 0.934
Succ	5.393 ± 1.566	2.659 ± 2.189	4.184 ± 4.319	1043.00 ± 98.507
Pyr	nd	nd	nd	nd
6PG	0.150 ± 0.048	0.105 ± 0.065	0.281 ± 0.094	0.851 ± 0.238
T6P	nd	nd	0.010 ± 0.004	0.072 ± 0.028
G3P	0.572 ± 0.044	0.093 ± 0.038	0.164 ± 0.097	8.097 ± 3.053
UDP-Glc	0.096 ± 0.011	0.018 ± 0.022	0.003 ± 0.001	0.106 ± 0.021
M1P	1.021 ± 0.052	0.565 ± 0.232	0.888 ± 0.296	24.488 ± 8.380
aKG	0.172 ± 0.004	0.239 ± 0.014	0.237 ± 0.005	4.614 ± 1.197
Fum	0.227 ± 0.041	0.254 ± 0.027	0.322 ± 0.008	nd
Mal	1.251 ± 0.042	0.227 ± 0.100	0.559 ± 0.061	563.640 ± 0.000
Cit	0.644 ± 0.027	1.148 ± 0.115	1.860 ± 0.078	5.431 ± 1.225
iCit	0.009 ± 0.001	0.015 ± 0.001	0.031 ± 0.002	0.136 ± 0.028
2PG	0.172 ± 0.010	0.632 ± 0.079	0.750 ± 0.016	0.506 ± 0.101
DHAP	0.492 ± 0.014	0.279 ± 0.003	0.258 ± 0.106	13.029 ± 3.169
3PG	1.737 ± 0.053	6.111 ± 0.718	6.905 ± 0.056	5.868 ± 1.075
Rib5P	0.279 ± 0.005	0.312 ± 0.028	0.293 ± 0.006	0.503 ± 0.108
Ribu5P	0.235 ± 0.012	0.122 ± 0.012	0.133 ± 0.001	0.773 ± 0.177
Xyl5P	0.158 ± 0.007	0.094 ± 0.015	0.099 ± 0.007	0.645 ± 0.133
F6P	0.307 ± 0.006	0.370 ± 0.032	0.357 ± 0.000	9.409 ± 1.471
G6P	1.006 ± 0.076	1.179 ± 0.089	1.086 ± 0.010	8.719 ± 1.715
AcCoA	na	na	na	na
S7P	0.258 ± 0.006	0.244 ± 0.029	0.264 ± 0.025	0.428 ± 0.080
Tre	nd	4.785 ± 0.549	10.812 ± 0.138	41.379 ± 7.756
E4P	0.004 ± 0.000	0.006 ± 0.001	0.007 ± 0.001	0.016 ± 0.003

nd = not detected

na=not applicable

Table D2. Central metabolites in the total broth of the strain K12GAPNΔzwf+pPHB expressed in μmol/g_{cdw}.

	Aerobic						
μ (h^{-1})	0.047	0.093	0.197	0.100	0.100	0.100	0.100
O_2/S	3.355	3.089	2.782	1.763	1.543	1.378	1.053
FBP	0.700 ± 0.016	1.222 ± 0.027	3.924 ± 0.134	2.744 ± 0.136	3.270 ± 0.450	4.224 ± 1.514	3.264 ± 0.256
PEP	4.092 ± 0.368	2.233 ± 0.119	1.116 ± 0.049	0.946 ± 0.017	0.603 ± 0.138	0.365 ± 0.088	0.218 ± 0.018
Succ	7.122 ± 1.810	17.261 ± 11.237	9.284 ± 0.867	14.205 ± 1.756	58.585 ± 25.851	14.23 ± 4.369	61.563 ± 7.312
Pyr	0.323 ± 0.255	0.320 ± 0.104	0.607 ± 0.205	2.967 ± 0.141	2.053 ± 1.453	nd	nd
6PG	0.001 ± 0.001	nd	0.001 ± 0.001	nd	nd	0.175 ± 0.125	0.113 ± 0.012
T6P	0.096 ± 0.025	0.003 ± 0.000	nd	nd	nd	nd	0.013 ± 0.007
G3P	0.756 ± 0.209	0.442 ± 0.063	0.678 ± 0.033	2.500 ± 0.220	2.562 ± 0.467	2.416 ± 0.673	2.922 ± 0.630
UDP-Glc	2.216 ± 0.126	2.394 ± 0.084	3.246 ± 0.066	1.319 ± 0.064	0.819 ± 0.534	0.929 ± 0.255	0.526 ± 0.008
M1P	0.844 ± 0.038	0.956 ± 0.025	1.222 ± 0.066	3.010 ± 0.041	2.527 ± 0.242	1.256 ± 0.378	0.902 ± 0.225
aKG	0.280 ± 0.009	0.323 ± 0.084	0.391 ± 0.005	0.200 ± 0.018	0.298 ± 0.072	0.169 ± 0.036	0.187 ± 0.035
Fum	0.355 ± 0.031	0.454 ± 0.097	0.260 ± 0.184	0.691 ± 0.026	0.606 ± 0.462	0.464 ± 0.232	nd
Mal	1.295 ± 0.171	3.393 ± 2.269	1.001 ± 0.710	3.792 ± 0.312	18.184 ± 4.178	3.752 ± 0.000	nd
Cit	3.577 ± 0.256	3.541 ± 0.169	4.312 ± 6.098	5.405 ± 7.644	nd	nd	nd
iCit	0.054 ± 0.005	0.046 ± 0.007	0.131 ± 0.009	nd	nd	nd	nd
2PG	0.993 ± 0.038	0.564 ± 0.014	0.297 ± 0.005	nd	nd	nd	nd
DHAP	0.683 ± 0.103	1.020 ± 0.052	1.972 ± 0.055	nd	nd	nd	nd
3PG	9.348 ± 0.607	5.157 ± 0.199	2.971 ± 0.060	2.335 ± 0.044	nd	nd	nd
Rib5P	0.388 ± 0.021	0.184 ± 0.184	0.433 ± 0.019	0.258 ± 0.003	0.250 ± 0.011	0.200 ± 0.056	0.165 ± 0.008
Ribu5P	0.080 ± 0.016	0.251 ± 0.150	0.077 ± 0.002	nd	nd	nd	nd
Xyl5P	0.065 ± 0.007	0.096 ± 0.019	0.123 ± 0.005	nd	nd	nd	nd
F6P	0.231 ± 0.026	0.214 ± 0.132	0.761 ± 0.037	0.950 ± 0.020	0.775 ± 0.113	0.999 ± 0.511	0.504 ± 0.105
G6P	0.787 ± 0.059	0.679 ± 0.330	1.533 ± 0.043	4.285 ± 0.208	6.731 ± 0.552	7.369 ± 1.967	6.410 ± 1.157
AcCoA	0.2504 ± 0.01	0.413 ± 0.021	0.59 ± 0.09	1.321 ± 0.08	1.004 ± 0.328	1.126 ± 0.381	0.997 ± 0.397
S7P	0.123 ± 0.004	0.872 ± 0.735	0.175 ± 0.002	0.063 ± 0.002	0.066 ± 0.002	0.057 ± 0.019	0.060 ± 0.006
Tre	7.169 ± 0.624	0.338 ± 0.188	0.101 ± 0.076	1.052 ± 0.040	2.384 ± 0.2258	1.457 ± 0.227	3.415 ± 0.538

nd = not detected

Annex E. Amino acids

The tables presented from the amino acids obtained in μmol/g_{cdw} at different dilution rates and O_2/S ratios (mmolO_2/mmol$_S$);

Table E1. Amino acids expressed in μmolAAS/g_{cdw} measured in the total broth in the strain K12+pPHB.

	Aerobic						
μ (h^{-1})	0.047	0.093	0.197	0.100	0.100	0.100	0.100
O_2/S	3.355	3.089	2.782	1.763	1.543	1.378	1.053
Ala	1.537 ± 0.259	1.420 ± 0.033	1.556 ± 0.062	3.725 ± 0.350	4.383 ± 0.287	4.316 ± 1.716	3.078 ± 0.132
Gly	7.802 ± 0.813	7.650 ± 0.090	8.296 ± 0.242	6.217 ± 1.875	4.421 ± 0.436	2.805 ± 1.057	1.539 ± 0.390
Val	0.993 ± 0.400	0.427 ± 0.038	1.019 ± 0.743	3.359 ± 0.155	4.097 ± 0.753	3.845 ± 1.181	2.370 ± 0.065
Leu	1.187 ± 0.522	0.373 ± 0.031	0.508 ± 0.168	0.958 ± 0.050	1.671 ± 0.177	1.779 ± 0.534	1.667 ± 0.017
Ile	0.507 ± 0.260	0.124 ± 0.023	0.262 ± 0.136	0.244 ± 0.023	0.440 ± 0.023	0.214 ± 0.097	0.198 ± 0.041
Pro	0.470 ± 0.065	0.474 ± 0.005	0.535 ± 0.004	0.592 ± 0.030	0.679 ± 0.033	0.434 ± 0.091	0.353 ± 0.008
Ser	0.493 ± 0.137	0.318 ± 0.002	0.518 ± 0.024	0.626 ± 0.051	0.767 ± 0.017	0.366 ± 0.105	0.414 ± 0.028
Thr	0.434 ± 0.081	0.420 ± 0.025	0.750 ± 0.031	0.853 ± 0.020	0.861 ± 0.124	0.761 ± 0.222	0.496 ± 0.055
Meth	0.129 ± 0.025	0.102 ± 0.002	0.160 ± 0.008	0.114 ± 0.007	0.163 ± 0.021	0.102 ± 0.034	0.132 ± 0.017
Phe	0.594 ± 0.208	0.287 ± 0.010	0.397 ± 0.062	2.035 ± 0.258	2.407 ± 0.610	1.261 ± 0.381	0.875 ± 0.116
Asp	3.128 ± 0.178	3.490 ± 0.150	4.077 ± 0.085	4.018 ± 0.221	3.646 ± 0.658	3.175 ± 1.029	1.680 ± 0.044
Cys	0.065 ± 0.010	0.080 ± 0.008	0.124 ± 0.008	0.160 ± 0.027	0.202 ± 0.023	0.105 ± 0.030	0.106 ± 0.011
Lys	2.474 ± 0.288	2.193 ± 0.015	1.973 ± 0.056	2.414 ± 0.551	1.896 ± 0.210	1.828 ± 0.863	1.609 ± 0.334
Asn	0.768 ± 0.046	0.759 ± 0.026	0.873 ± 0.032	0.933 ± 0.078	0.763 ± 0.156	0.872 ± 0.288	0.551 ± 0.121
Gln	3.700 ± 0.221	4.838 ± 0.342	6.297 ± 0.143	4.785 ± 0.194	5.060 ± 0.599	6.759 ± 2.180	6.696 ± 1.859
Tyr	0.243 ± 0.049	0.150 ± 0.002	0.193 ± 0.029	0.345 ± 0.016	0.481 ± 0.087	0.246 ± 0.059	0.245 ± 0.012
His	0.185 ± 0.020	0.142 ± 0.003	0.153 ± 0.015	0.068 ± 0.015	0.079 ± 0.001	0.031 ± 0.031	0.000 ± 0.000
Trp	0.024 ± 0.003	0.022 ± 0.001	0.026 ± 0.001	0.024 ± 0.000	0.035 ± 0.004	0.022 ± 0.005	0.010 ± 0.010
Glu	57.067 ± 3.658	56.788 ± 2.381	73.267 ± 2.751	36.171 ± 0.171	40.263 ± 9.362	56.648 ± 18.348	43.107 ± 1.356

Table E2. Amino acids expressed in μmolAAS/g_{cdw} measured in the total broth in the strain K12GAPNΔzwf+pPHB.

	Aerobic		Oxygen Limited	
μ (h^{-1})	0.04	0.08	0.04	0.05
O_2 /S	3.554	2.880	3.276	0.939
Ala	0.977 ± 0.141	1.013 ± 0.128	0.000 ± 0.000	5.822 ± 0.000
Gly	1.204 ± 0.071	1.297 ± 0.147	0.000 ± 0.000	8.142 ± 0.000
Val	0.733 ± 0.534	0.287 ± 0.066	5.130 ± 1.58	1.935 ± 0.000
Leu	0.194 ± 0.038	0.196 ± 0.026	0.686 ± 0.202	1.259 ± 0.000
Ile	0.122 ± 0.077	0.059 ± 0.014	0.036 ± 0.008	0.258 ± 0.000
Pro	0.265 ± 0.012	0.195 ± 0.025	0.114 ± 0.029	1.680 ± 0.000
Ser	0.240 ± 0.004	0.337 ± 0.033	0.074 ± 0.019	1.363 ± 0.000
Thr	0.354 ± 0.002	0.323 ± 0.033	0.127 ± 0.035	2.022 ± 0.000
Meth	0.132 ± 0.009	0.083 ± 0.018	0.005 ± 0.001	0.584 ± 0.000
Asp	1.830 ± 0.025	2.346 ± 0.265	67.038 ± 16.17	16.336 ± 0.000
Phe	0.227 ± 0.040	0.221 ± 0.024	0.265 ± 0.063	1.260 ± 2.023
Cys	0.086 ± 0.005	0.100 ± 0.011	0.109 ± 0.027	0.540 ± 0.000
Glu	33.504 ± 0.794	43.381 ± 4.409	64.078 ± 19.72	304.556 ± 115
Lys	0.754 ± 0.043	1.278 ± 0.161	0.128 ± 0.036	8.279 ± 11.18
Asn	0.450 ± 0.011	0.548 ± 0.060	0.069 ± 0.049	3.409 ± 0.000
Gln	2.651 ± 0.097	2.491 ± 0.277	0.326 ± 0.118	14.835 ± 0.000
Tyr	0.094 ± 0.010	0.098 ± 0.011	0.040 ± 0.010	0.583 ± 0.000
His	0.082 ± 0.004	0.135 ± 0.014	0.000 ± 0.000	0.862 ± 0.000
Trp	0.011 ± 0.001	0.013 ± 0.002	0.104 ± 0.017	0.087 ± 0.000

Annex F. Nucleotides

The tables presented from the nucleotides obtained in μmol/g_{cdw} at different dilution rates and O_2/S ratios (mmolO_2/mmolS);

Table F1. Nucleotides and coenzyme expressed in μmol/g_{cdw} measured in the total broth in the strain K12+pPHB.

	Aerobic		Oxygen Limited	
μ (h^{-1})	0.04	0.08	0.04	0.05
O_2/S	3.554	2.880	3.276	0.939
AMP	1.697 ± 0.721	0.442 ± 0.000	1.182 ± 0.320	1.600 ± 0.367
ADP	1.588 ± 0.065	2.375 ± 0.280	2.547 ± 0.088	1.871 ± 0.369
ATP	2.179 ± 0.050	3.238 ± 0.443	3.384 ± 0.113	2.139 ± 0.624
c_AMP	0.279 ± 0.034	0.072 ± 0.009	0.090 ± 0.001	0.129 ± 0.027
UDP	0.306 ± 0.029	0.403 ± 0.061	0.454 ± 0.030	0.375 ± 0.093
UTP	1.127 ± 0.020	1.574 ± 0.216	2.091 ± 0.012	0.780 ± 0.243
GDP	0.231 ± 0.017	0.252 ± 0.028	0.257 ± 0.019	0.368 ± 0.072
GTP	1.082 ± 0.008	1.061 ± 0.088	1.311 ± 0.109	1.442 ± 0.247
CDP	0.206 ± 0.009	0.224 ± 0.012	0.188 ± 0.041	0.129 ± 0.025
CTP	0.276 ± 0.100	0.000 ± 0.000	0.090 ± 0.001	0.129 ± 0.027

Table F2. Nucleotides expressed in μmol/g_{cdw} measured in the total broth in the strain K12GAPNΔzwf+pPHB.

	Aerobic						
μ (h^{-1})	0.047	0.093	0.197	0.100	0.100	0.100	0.100
O_2/S	3.355	3.089	2.782	1.763	1.543	1.378	1.053
ADP	2.129 ± 0.442	2.339 ± 0.021	2.640 ± 0.142	2.418 ± 0.062	1.989 ± 0.495	2.137 ± 0.712	2.687 ± 1.123
ATP	3.580 ± 0.260	3.253 ± 0.052	3.412 ± 0.109	2.752 ± 0.057	2.092 ± 0.647	2.509 ± 0.724	2.927 ± 1.411
c_AMP	1.366 ± 0.284	0.926 ± 0.037	1.309 ± 0.023	0.441 ± 0.154	0.212 ± 0.030	0.149 ± 0.033	0.313 ± 0.087
UDP	0.623 ± 0.182	0.415 ± 0.001	0.318 ± 0.065	0.482 ± 0.096	0.505 ± 0.136	0.450 ± 0.130	0.619 ± 0.268
UTP	2.526 ± 0.222	1.919 ± 0.124	1.814 ± 0.022	1.505 ± 0.027	1.168 ± 0.205	1.303 ± 0.229	1.510 ± 0.531
GDP	0.154 ± 0.023	0.132 ± 0.000	0.201 ± 0.010	0.220 ± 0.020	0.211 ± 0.041	0.154 ± 0.008	0.302 ± 0.122
GTP	0.889 ± 0.184	1.117 ± 0.063	1.365 ± 0.103	0.973 ± 0.065	0.902 ± 0.474	0.969 ± 0.261	1.416 ± 0.678
NAD	4.080 ± 0.027	4.617 ± 0.138	4.846 ± 0.118	3.608 ± 0.230	2.963 ± 1.105	3.309 ± 1.180	4.322 ± 2.126
NADPH	0.390 ± 0.139	0.254 ± 0.021	0.288 ± 0.015	0.258 ± 0.008	0.240 ± 0.030	0.194 ± 0.049	0.353 ± 0.080
CoA	0.883 ± 0.148	0.755 ± 0.080	0.732 ± 0.123	0.490 ± 0.059	0.430 ± 0.112	0.473 ± 0.169	0.637 ± 0.309
FAD	0.164 ± 0.029	0.172 ± 0.004	0.179 ± 0.004	0.228 ± 0.007	0.200 ± 0.049	0.192 ± 0.064	0.270 ± 0.137

Annex G. Representation of the amino acids concentration with respect to glucose uptake of the strain K12GAPNΔzwf+pPHB.

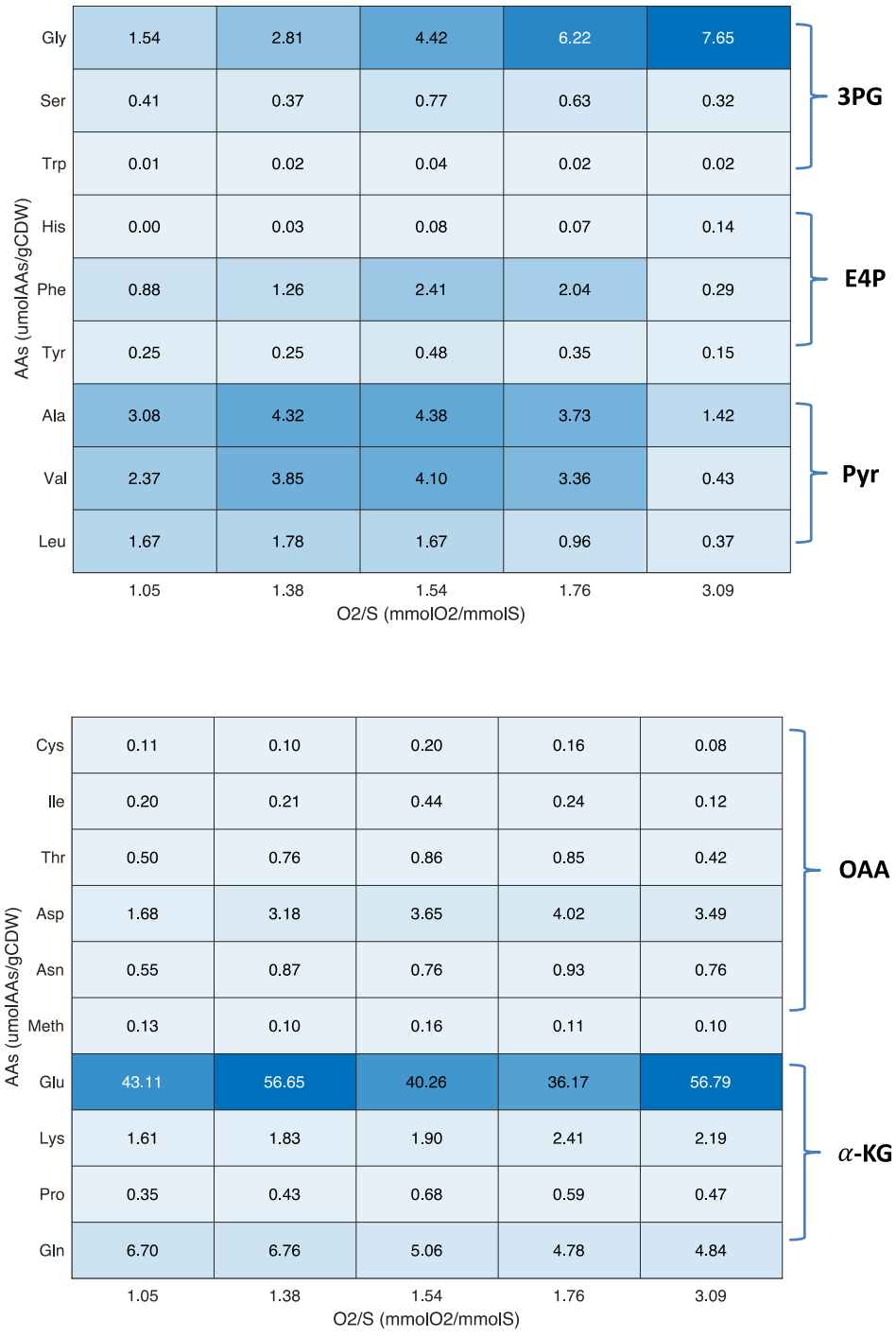

Figure G1. Heatmap of the total broth of amino acids, presented as Metabolite ($mmol_{AAS}/g_{CDW}$), grouped according to the metabolite they are derived from. The data is presented from aerobic to oxygen limited conditions in the strain K12GAPNΔzwf+pPHB. Aerobic: O_2/S =3.09 at D= 0.1 h^{-1}. Oxygen limited: data of O_2/S from 1.05 to 1.76 at a D= 0.1 h^{-1}.

Chapter 4.

Microscale quantitative analysis of polyhydroxybutyrate in prokaryotes using IDMS

Mariana I. Velasco Alvarez, Angela ten Pierick, Patricia T. N. van Dam, Reza Maleki Seifar , Mark van Loosdrecht and S. Aljoscha Wahl

Abstract

Polyhydroxybutyrate (PHB) is an interesting biopolymer for replacing petroleum-based plastics, its biological production is performed in natural and engineered microorganisms. Current metabolic engineering approaches rely on high-throughput strain construction and screening. Analytical procedures have to be compatible with the small scale and speed of these approaches. Here, we present a method based on isotope dilution mass spectrometry (IDMS) and propanolysis extraction of polyhydroxybutyrate from an *Escherichia coli* strain engineered for PHB production. As internal standard we applied an uniformly labelled ^{13}C-cell extract, of an *E. coli* PHB producing strain, grown on U-^{13}C- glucose as C-source. This internal ^{13}C-PHB standard enables to quantify low concentrations of PHB (LOD of 0.01 ug/gDW) from several micrograms of biomass. With the method, a technical reproducibility of about 2 % relative standard deviation is achieved. Furthermore, the internal standard is robust towards different sample backgrounds and dilutions. The early addition of the internal standard also makes the quantification reproducible with a higher sensibility and allows a significantly increased throughput.

1. Introduction

Since the discovery of PHB accumulating microorganisms, different approaches have been proposed for a precise and accurate measurement of the PHB content [1]. The first method was developed by Lemoigne [2], which was followed by a series of improvements. Especially, different reagents for extraction like dichloroethane or free chlorinated solvents replacing the chloroform [3,4] . Nowadays, one of the most commonly used methods is propanolysis and GC-based quantification [5–8]. The method can be applied to a wide range of microorganisms [9,10]. Next to propanolysis an approach based on derivatization with N-tert-butyldimethylsilyl-N-methyltrifluoroacetamide (MTBSTFA) and GC-MS/MS has been proposed [11]. A comparison of the described methods including required sample amounts and accuracy can be found in Table 1. Unfortunately, not all methods are fully documented with the respective detection limits and accuracies.

Table 1. Comparison of most common approaches for PHB quantification in biomass.

	Methods				
	GC-FID[5]	**GC-MS/MS**[11]	**HPLC**[12]	**IC**[13]	**GC-IDMS [this study]**
Minimal biomass amount (mg_{DW})	10	50	1000	10	1
Limit of detection ($\mu g_{PHB}/g_{DW}$)	93000	0.0003 *	0.853	-	0.011
Internal standard	Benzoic acid	β-hydroxyoctanoic acid	Adipic acid	NA	U ^{13}C-PHB
External standard	PHB	3-HBNa**	Crotonic acid	3.3:1 PHB:PHV***	3-HBNa

DW: dry weight of biomass. LOD: limit of detection was calculated taking three times the standard deviation divided by the slope [14]. Value reported in the article.**3-HBNa: sodium 3-hydroxybutyrate. *** PHV: Polyhydroxyvalerate.*

In this study, the LOD reported is based on a split 1/500 injection meaning that only 2 nL is injected on the column, the GC-MS/MS method is used in SL (splitless) mode, which means

that the full 1 µl is injected. Therefore, there is also the possibility to lower the LOD for at least 100 times.

There are two main limitations in the current methods: (1) laborious and time consuming sample preparation and (2) the requirement of large amounts of biomass [1]. In view of high-throughput experimentation, a fast and small-scale method is needed. Especially, the cultivation volume will be limited and only small sample volumes can be obtained. Further, a high amount of samples is only feasible with a robust and simple protocol [15,16].
Here, we present an approach that is robust towards the cellular matrix, requires small sample volumes and less preparation sample steps, especially the weighing step of samples and standards for the PHB quantification. The major difference to previous methods is the application of a labelled internal standard [17,18].

2. Materials and methods

Strain and preculture

The *E. coli* MG1655-PHB strain was obtained from a transformation with a plasmid (pBBR1MCS-2::*phaCAB)*, constructed in the University of São Paulo (Brazil) containing the genes of *Cupriavidus necator* for polyhydroxybutyrate production [19]. The stock cells were grown in mineral medium and aliquots containing glycerol were stored at -80 °C, until further use for inoculation (80% v/v glycerol).

Cultivation of labeled PHB

A shake flask cultivation of 0.1 L using *E. coli* MG1655-PHB was grown at 37°C and 220 rpm. A low ammonium minimal medium concentration composition for one liter was used: 2.0 g $(NH_4)_2SO_4$, 2.0 g KH_2PO_4, 0.5 g $MgSO_4.7H_2O$, 0.5 g NaCl, 0.001 g vitamin (Thiamine-HCl), 0.05 g kanamycin and 1 mL of trace elements solution (Sctra-1) [20]. The carbon source was U-^{13}C-glucose 99% purchased from Cortecnet (Paris, France) in a concentration of 20 g/L. The pH of the medium was adjusted to 7 with 1 M K_2HPO_4, and 8.37 mg/mL of MOPS was added as a buffer. After adjusting the pH, the medium was sterilized with a 0.2 µm pore size filter, cellulose acetate (FP 30/0.2, Whatman GmbH, Dassel, Germany).

Preparation of labeled cell extracts

The labelled broth obtained was centrifuged and then distributed in falcon tubes until further dilution, and kept at -80°C, until further usage.

Calibration Lines of 3-HB

The sodium 3-hydroxybutyrate (95.2% purity) was purchased from Sigma Aldrich (Darmstadt, Germany). The concentration range of the calibration lines were from 0.001 to 11 mmol/L. The stock solutions of the internal standards PAA (phenylacetic acid) and BA (benzoic acid) was prepared in a concentration of 2 mg/mL. The concentration of the $(PHB)_1$ in the cell extract was 0.8 mg/mL.

A duplicate of calibration lines was performed to check reproducibility within the same concentration range. The standards were measured with a three times injection.

In addition, a duplicate of calibration lines was performed without the addition of the IS ^{13}C-PHB.

For convenience of the results shown, the units of the monomer measured in the calibration lines and in the validation results is expressed as $(PHB)_1$ mmol/L.

Quantification of PHB

One milliliter of broth was transferred into a 1.5 mL microcentrifuge Eppendorf tube and centrifuged. The pellet was resuspended in a mixture of 200 µL of the labelled extract (^{13}C-PHB), 50 µl PAA and 500µL milli-Q water and transferred to a silanized glass GC vial with screw cap (w/spot 2mL, Agilent Technologies, California, USA). The sample was then freeze-dried overnight.

The dried samples were derivatized using the propanolysis reaction [5] . I.e. 50 µL of 2 g/L of benzoic acid (Acros Organics, Antwerp, Belgium) in 1-propanol (99.9% Thermo Fisher Scientific, Massachussetts, USA), 100 µl of 3:7 HCl:1-propanol and 150 µl of 1,2 Dichloroethane (99.9% Thermo Fisher Scientific, Massachussetts, USA). The screw cap (w/spot 2 mL, Agilent Technologies, California, USA) vials were then placed in a heating block at 100°C for 2 hours. During the heating, the vials were shortly vortexed every 30 minutes. After cooling down, the lower organic phase was transferred into a 1 mL shell vial 8x40 mm; Grace, Maryland, USA) and 150 µl of 1,2 Dichloroethane and 300 µl of milli-Q water were added. The mixture was vortexed for 5-10 seconds and centrifuged for 1 minute at 10000 G. The lower organic phase was recovered in a fresh shell glass vial. Remaining traces of water were removed by the addition of about 5 mg of Na_2SO_4 and centrifuged for 1 minute

at 10000 G. A volume of 120 µL was transferred into the GC vial with an insert (250 µL pulled point glass Agilent Technologies, California, USA).

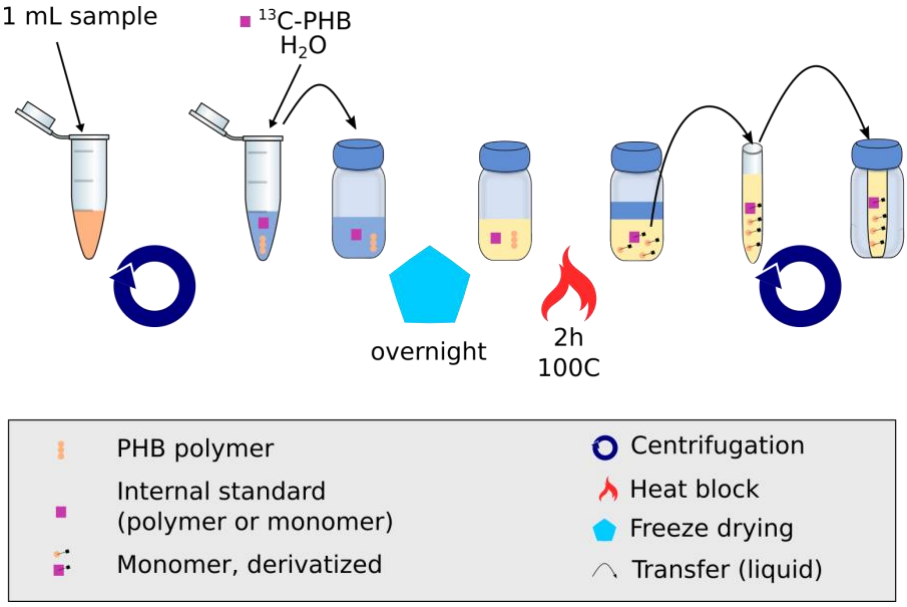

Figure 1: **Sample processing steps for the measurement of $(PHB)_1$ using the IDMS approach**. Broth is centrifuged and re-suspended to remove extracellular matrix. After freeze-drying, the sample is further cleaned and derivatized.

GC-IDMS condition analysis

GC–MS measurements were carried out on a 7890A GC coupled to a 5975C Quadrupole MSD (both from Agilent, California, USA). The conditions were optimized for the measurement of the metabolites of interest and were set to: 1 µL of derivatized sample was injected with a split ratio of 1:500. Straight ultra-inert glass liners with glass wool were used (Agilent). The Multimode Inlet (MMI; Agilent) temperature was set to 80 °C with a hold time of 3 seconds. The MMI temperature was raised to 220 °C with a gradient of 720 °C/min and held for 5 min. Subsequently, the temperature was further raised to 300 °C for cleaning purposes.

The column was a Zebron ZB-50 column (30 m × 250 µm internal diameter, 0.25 µm film thickness; Phenomenex, California, USA). The carrier (helium) flow during the analysis was set at 1 mL/min. The GC oven temperature was held for 0.5 min at 80 °C, then raised with 10 °C/min up to 175 °C. At the end of a GC run, the column was back flushed with 5 column volumes at 300 °C.

The temperature of the transfer line to the MS was set to 250 °C, the MS source to 230 °C and the quadruple to 150 °C. Electron impact ionization (EI) was operated at 70 eV. For quantitative measurements the MS was used in SIM (Single Ion Mode). The mass resolution was set to 0.6 mass units. Raw MS data were processed using Mass Hunter Quantitative Analysis software for MS (version B.07.00; Agilent).

3. Results and discussion

The development of the novel PHB measurement method, required a series of experiments to verify the potential use of the proposed IS and the reduction of steps involved in the analytical protocol. Besides establishing calibration lines and the study of a matrix effect, other experiments were performed such as complete assessment of the derivatization time, homogeneity and simultaneous biomass quantification, which can be found in the supplementary material.

PHB Extraction from small sample volume

To test if the extraction and derivatization from small sample volumes would bias the results, the results were compared to the conventional method. The results showed a PHB content of 14.4 ± 1.687% with the new method and 12.7 ± 2.01% with the conventional method. The t-test ($p<0.05$) demonstrate no significant difference between methods.

Calibration with labeled PHB as internal standard

Equal amounts of labeled PHB (^{13}C cell extract) were added to each standard (3HB). The peak area ratio was then measured by GC-IDMS. Linear calibration lines were obtained from the ratio between the ^{12}C-3HB and the IS (U ^{13}C-PHB). The standard deviation of the ratio (^{12}C-PHB/IS) measurements was used to calculate the relative and the absolute error: 0.0053 mmol/L and $3x10^{-5}$ respectively. The resulting heteroscedastic error model was used for weighted linear regression.

A calibration line, valid over 4 orders of magnitudes was obtained (Figure 2).

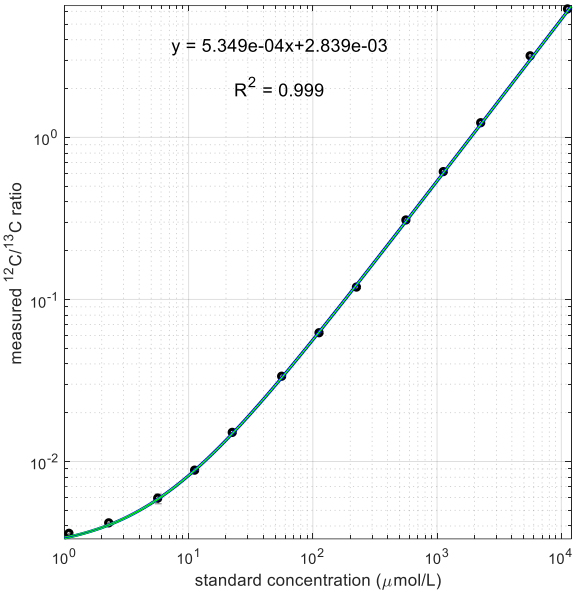

Figure 2. Measured $^{12}C/^{13}C$ ratio and linear regression line. Both standard concentration and measured ratio are in log scale.

4. Validation experiments

Representative samples were produced by cultivation of *E. coli* MG1655-PHB in minimal medium in aerobic shake flasks. Samples were taken at the end of the cultivation, containing about 1.2 g_{DW}/L biomass with a PHB content of about 20% (g/g_{DW}). The following analytical tests were performed:

1. Technical reproducibility
2. Sample background impact (matrix effect)
3. Putative Influence of the Cell Matrix

1. Technical reproducibility including sample processing

The technical variability of sample processing and measurement was determined by three replicate broth samples from two different cultures (biological duplicate). Each sample was measured three times (analytical variability, see data in the supplementary material, Table D1). The relative standard deviation of the analytical replica measurement was 1.5 % while the technical reproducibility (measurement and processing) was around 1.9%.

2. *Putative Influence of Sample background (matrix effect)*

In contrast to pure standards, samples may contain interfering compounds. To exclude an influence from the cellular matrix, experiments with diluted matrix and standard addition were performed. Six samples (three replicates from two different cultures) were spiked with a known $(PHB)_1$ concentration of 2.33 mmol/L. The recovery of the standard addition was analyzed through comparing the ratios at the standard made with such concentration and the recovered ratios. The recovery obtained was 100% ± 2.2 % for the first culture and 103 % ± 1.8 % for the second culture. To confirm that there is no matrix effect, a one sample t-test was performed. The recoveries obtained were compared based on a mean (μ) of 100% recovery. Two hypothesis were formulated: no significant difference was observed in all the recoveries obtained (H_0) and a difference between the true mean and the values obtained was observed (H_1). The null hypothesis was accepted (t-test, $p<0.05$), thus we can confirm that there is no effect from the cellular matrix.

3. *Putative Influence of the Cell Matrix*

The impact of cellular matrix was evaluated by preparing different ratios of ^{12}C over ^{13}C sample volume. The dilution ranged from 0.05 to 3.7 compared to the regular sample preparation (1mL sample, 200 µL ^{13}C cell extract). Each sample was prepared in triplicate and measured three times. If there was no matrix effect, the obtained change in ratio is equal to the applied dilution, resp. the concentration of the original sample is independent of the ^{12}C to ^{13}C volume ratio (Figure 4). and no relation between dilution and the obtained (recalculated) sample concentration (H_0) is obtained. In case of a matrix effect, a (linear) trend should become visible (H_1). H_1 is rejected in a chi-test with $p>0.05$ [15].

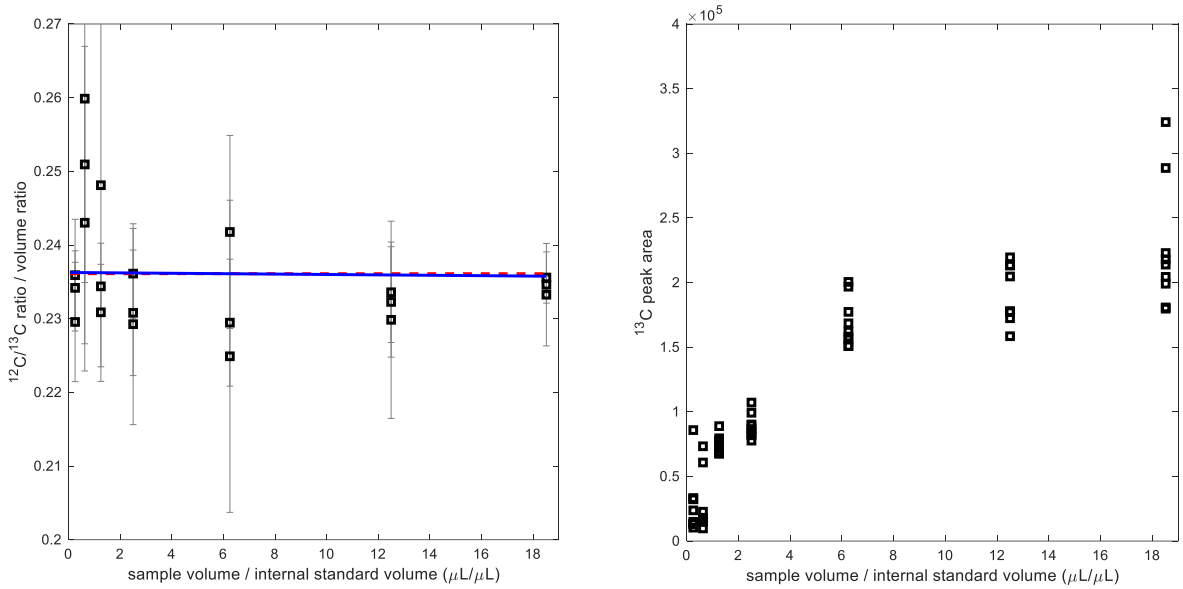

Figure 4. A: Calculated $^{12}C/^{13}C$ ratio (measured ratio divided by the volume ratio) as a function of the volume ratio ^{12}C /^{13}C. In blue the regression assuming an influence of the matrix (H_1), H_0 in red. B: ^{13}C peak area with different matrix background (sample / internal standard volume)

While the ^{12}C /^{13}C ratio measurement was not influenced by the matrix composition, the measured peak area was influenced. We observed that always an equal amount of ^{13}C PHB led to significantly different signal responses (Fig 4B). As the concentration of cell matrix background and/or the analyte $(PHB)_1$ increases, the response of the peak area of ^{13}C also increases. Such behavior of either enhancement or suppression has already been reported in other studies using MS(/MS) [21]. The relevance of such matrix effect is reflected on the signal intensity, which can vary from measurement to measurement. For instance in the sample background analysis (Test 3.) was observed that the peak areas increased by 40% in the standards when the IS ^{13}C-PHB was added, compared to samples with no addition of the IS. Thus, the importance of an internal standard is confirmed since the ratio gives more stability to fluctuations in the sample preparation and process. Here, a good balance between saving internal standard and high accuracy in the ratio measurement was found at a volume ratio of 0.2 (sample vs IS). Clearly, this ratio may vary depending on the concentration determined of the ^{13}C-PHB but also the sample concentration (biomass concentration and PHB content).

4. Conclusion

Using a sensitive detection system (GC-MS) together with an appropriate internal standard, a robust, easy to perform PHB quantification method was achieved. The ^{13}C PHB standard not only corrects for matrix effects but also variations in the sample preparation process that is suitable for low sample amount measurements. A low sample volume can provide flexibility and convenience for the researcher to design experiments. For instance, low volume cultivation experiments using shake flasks, falcon tubes, or even a microtiter plate.

The technical reproducibility for sample measurements was 1.9%. Including the sample processing steps, a reproducibility of 2% was observed, supporting that the internal standard can correct for sample processing variability [22]. While the reported method was focused on PHB, different polymers are produced by microorganisms. The presented approach can be extended to the quantification of PHV, P4HB (poly-4-hydroxybutyrate) and other polyhydroxyalkanoates.

Acknowledgements

This work was supported by the joint research program NWO-FAPESP from the The Netherlands Organization for Scientific Research (NWO) and São Paulo Research Foundation (FAPESP) with grant number BRAZIL.2013.018. The author MIVA would like to thank the whole CSE group for the help and assistance during the experiments and analysis, especially to Karel Olavarria-Gamez, Leonor Guedes da Silva, Andy Wiranata Wijaya, Hugo Cueto-Rojas, Hector Sangüensa and Zeijan Wang for their collaboration.

Authors contributions:

MIVA: Designed, performed and evaluated the PHB quantification experiments and wrote the manuscript. AtP and PvD performed the GC-MS analysis and contributed to the methods section. AW designed and evaluated the experiments, wrote sections and revised the manuscript. RMS and MvL critically reviewed the manuscript. All authors have read and approved the final manuscript.

Conflicts of Interest: The authors declare no conflict of interest.

References

1. de Rijk TC, van de Meer P, Eggink G, Weusthuis R a. Methods for Analysis of Poly (3-hydroxyalkanoate)(PHA) Composition. Biopolymers [Internet]. 2005;1–12. Available from: http://onlinelibrary.wiley.com/doi/10.1002/3527600035.bpol3b01/full

2. Lemoigne M. Produits de dehydration et de polymerisation de l'acide ß-oxobutyrique. Bull Soc Chim Biol (Paris). 1926;8:770–8.

3. Werker A, Lind P, Bengtsson S, Nordström F. Chlorinated-solvent-free gas chromatographic analysis of biomass containing polyhydroxyalkanoates. Water Res. 2008;42:2517–26.

4. Braunegg G, Sonnleitner B, Lafferty RM, Springer-veriag I. A Rapid Gas Chromatographic Method for the Determination of Poly-β-hydroxybutyric Acid in Microbial Biomass. Eur J Appl Microbiol Biotechnol. 1978;6:29–37.

5. Riis V, Mai W. Gas chromatographic determination microbial biomass after hydrochloric of poly-beta-hydroxybutyric acid propanolysis. J Chromatogr. 1988;445:285–9.

6. Carlson R, Wlaschin A, Srienc F. Kinetic Studies and Biochemical Pathway Analysis of Anaerobic Poly- (R) -3-Hydroxybutyric Acid Synthesis in Escherichia coli. Society. 2005;

7. Kacmar J, Carlson R, Balogh SJ, Srienc F. Staining and quantification of poly-3-hydroxybutyrate in Saccharomyces cerevisiae and Cupriavidus necator cell populations using automated flow cytometry. Cytom Part A. 2006;69:27–35.

8. Mahishi LH, Tripathi G, Rawal SK. Poly(3-hydroxybutyrate) (PHB) synthesis by recombinant Escherichia coli harbouring Streptomyces aureofaciens PHB biosynthesis genes: effect of various carbon and nitrogen sources. Microbiol Res. 2003;158:19–27.

9. Baetens D, Aurola AM, Foglia A, Dionisi D, Van Loosdrecht MCM. Gas chromatographic analysis of polyhydroxybutyrate in activated sludge: A round-robin test. Water Sci Technol. 2002. p. 357–61.

10. Du, GC; Chen, J; Yu, J; Lun S. Continuous production of poly-3-hydrobutyrate by

Ralstonia eutropha in a two-stage culture system. J Biotechnol. 2001;88, 59-65.:59–65.

11. Elhottová D, Tríska J, Petersen SO, Santrůcková H. Analysis of poly-beta-hydroxybutyrate in environmental samples by GC-MS/MS. Fresenius J Anal Chem [Internet]. 2000;367:157–64. Available from: http://www.ncbi.nlm.nih.gov/pubmed/11225876

12. Karr DB, Waters JK, Emerich DW. Analysis of Poly- , 3-Hydroxybutyrate in Rhizobium japonicum Bacteroids by Ion-Exclusion High-Pressure Liquid Chromatography and UV Detectiont. Appl Environ Microbiol. 1983;46:1339–44.

13. Hesselmann RPX, Fleischmann T, Hany R, Zehnder AJB. Determination of polyhydroxyalkanoates in activated sludge by ion chromatographic and enzymatic methods. J Microbiol Methods. 1999;35:111–9.

14. Shrivastava A, Gupta V, Article R. Methods for the determination of limit of detection and limit of quantitation of the analytical methods. Chronicles Young Sci [Internet]. 2011;2:21–5. Available from: http://www.cysonline.org/article.asp?issn=2229-5186;year=2011;volume=2;issue=1;spage=21;epage=25;aulast=Shrivastava

15. Wu L, Mashego MR, van Dam JC, Proell AM, Vinke JL, Ras C, et al. Quantitative analysis of the microbial metabolome by isotope dilution mass spectrometry using uniformly 13C-labeled cell extracts as internal standards. Anal Biochem [Internet]. 2005 [cited 2015 Aug 20];336:164–71. Available from: http://www.ncbi.nlm.nih.gov/pubmed/15620880

16. Noack S, Wiechert W. Quantitative metabolomics: a phantom? Trends Biotechnol [Internet]. Elsevier Ltd; 2014 [cited 2015 May 20];32:238–44. Available from: http://www.ncbi.nlm.nih.gov/pubmed/24708998

17. Mashego MR, van Gulik WM, Vinke JL, Visser D, Heijnen JJ. In vivo kinetics with rapid perturbation experiments in Saccharomyces cerevisiae using a second-generation BioScope. Metab Eng. 2006;8:370–83.

18. Niedenführ S, ten Pierick A, van Dam PTN, Suarez-Mendez CA, Nöh K, Wahl SA. Natural isotope correction of MS/MS measurements for metabolomics and 13C fluxomics. Biotechnol Bioeng. 2016;113:1137–47.

19. Gomes R de S. Obtenção de mutantes deficientes no acúmulo de PHA e construção de linhagens recombinantes para o controle da composição monomérica. 2009.

20. Taymaz-Nikerel H, de Mey M, Ras C, ten Pierick A, Seifar RM, van Dam JC, et al. Development and application of a differential method for reliable metabolome analysis in Escherichia coli. Anal Biochem [Internet]. Elsevier Inc.; 2009 [cited 2014 Nov 19];386:9–19. Available from: http://www.ncbi.nlm.nih.gov/pubmed/19084496

21. Niessen WMA, Manini P, Andreoli R. Matrix effects in quantitative pesticide analysis using liquid chromatography-mass spectrometry. Mass Spectrom Rev [Internet]. 2009;25:881–99. Available from: http://www.ncbi.nlm.nih.gov/pubmed/20329703

22. Wahl SA, Seifar RM, ten Pierick A, Ras C, van Dam JC, Heijnen JJ, et al. Quantitative Metabolomics Using ID-MS. Methods Mol Biol [Internet]. 2014. p. 91–105. Available from: http://link.springer.com/10.1007/978-1-4939-1170-7_6

Annexes

A. Fragmentation of derivatized 3-HB

Two major fragments were identified by GC-MS for PHB analyses: m/z 131 and m/z 145. The fragment m/z 131 was used for the quantification, the mass of the internal standard was m/z 134. The retention time of the fragments was 4.53 minutes.

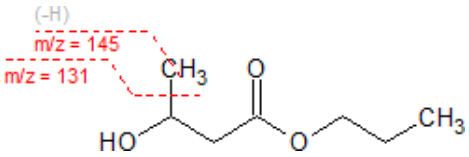

Figure A1. Chemical structure of derivatized 3-HB and observed fragments.

B. Calibration Standards

Table B1: Preparation of a standard calibration (external) using the following standard concentrations (13 points).

	S1	S2	S3	S4	S5	S6	S7	S8	S9	S10	S11	S12	S13
3-HB (mmol/L)	0.001	0.002	0.006	0.011	0.023	0.057	0.113	0.227	0.567	1.134	2.268	5.671	11.341

Table B2: Preparation of a standard calibration (external) using the following standard concentrations (18 points).

	S1	S2	S3	S4	S5	S6	S7	S8	S9	S10	S11	S12	S13	S14	S15	S16	S17	S18
3-HB(mM)	0.001	0.002	0.006	0.011	0.022	0.056	0.111	0.222	0.389	0.555	0.833	1.110	1.666	2.221	2.776	5.552	8.328	11.104

C. Estimation of the analytical standard deviation of the measurements ($^{12}C/^{13}C$-PHB)

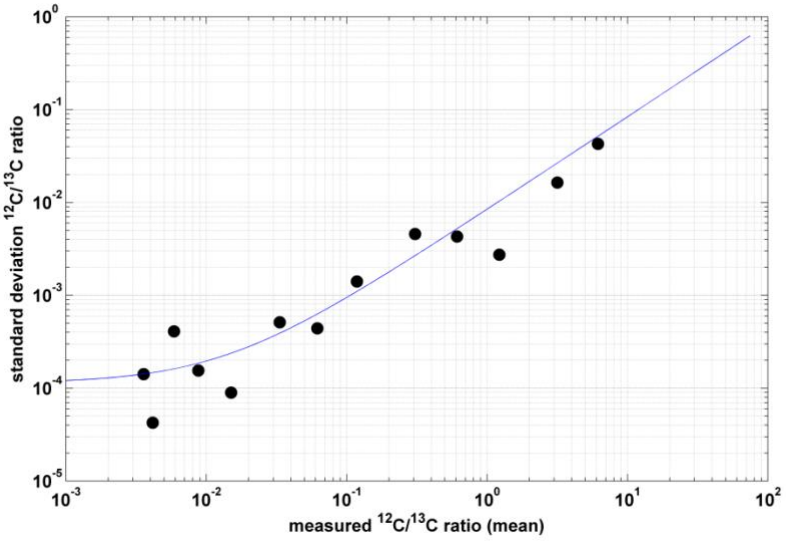

Figure C1. Observed standard deviation as a function of the measured average ratio in log scale. Based on the observed linearity, a heteroscedastic error model was assumed (blue line).

D. Technical and sample processing reproducibility

Table D1. Measurement of the $(PHB)_1$ concentration from the two different cultivations, each sample is measured in triplicate .

	Concentration*	**SE****	**SE**	***SE Concentration**	**SE**
	(mmol/L)	**(mmol/L)**	**(%)**	**(mmol/L)**	%
	2.754	0.008	0.279		
1	2.802	0.042	1.493		
	2.881	0.072	2.503		
Average	2.812	0.041	1.441	0.052	1.86
	3.054	0.061	2.011		
2	3.033	0.057	1.894		

	3.029	0.026	0.848		
Average	3.038	0.048	1.584	0.011	0.37

Average concentration of three times injection. **Standard deviation of three times injection (analytical reproducibility).*** Standard deviation of the three samples concentration (first column, process reproducibility).

E. Additional tests on sample processing steps

I. Complete degradation of the polymer:

The standard method suggests a time for derivatization of 2 hours. Thus, was desired to confirm whether a complete degradation of the polymer could be achieved in less time. The $(PHB)_1$ concentration at different time points 30, 60, 120, 150 and 180 minutes was tested. One millilitre samples were taken from one shake flask in triplicate, the peak areas obtained were corrected with the IS-^{13}C-PHB . The concentration in the broth was 2.925 ± 0.044. The t-test ($p<0.05$) indicated no significant differences between the time points measured and the concentration in the broth.

Table E1. Comparison of concentration of $(PHB)_1$ in different derivatization times.

Derivatization time (h)	**Average (mmol/L)**	**SE (mmol/L)**
0.5	2.685	0.022
1	2.725	0.051
2	2.885	0.046
2.5	2.788	0.037
3	2.826	0.056

II. **Homogeneity:**

During derivatization, vortexing is an important step for the complete mixing of the sample. The standard method recommends to vortex every 30 minutes during derivatization. Hence, was determined if the mixing is enough with the boiling itself. Three samples from one shake flask were measured without vortexing during derivatization. The concentrations were corrected with the IS-^{13}C-PHB . The results show that there is no need for vortexing during derivatization. However this was only tested with *E. coli*, is possible that other species might not deliver the same result if not vortexed.

Table E2. Comparison of concentration $(PHB)_1$ obtained with and without vortexing.

Repeat #	**Homogeneity**		**Reproducibility**	
	Average (mmol/L)	**SE** (mmol/L)	**Average** (mmol/L)	**SE** (mmol/L)
1	2.793	0.011	2.754	0.008
2	2.820	0.008	2.802	0.042
3	2.853	0.037	2.881	0.072

III. **Biomass quantification:**

In order to know the content of PHB in biomass. Cell dry weight was compared by two methods: filtration and freeze drying.

To determine biomass content by filtration a 5 mL sample in triplicate was taken from one shake flask. Through freeze drying, first was determined the weight of IS-^{13}C-PHB and PAA only, as a blank. Then the biomass was measured subtracting such value to obtain the actual value of cell dry weight per one milliliter. Each vial was weighted before adding sample and after freeze drying.

There was no significant difference between the two methods used for the biomass determination.

Table E3. Comparison of biomass determination in g/L through freeze drying and filtration.

Biomass		
	Freeze drying	**Filtration**
Average (g_{DW}/L)	1.185	1.300
SE (g_{DW}/L)	0.035	0.0013

F. Calibration lines with the internal standards Benzoic acid (BA) and Phenyl acetic acid (PAA)

Calibration using Benzoic Acid as Internal Standard

The stock solutions of the internal standards PAA and BA were prepared in a concentration of 0.02 mmol/mL. A volume of 50 µL of each internal standard was added to the samples. The step in which the internal standards were added in the samples differs, BA was added after freeze drying and PAA before freeze drying. The calibration lines obtained were analyzed with and without the addition of$IS\text{-}^{13}C\text{-}PHB$. The internal standard BA was added to compare with the IS proposed in this study. The relative and the absolute error of the data obtained with BA, was calculated with the presence of $IS\text{-}^{13}C\text{-}PHB$ that was 0.0045 and 0.0004 respectively.

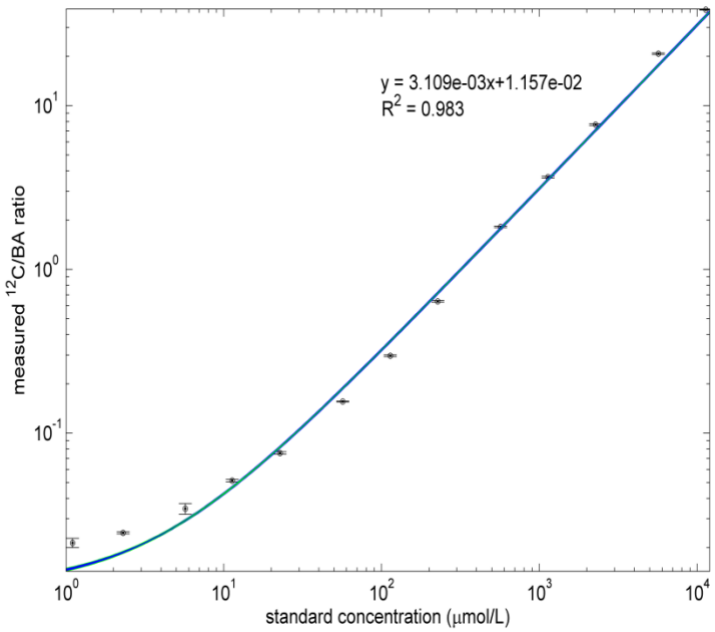

Figure F1. Measured ^{12}C/BA ratio and linear regression line. Both standard concentration and measured ratio are in log scale.

Calibration using Phenyl acetic acid as Internal Standard

The calibration lines obtained were analyzed in the same way as with BA with and without the presence of the IS-^{13}C-PHB. The purpose of adding the internal standard PAA was to have a similar correction as the ^{13}C-PHB, because was added before freeze drying. The relative and the absolute error with the presence of IS-^{13}C-PHB was calculated that was 0.0137 and 0.00005 respectively. Therefore such internal standards were not reliable for quantification with GC-IDMS.

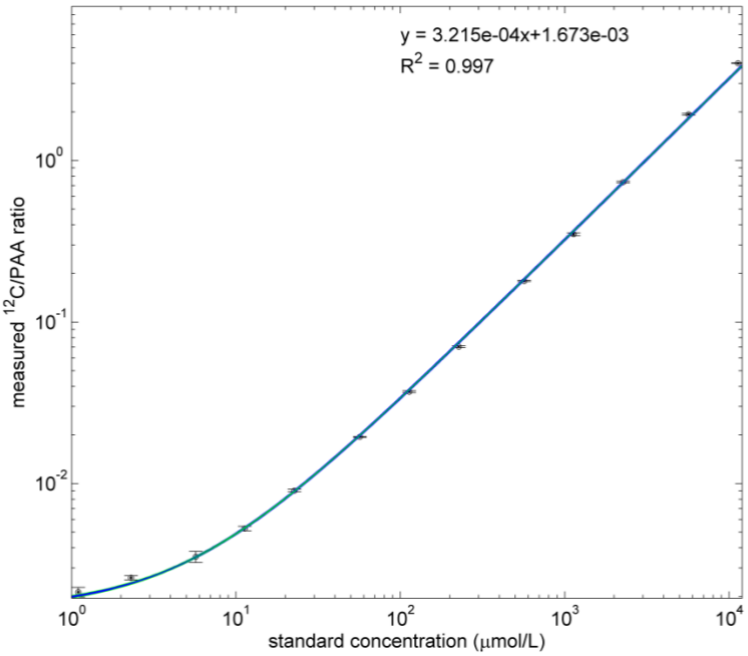

Figure F2. Measured 12C/PAA ratio and linear regression line. Both standard concentration and measured ratio are in log scale.

The internal standards PAA and BA showed lower reproducibility and when spiked with a known amount of $(PHB)_1$ the recoveries were overestimated with BA and underestimated with PAA. The overestimation using BA comes from adding the internal standard after the freeze drying. Therefore the correction does not take into account losses of the first steps.

Chapter 5.

Recommendations and outlook

Redox metabolism in *Escherichia coli* is very flexible and adjusts to environmental conditions and/or metabolic engineering approaches robustly. The experimental and model-based analysis revealed that *E. coli* has flexibility in redox sinks that released an engineered coupling of NADPH regeneration and consumption in the product pathway (PHB). Based on the main findings, specific conclusions and recommendations are formulated in the following sections.

1. Thermodynamic analysis as a tool to identify bottlenecks in metabolic pathways

Studies related to co-factor availability for the synthesis of interesting industrial products, has promoted the use of several tools to investigate the co-factor role such as metabolomics, fluxomics and genomics [1,2]. In this research thermodynamics was integrated with metabolomics for the assessment of metabolic pathways. The product investigated was polyhydroxybutyrate, a cell internal sink for reducing equivalents that finds an application as biodegradable plastic. In **Chapter 2** three different pathways were analyzed: EMP, mEMP and EDP. The thermodynamic pathway analysis suggested that the main bottleneck for PHB production is not so much the redox state of the cell but the acetyl-CoA/CoA ratio in the cell.

In literature, the formation of acetoacetyl-CoA was suggested to be inhibited by the CoA concentration [3,4]. The thermodynamic analysis presented in this thesis showed that a thermodynamic constraint in the reaction to form acetoacetyl-CoA governed the reaction rather than allosteric control or inhibition by free CoA levels. This shows that evaluating the Gibbs free energy of PHB formation pathway could help to improve the process design and strain engineering in product development.

1.1 Adding enzyme properties and resource allocation in the thermodynamic analysis

Not only thermodynamic based on reaction stoichiometry should be considered but also enzyme concentrations and capacities. The (calculated) required enzyme amounts to generate a set of reactions in a pathway give relevant insights for the metabolic engineering strategies and avoid bottlenecks. Especially, the Enzyme Cost Minimization (ECM) tool developed by Noor et. al. could be applied [5]. The ECM optimization includes enzyme concentrations, as well as metabolite concentrations of substrates and products, leading to a result balancing between enzyme expression and thermodynamic optimality [6].

Enzyme kinetic studies showed that there can be significant difference between microorganisms. Acetyl-CoA C-acetyltransferase (EC 2.3.1.9) which is involved in the condensation of acetoacetyl-CoA in *Cupriavidus necator* has a K_m of 158 μM for acetoacetyl-CoA [7], while in *Azotobacter beijerinckii* the K_m is lower at 1.8 μM. Therefore, a more elaborate model where the enzymes characteristics are considered next to thermodynamic driving forces in the pathway, could increase the robustness of the analysis and enable best choices of enzymes.

2. Metabolic engineering and PHB formation

Following the thermodynamic and stoichiometric calculations, the *E. coli* strain (K12GAPNΔzwf+pPHB) was constructed and studied experimentally. The experimental results shown in **Chapter 3** confirm the outcome from the thermodynamic analysis: the strain K12GAPNΔzwf+pPHB showed increased PHB production compared to a strain with non-modified glycolysis (K12+pPHB).

2.1 Stability of the production strain

In this study modified strains of *E. coli* harboring a plasmid with the genes of *Cupriavidus necator* for the PHB synthesis were applied. The plasmid based strategy has several drawbacks during the cultivation of the cells, the instability and burden of the plasmid generates a limitation for obtaining a successful design. Especially, the plasmid instability using engineered strains, is a recurrent problem in the industry, For instance, the addition of antibiotics in large-scale cultivations to stabilize plasmids is not advantageous [8]. To solve this problem, a future integration of the PHB pathway in the chromosome could prevent replication problems [9].

2.2 Tracing redox metabolism

The reactions that were consuming most of the NADPH in the engineered cells could not be fully identified. To better investigate the distribution of the internal fluxes in the cells, ^{13}C experiments [10,11] should be performed and elucidate the fate of carbon and consequently also the cofactors in the cells, not only NADPH but also acetyl-CoA.

2.3 Modifying co-factor preference in the PHB pathway to NADH-dependent

The approach used in this study relied on the modifications of glycolysis, however a PHB NADH-dependent pathway can be a good alternative for oxygen limited or anaerobic conditions. Anaerobic production can be favored in a NADH-dependent PHB pathway, since the reduced co-factors produced in the glycolysis (NADH) could be directly used for PHB production. Some efforts are being performed in this line of research by Olavarria et al. (unpublished results).

2.4 Strategies to regulate CoA levels in the cell

Two main strategies can be applied: (1) co-feeding of acetate (or other substrate) or (2) improved stoichiometry to increase acetyl-CoA from glucose.

The shortest pathway to form acetyl-CoA is from acetate, adding acetate as a co-substrate could increase the ratio of AcCoA/CoA. However, it has been well documented that *E. coli* cannot consume glucose and acetate simultaneously due to catabolite repression in batch conditions [12,13]. However, in chemostat cultivations catabolite repression is not active and could therefore be applied [14,15].

Moreover, another study used acetate to favor the production of N-acetylglutamate through the enhancement of acetyl-CoA levels, an increase of 77.9% of acetyl-CoA supply was achieved [16].

Another possible strategy to increase acetyl-CoA/CoA ratio is a reversible glyoxylate shunt that could increase the acetate yield on glucose by 50 % [17] or a non-oxidative glycolysis, in both cases 3 mol acetyl-CoA from 1 mol glucose could be attained [18] see **Figure 1**.

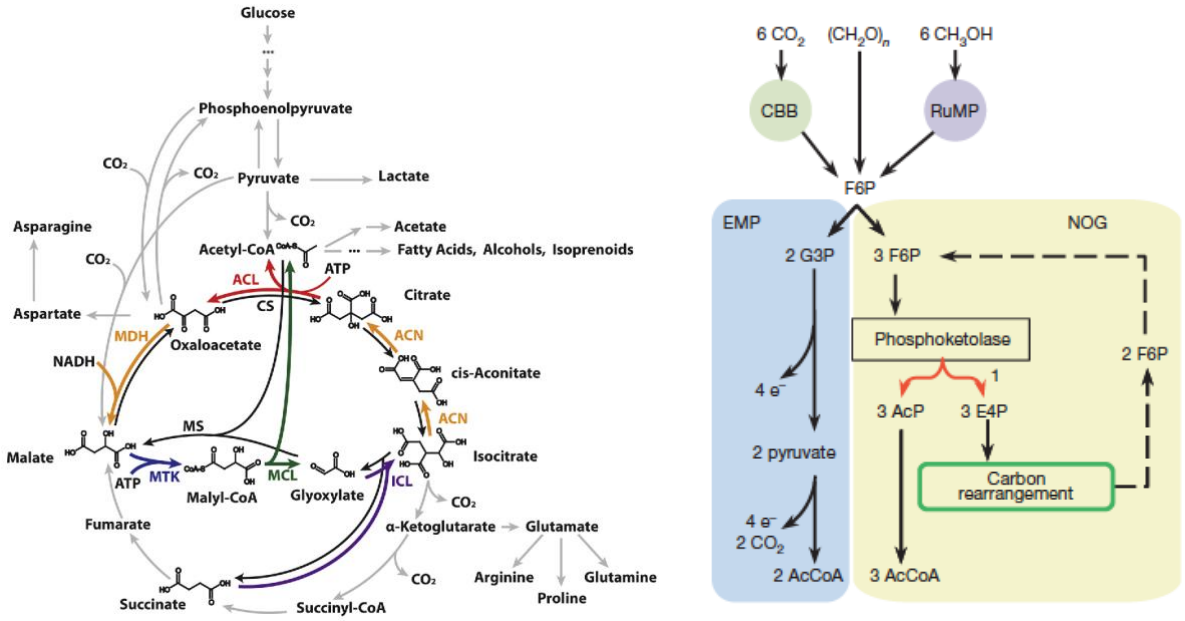

Figure 1. Strategies for the increase of acetyl-CoA production. Left: Reversible glyoxylate shunt [17]. Right: Non-oxidative glycolysis pathway [18].

For the control and regulation of CoA, in *E. coli* four main pools of CoA have been identified that are acetyl-CoA, non-esterified CoA, succinyl-CoA and, in a minor level malonyl-CoA [19]. The main precursor of CoA is the vitamin pantothenic acid, which has been studied for the regulation and control of CoA levels in the cell [20]. Nonetheless, if the concentrations of CoA are too low a negative effect in the cells can occur. One study demonstrated that the CoA depletion caused a change in the saturated/unsaturated fatty acid ratio in the membrane phospholipids, that resulted in the inability of the cells to generate precursors in the TCA cycle for the synthesis of amino acids and proteins [19]. As a result, a careful analysis should be done to obtain an optimal CoA content in the cell that can increase PHB flux but is not detrimental for the cells when lowering CoA levels.

2.5 Expanding the knowledge to other industrial chemicals

The insights generated in this thesis can be beneficial to a large number of current compounds that are promising for industrial production [21,22]. Several of these chemicals are dependent on acetyl-CoA and/or NADPH. For instance, bioplastics like PHAs (Polyhydroxyalkanoates) not only PHB but PHV (Polyhydroxyvalerate) are dependent on both co-factors. Other bioplastics like PLA (Polylactic acid) are dependent on acetyl-CoA [23]. The terpenes farnesene and lycopene require acetyl-CoA in the pathway synthesis [24,25], among other

organic compounds. Consequently, the observations presented in this work can contribute to the further design and evaluation of favorable metabolic pathways for their production.

References

1. Molenaar D, Van Berlo R, De Ridder D, Teusink B. Shifts in growth strategies reflect tradeoffs in cellular economics. Mol Syst Biol [Internet]. Nature Publishing Group; 2009;5:1–10. Available from: http://dx.doi.org/10.1038/msb.2009.82

2. Taymaz-Nikerel H, Borujeni AE, Verheijen PJT, Heijnen JJ, van Gulik WM. Genome-derived minimal metabolic models for Escherichia coli MG1655 with estimated in vivo respiratory ATP stoichiometry. Biotechnol Bioeng. 2010;107:369–81.

3. Senior PJ, Dawes EA. The regulation of poly β hydroxybutyrate metabolism in Azotobacter beijerinckii. Biochem J. 1973;134:225–38.

4. Dawes E. Polyhydroxybutyrate: an intriguing biopolymer. Biosci Rep [Internet]. 1988 [cited 2015 Mar 30];8:537–47. Available from: http://link.springer.com/article/10.1007/BF01117332

5. Noor E, Flamholz A, Bar-Even A, Davidi D, Milo R, Liebermeister W. The Protein Cost of Metabolic Fluxes: Prediction from Enzymatic Rate Laws and Cost Minimization. PLoS Comput Biol. 2016;12:1–29.

6. Noor E, Bar-Even A, Flamholz A, Reznik E, Liebermeister W, Milo R. Pathway Thermodynamics Highlights Kinetic Obstacles in Central Metabolism. PLoS Comput Biol. 2014;10.

7. Kim J, Kim KJ. Purification, crystallization and preliminary X-ray diffraction analysis of 3-ketoacyl-CoA thiolase A1887 from Ralstonia eutropha H16. Acta Crystallogr Sect FStructural Biol Commun. International Union of Crystallography; 2015;71:758–62.

8. Lee SY, Lee Y. Metabolic Engineering of Escherichia coli for Production of Enantiomerically Pure (R) - (𝛘) -Hydroxycarboxylic Acids. Appl Environ Microbiol. 2003;69:3421–6.

9. Lee SY, Lee KM, Chan HN, Steinbüchel A. Comparison of recombinant Escherichia coli strains for synthesis and accumulation of poly-(3-hydroxybutyric acid) and morphological changes. Biotechnol Bioeng. 1994;44:1337–47.

10. Nanchen A, Schicker A, Sauer U. Nonlinear dependency of intracellular fluxes on growth rate in

miniaturized continuous cultures of Escherichia coli. Appl Environ Microbiol. 2006;72:1164–72.

11. Chen X, Alonso AP, Allen DK, Reed JL, Shachar-Hill Y. Synergy between 13C-metabolic flux analysis and flux balance analysis for understanding metabolic adaption to anaerobiosis in E. coli. Metab Eng [Internet]. Elsevier; 2011;13:38–48. Available from: http://dx.doi.org/10.1016/j.ymben.2010.11.004

12. Enjalbert B, Millard P, Dinclaux M, Portais J-C, Létisse F. Acetate fluxes in Escherichia coli are determined by the thermodynamic control of the Pta-AckA pathway. Sci Rep [Internet]. Nature Publishing Group; 2017;7:42135. Available from: http://www.nature.com/articles/srep42135

13. Goldie H. Regulation of transcription of the Escherichia coli phosphoenolpyruvate carboxykinase locus: Studies with pck-lacZ operon fusions. J Bacteriol. 1984;159:832–6.

14. Novak K, Flöckner L, Erian AM, Freitag P, Herwig C, Pflügl S. Characterizing the effect of expression of an acetyl-CoA synthetase insensitive to acetylation on co-utilization of glucose and acetate in batch and continuous cultures of E. coli W. Microb Cell Fact [Internet]. BioMed Central; 2018;17:1–15. Available from: https://doi.org/10.1186/s12934-018-0955-2

15. Taymaz-Nikerel H. Quantitative analysis of relationships between fluxome and metabolome in Escherichia coli. TU Delft - Dep. Biotechnol. - Bioprocess Technol. Gr. 2010.

16. Zhang S, Yang W, Chen H, Liu B, Lin B, Tao Y. Metabolic engineering for efficient supply of acetyl-CoA from different carbon sources in Escherichia coli. Microb Cell Fact [Internet]. BioMed Central; 2019;18:1–11. Available from: https://doi.org/10.1186/s12934-019-1177-y

17. Mainguet SE, Gronenberg LS, Wong SS, Liao JC. A reverse glyoxylate shunt to build a non-native route from C4 to C2 in Escherichia coli. Metab Eng [Internet]. Elsevier; 2013;19:116–27. Available from: http://dx.doi.org/10.1016/j.ymben.2013.06.004

18. Bogorad IW, Lin TS, Liao JC. Synthetic non-oxidative glycolysis enables complete carbon conservation. Nature. Nature Publishing Group; 2013;502:693–7.

19. SUZANNE JACKOWSKI C 0. R. Consequences of Reduced Intracellular Coenzyme A Content in Escherichia coli. J Bacteriol. 1986;166:866–71.

20. Vallari DS, Jackowski S. Biosynthesis and degradation both contribute to the regulation of coenzyme A content in Escherichia coli. J Bacteriol. 1988;170:3961–6.

21. Adrie J. J. Straathof AB. Potential of commodity chemicals to become bio-based according to maximum yields and petrochemical prices. Biofuels, Bioprod Biorefining. 2017;11:798–810 (2017);

22. Li Z, Yang J, Loh XJ. Polyhydroxyalkanoates: Opening doors for a sustainable future. NPG Asia Mater. Nature Publishing Group; 2016;8:1–20.

23. Rehm BH a. Bacterial polymers: biosynthesis, modifications and applications. Nat Rev Microbiol [Internet]. Nature Publishing Group; 2010 [cited 2014 Jul 10];8:578–92. Available from: http://www.ncbi.nlm.nih.gov/pubmed/20581859

24. Martínez I, Zhu J, Lin H, Bennett GN, San K-Y. Replacing Escherichia coli NAD-dependent glyceraldehyde 3-phosphate dehydrogenase (GAPDH) with a NADP-dependent enzyme from Clostridium acetobutylicum facilitates NADPH dependent pathways. Metab Eng [Internet]. 2008 [cited 2015 Mar 30];10:352–9. Available from: http://www.ncbi.nlm.nih.gov/pubmed/18852061

25. Straathof AJJ. Transformation of biomass into commodity chemicals using enzymes or cells. Chem Rev. 2014;114:1871–908.

List of publications

- Velasco Alvarez MI, Ten Pierick A, van Dam PTN, Maleki Seifar R, van Loosdrecht MCM, Wahl SA. Microscale quantitative analysis of polyhydroxybutyrate in prokaryotes using IDMS. Metabolites. 2017;7:1–8.

- K. Olavarria, A. Fina, M. I. Velasco, M. C. M. van Loosdrecht, and S. A. Wahl, “Metabolism of sucrose in a non-fermentative Escherichia coli under oxygen limitation,” Appl. Microbiol. Biotechnol., vol. 103, no. 15, pp. 6245–6256, 2019.

Curriculum vitae

Mariana Itzel Velasco Alvarez was born on the 11th of August of 1988 in Mexico City. She became interested in organic chemistry during high school, specifically in the compounds that fruit release and give aroma, she became fascinated by esters. As a result, she decided to do a bachelor's in Food engineering in 2006 at the "*Universidad Autónoma Metropolitana- Iztapalapa México*". As a graduation team project, she developed a feasibility study for a plant to produce beetroot marzipan. As part of the study, it was essential to include the wastewater treatment process. As a result, she became interested in the process of waste streams in the industry and joined a project for the removal of volatile organic acids that are generated in wastewater treatment plants in the Department of Process and Technology. This project inspired her to pursue a master's in Environmental Science and Engineering that was a joint program between UNESCO-IHE, Ghent University, and the Institute of Chemistry of Prague, she was part of the 2012-2014 batch. After the first year of the master's program, she did an internship at Biothane, Delft. There she studied the performance of anaerobic membrane bioreactors to treat industrial effluents. She finalized her master's thesis with a research project about the metabolic capacities of anammox bacteria in Nijmegen at Radboud University.

Afterward, she was motivated to continue doing research pursuing a PhD in Delft in 2014. She joined the Cell Systems Engineering group at the Biotechnology department. The research project was in collaboration with the University of Sao Paulo and was supervised by Aljoscha Wahl and Mark van Loosdrecht. By coincidence or not the research project was related to a form of polyester, polyhydroxybutyrate.

In August 2020, she joined the Vaccine Launch Facility at Janssen Biologics (Leiden). She is part of the Downstream Manufacturing Specialists team, currently working for the production of the COVID-19 vaccine.

Acknowledgements

Today while cycling I was thinking about how the weather influences greatly our estate of mind. However, no matter how harsh can be sometimes the winter, there is still beauty in the bare trees, holding on to the time when they can show their beautiful leaves. Then, observing provides the tools for gratitude.

That being said, gratitude is something we might forget sometimes. These times are certainly difficult for all the people around world, for some more than others. The importance of appreciating every small detail in daily life can help to ease the moments of uncertainty.

Even though not everyone might be able to read this thesis, I would like to express my sincere gratitude for all the people that were around during my PhD project, thank you for the support, help and presence. Graduating during lockdown, feels strange, however I will imagine that all of you are present.

I would like to thank my family for giving unconditional support, thank you for believing me and encouraging me during the darkest moments. Dear mom (Lulú), you are the big star here, la que me cuidó a pesar de la distancia, gracias por hacerme reír a pesar de las adversidades, por celebrar logros aunque para mí a veces eran insignificantes, gracias por recordarme la fortaleza de la naturaleza, y por hacerme apreciar cada pequeño detalle de la vida, tu luz me ha guiado siempre.

Hermanito (Andrés), el mejor hermano del mundo, aunque siempre me dices que soy la hermana menor, después del doctorado ya hasta me salieron canas jeje. Gracias por hacerme reír todo el tiempo, por hacer todo más ligero, por nuestras largas pláticas nocturnas sobre la vida. Fernando, gracias por todo el apoyo, por darle la importancia a la educación, no sólo académica pero también espiritual.

Lupita, mi tía favorita. Gracias por acompañarme en esta trayectoria y compartir tu sabiduría de la vida. Por creer siempre en mis habilidades y siempre estar presente ante cualquier momento a pesar de la distancia.

Abuelitos, gracias por siempre recibirme siempre con una cálida sonrisa, por las historias contadas y por el cariño incondicional.

Mark, thank you for teaching me great lessons of how to explain science, and being clear. Thank you for all the support and encouragement to get to the finalization of the thesis.

You were always open to discuss not only scientific topics but also life matters. Aljoscha, thank you for giving me the opportunity to do research. It was certainly not an easy path, but the end came accordingly. Thank you for teaching me the tools to analyze metabolic networks and to be consistent. Walter, thank you for all your insights in metabolic engineering, and for providing help at all times.
Lina, my supervisor during my master thesis, thank you for inspiring me to pursue a PhD. I appreciate everything I learned from you during the master and making me interested in understanding metabolic routes. You were such an inspiration to me, thank you. Peter, Huub and Jack, thank you for supporting me to start this journey, thank you for everything.

To my students: Vincenzo, thank you for being a team with me at the start of the PhD, thank you for all your dedication. Your collaboration was key to the project.
Héctor, thank you for all your hard-work and you scientific intuition, for your dedication despite the hard times you were going through. Samantha, definitely we had a lot of fun in the lab, thank you for all your expertise in modeling, it was definitely an important input in this thesis. Thank you for all the commitment to the project. Jolijn, thank you for your enthusiasm and dedication to the project, it was fun. Noortje, thank you for all your effort and input.

Zeijang, thank you for all the support and help with the bioreactor experiments, for all the insights at the laboratory and the lessons learned with *E. coli.*
A big thank you to Apilena, Astrid and Janine without your support many experiments would not have gone smoothly ☺. Apilena, thank you for your kindness and cheerfulness, you always had a smile to give. Astrid thank you for sharing all the art and cultural news during the lunch breaks. Janine, thank you for always being there to help.
Rob and Dirk, thank you for your support at the lab at all times. You were always ready to give support and solve lab issues. Johan, you always made time to measure samples, thank you for all the assistance and help.
Jenifer, thank you for your support an care, you were always available to provide any kind of help. Thank you for everything.

Cor, your help and support was crucial for delivering all the final results of this thesis. Thank you for your kindness and for your support at all times. Angie, it was a pleasure

meeting you during the first half of the PhD. You always came up with great ideas, thank you for all the enthusiasm and support, it was great working with you. Song, thank you for all the help with the bioreactors and being always available to assist, also thank you for your friendship. Patricia, Reza, thank you for making possible the measurement of so many samples in every experiment. Your support was of great impact to the thesis development. Sylvia, it was a pleasure working with you, thank you for your assistance.
Koen, Leonor, Lucas, thank you for all the help in the lab, and for all the fun while doing the 13C vials. Maxime, it was fun knowing you and sharing lunch together.
To the EBT gang, Jelmer, Monica, Ema, Gerben, David, thank you for creating a great environment at the faculty, I enjoyed the times I could attend the presentations about the research you were doing.
To the BPE team, Carlos, David, Joana, Sylvia, thank you for all the nice times at the faculty, for the muffin breaks and all the fun in the lab.
To the latin gang, Raúl, Ricardo, Pablo, Nati, thank you for all the lunch conversations and the summer gatherings. To the Krashna gang, Ranko, Alexey, Arturo, it was really fun being part of the choir, thank you for the great times.

To my family in the Netherlands: Susana, you are for me an example to follow, a beautiful woman with incredibly amazing creativity and intelligence. Thank you for the invaluable friendship, for the laughs, the hugs (I hope I will be able to give you one soon), and all the stories we shared of life, even though you always say that you are the only one that talks when we meet, hehe. Mar, like the sea, you were always calming the storms during the hard times of the finalization of the thesis. Thank you for all the talks in the faculty, for always making time to discuss life reflections and science topics. I admire your way of thinking, your sense of justice and freedom. Mario Coutiño, I met you at the start of the PhD, time went too fast, I feel fortunate to have you as a friend. Thank you for taking care of me, and for sharing your intelligence in everything. You are an amazing person, your friendship has been a sparkle in my life. Arturito, gracias por todo. Thank you for motivating me to learn dutch, to laugh about our gray days. You are a great human being, thank you for listening always and making amazing mexican food :P.
Yaya, you have been a lovely friend, always caring for the people close to you. Thank you for sharing your gentleness and wisdom. I have warm memories of the times in the lab, or going together on holidays. Flor, you are such a beautiful woman, thank you for

always caring, for your infinite tenderness. Thank you for all the support and help, you were the flower that gave color to the rainy days.
Carlita, muito obrigada!, thank you for all the support and encouragement. We have shared many fun moments during the PhD. I am glad that we met and we keep sharing smiles. Thank you for always being there to listen and see the bright side of life. Ana, we shared the final years of the PhD, it was a great adventure. You always had a warm spirit to brighten the cold days. Thank you for all the support and for reminding me all what we are capable to do.
Lore, you were always there for encouraging me, thank you for all the adventures and for the long talks that always ended with big laughs.

Hugo C. thank you for sharing all your wisdom and knowledge about bioreactors during my first months, for all the laughs. I was lucky to meet you at the beginning of the PhD. Thank you for always making time to review something from my thesis and for sharing your sense of humor.
Karel, muchas gracias por todo. I am extremely grateful for all the help and support you gave me during the project. Generating scientific curiosity, while spending long hours in the lab, but always with a smile or singing a tropical song (salsa, cumbia, son, etc). You were always willing to teach with delight, I learned so much from you. Thank you for sharing your wisdom in life and your joy for science. Hugo K. Thank you for supporting me at the finalization of my thesis, were tough times and music was always our companion. Thank you for your care and for lighten up moments with funny stuff. Francisca, thank you for all the beautiful moments during the PhD for teaching me and guiding me at the beginning. Mihir, thank you for always sharing your light spirit, “as everything is as expected there is nothing to worry”, this is the lesson I learned from you. Cris B. your simplicity and your charisma was always present. Thank you for always spreading a cheerful atmosphere that was much needed under times of stress.
Fahimeh, we met at the beginning of the PhD, it was great meeting you and I am happy to still keep sharing nice moments with you. Thank you for you sharing your bright and cheerful character. Eleni, it was fun our times at the lab, assisting courses, working together at the library, thank you for all the support. Pilar, you always had a gentle spirit, thank you for your support, for listening and being there to give comfort when needed. Cris, las risas nunca faltaron, gracias por las pláticas y por hacer un ambiente genial.

Pau, mi chilena favorita, a pesar del tiempo y la distancia, siempre te recordaré con cariño. Gracias por todas las risas que compartimos, por tu alegría y sencillez, espero que pronto podamos volvernos a ver.

Nadya, Gilda, Shilpi, thank you for your friendship and for supporting me to start the PhD journey. I miss you a lot, I hope we can see each other soon.
Ile, Anita, mis amigas de vida, a pesar de la distancia esto no nos ha impedido a seguir con nuestra amistad. Los años pasan y aquí seguimos comaprtiendo risas y contando historias de nuestra niñez.
Rulo, Pichi the best bears of the world y una cosa que nunca olvidaré es que "una cosa es una cosa", frase célebre de Rulo. Pichi, your laugh has been always contagious, I keep all the good memories of our youth.

Wim, to the best saxophone teacher. Thank you for inspiring me to play saxophone and to find my own style. Also, for motivating me to improve and to learn from mistakes. Even in music, a mistake can derive into a nice melody. Music was an important factor to finalizing the PhD.

My dear Pimeje, I met you when I never expected it, you have been a calm wave in the turbulent sea. Thank you for all the love and care, and enduring the hard times. You have been next to me during this transition, I feel grateful for your immense patience and warmth.

I hope I did not forget anyone, and if I did, my apologies. I will make sure to share my gratitude by a message.